



**UNIVERSITÀ
DEGLI STUDI DELLA
BASILICATA**

Dottorato di Ricerca in
“Scienze di Base e Applicate (DiSBA)”

“RECOVERY SUBSTANCES WITH ANTIPATHOGENIC EFFECTS FROM ORGANIC AGRO-
INDUSTRIAL WASTE USING SUITABLE MICROORGANISMS”

Settore Scientifico-Disciplinare
“Biologia Applicata”

Coordinatore del Dottorato

Dottorando

Prof.ssa Patrizia Falabella

Dott.ssa Brigida Della Mura

Relatore

Prof. Giuseppe Martelli

Ciclo XXXVIII

*Certo, “Si può fare”, ma servono
audacia, perseveranza, lungimiranza,
sagacia e tanta indisponenza.
E io modestamente non manco di nessuna.*

Dedico questo lavoro a coloro che hanno visto in me tutto questo, permettendomi di brillare anche nei giorni più bui.

Table of Contents

Abstract	1
Abstract in italiano	2
1. Introduction	3
1.1 Reference agronomic context	3
1.2 BCAs and BAs as key factors for biological control.....	5
1.3 PGPR for plant health and environmental protection.....	7
1.4 Effects of PGPR on Plant Growth and Health.....	8
1.5 Application Methods of PGPR.....	9
1.6 <i>Bacillus subtilis</i> for plant health	10
1.6.1 <i>Bacillus subtilis</i> features	11
1.6.2 <i>B. subtilis</i> - plants interaction	13
1.6.3 <i>B. subtilis</i> : a source of antimicrobial lipopeptides.....	15
1.6.4 Industrial lipopeptides production	20
1.6.5 Limits and potential for a large-scale <i>B. subtilis</i> utilisation	25
1.6.6 Microbial biomass and whole-cell formulations as sustainable alternatives to chemical fertilisers	33
1.6.7 Seed coating with beneficial microorganisms	35
1.7 <i>Pseudomonas granadensis</i> and its role in the Rhizosphere.....	37
1.7.1 Overview of the Genus <i>Pseudomonas</i>	37
1.7.2 Taxonomy and Discovery of <i>P. granadensis</i>	38
1.7.3. Morphological and Physiological Characteristics	38
1.7.4 Genomic Architecture and Rhizosphere Competence.....	38
1.7.5 Ecological Significance and Plant-Microbe Interactions	39
1.7.6 The Endophytic Lifestyle of <i>P. granadensis</i>	39
1.7.7 Mechanisms of Biocontrol and Stress Resilience	40

1.7.8	Current State of the Literature	40
	Aim of the thesis.....	42
2.	Materials and Methods	44
2.1.	Production of biological preparations containing iturin A with antimicrobial action 44	
2.1.1	General Workflow for Microbial Cultivation and Iturin A Production.....	44
2.1.2	Microorganism selection	45
2.1.3	Selected bacterial strain	45
2.1.4	Fungal pathogens.....	45
2.1.5	Agro-industrial waste selection for breeding the chosen microorganism	46
2.1.6	Determination of the quantity of iturin A.....	47
2.1.7	Preparation of cell-free supernatant and crude lipopeptide extract	48
2.1.8	Antimicrobial activity evaluation during the scaling-up and optimisation process 48	
2.2	Microbial biomass production for plant biostimulation	51
2.3	Evaluation of the microbial biomass biostimulant activity	51
2.3.1	Pilot trials.....	51
2.3.2	Biostimulant test on Basil.....	65
2.3.3	Coating basil seeds with microbial biomass containing <i>B. subtilis</i> ET-1.....	76
2.4	Evaluation of the potential of <i>Pseudomonas granadensis</i> CT364 to colonise plant tissues 91	
2.4.1	Tomato Micro-Tom tissues colonisation.....	92
2.4.2	Cochise wheat sterilisation procedures	99
2.5	Data analysis.....	101
3	Results	103
3.1.	Microorganism selection	103
3.2	Agro-industrial waste selection for breeding the chosen microorganism	104

3.3	Antimicrobial activity evaluation during the scaling-up and optimisation process	107
3.3.1	<i>In vitro</i> test.....	107
3.3.2	<i>In vivo</i> test.....	109
3.4	Microbial biomass production for plant biostimulation	111
3.5	Biostimulant test on Basil.....	112
3.5.1	Phenotypic observations	112
3.5.2	Biometric measurements	116
3.5.3	Measurement of Chlorophyll Content Index	119
3.6	Evaluation of the biostimulant activity of microbial biomass through coating of Basil seeds.....	122
3.6.1	Germination percentage.....	122
3.6.2	Phenotypic observations	124
3.6.3	Biometric measurements	126
3.6.4	Measurement of Chlorophyll Content Index	129
3.7	Evaluation of the potential of <i>Pseudomonas granadensis</i> CT364 to colonise Tomato tissues	130
3.7.1	Visualisation of Tomato root colonisation by <i>P.granadensis</i> CT364	130
3.7.2	Visualisation of Tomato aerial tissues colonisation by <i>P.granadensis</i> CT364	132
3.7.3	Cochise wheat sterilisation procedures	137
4	Discussion.....	144
4.1.	Production of iturin A–based biological preparations with antimicrobial activity	144
4.1.1	Selection of <i>Bacillus subtilis</i> ET-1 as an effective biocontrol agent.....	144
4.1.2	Influence of substrate composition on growth and antifungal activity	144

4.1.3	Optimisation through agro-industrial waste and Response Surface Methodology	145
4.1.4	Biological validation <i>in vivo</i> and post-harvest systems.....	145
4.2	Microbial biomass production and biostimulant activity	145
4.2.1	Limitations associated with seed coating application.....	147
4.2.2	Nutritional Assessment as a Limiting Factor in Biostimulant Evaluation ...	148
4.3	Concluding remarks.....	149
4.4	Colonisation ability and plant interaction of <i>Pseudomonas granadensis</i> CT364	149
4.4.1	Root colonisation and early plant–microbe interactions	149
4.4.2	Colonisation of aerial tissues and endophytic behaviour	150
4.4.3	Effects on plant performance and stress tolerance	150
4.4.5	Biometric measurements and interpretation of statistical outcomes	151
4.4.6	Phytosanitary observations and environmental stress factors	151
4.4.7	Methodological constraints: seed sterilisation challenges.....	151
4.4.8	Concluding remarks.....	152
4.5	Complementary microbial strategies for sustainable crop management.....	152
4.6	Technology readiness and application potential of the investigated microbial systems.....	153
	Conclusions	154
	Acknowledgements	156
	Bibliography.....	158
	Annex A	179
	Scientific publications	179
	Scientific papers.....	179
	Conference contributions.....	179
	Annex B	181

Data and observations on the biostimulant activity of microbial biomass.....	181
Pilot trial on Basilico	181
Phenotypic observations.....	181
Biometric measurements.....	184
Chlorophyll Content Index.....	185
Summary evaluation of results.....	186
Pilot trial on potato plants	187
Phenotypic observations.....	187
Biometric measurements.....	189
Summary evaluation of results.....	190
Biostimulation test on basil.....	190
Biometric measurements	191
Chlorophyll Content Index.....	193
Testing chitosan coating on basil.....	193
Germination percentage	194
Phenotypic observations.....	194
Summary evaluation of results.....	197
Testing of microbial biomass coating on basil	198
Germination percentage	198
Biometric measurements	200
Chlorophyll Content Index.....	201
Annex C	203
Data on the assessment of <i>P. granadensis</i> CT364's ability to colonise plant tissues..	203
Tomato Micro-Tom tissues colonisation	203
Biometric measurements	203
Measurement of Chlorophyll fluorescence	206

Index of tables and figures

The index of figures and tables refers exclusively to the main body of the thesis. Figures and tables in the appendices are not included.

Table 1. Summary of the studies carried out on the antipathogenic action of lipopeptides produced by different strains of <i>B. subtilis</i> and other microorganisms on different plant hosts.	18
Table 2. Summary of the fermentation processes applied for the production of compounds using <i>B. subtilis</i> and other microorganisms.	21
Table 3. Recent studies on the BA and BCA attitudes of <i>B. subtilis</i>	28
Table 4. Design matrix generated with the Design of Experiments (DOE) software Modde 13.0.2.	46
Table 5. Timetable of the pilot experimental activity for evaluating the biostimulant effect of microbial biomass containing <i>B. subtilis</i> on basil.	55
Table 6. Water supply, treatments and fertilisation for the plants of the 3 considered trials (water, microbial biomass and ammonium sulphate). Fertiacetyl GZ (an organomineral NK fertiliser) was used in fertigation towards the end of the crop cycle for the plants in all trials.	57
Table 7. Timetable of the pilot experimental activity for evaluating the biostimulant effect of microbial biomass containing <i>B. subtilis</i> on potatoes plants.	62
Table 8. Water supply and treatments for the plants of the 3 considered trials (water, microbial biomass and ammonium sulphate).	64
Table 9. Timetable of the pilot experimental activity for evaluating the biostimulant effect of microbial biomass containing <i>B. subtilis</i> on basil plants.	70
Table 10. Maximum and minimum temperatures recorded in the laboratory during the growing cycle of basil plants.	72
Table 11. Water supply and treatments for the plants of the 3 considered trials (water, microbial biomass and ammonium sulphate).	73
Table 12. Timetable of the pilot experimental activity for evaluating the effect of coating with chitosan con on basil seeds.	79

Table 13. Maximum and minimum temperatures recorded in the laboratory during the basil seed coating test with chitosan.	80
Table 14. Water supply for chitosan-coated and uncoated basil seeds.	80
Table 15. Water supply for chitosan-coated and uncoated basil seeds.	80
Table 16. Weights of seeds of the thesis coated with pectin (C), coated with microbial biomass and pectin (B) and uncoated (N).	84
Table 17. Timetable of the experimental activity to evaluate the effects of coating with pectin and microbial biomass on basil seeds compared to seeds coated only with pectin and uncoated seeds.	85
Table 18. Water supply for pectin-coated, biomass-coated and uncoated basil seeds.	87
Table 19. Maximum and minimum temperatures recorded in the laboratory during the basil seed coating test with pectin and microbial biomass.	89
Table 20. Timetable of the experimental activity to evaluate the ability of <i>P. granadensis</i> CT364 to colonise Tomato Micro-Tom aerial tissues.	95
Table 21. Percentage of mycelial growth inhibition (MGI%) exhibited by the tested biocontrol agents (BCAs) against <i>B. cinerea</i> and <i>P. digitatum</i> under <i>in vitro</i> conditions.	103
Table 22. Effect of substrate composition on colony-forming units (CFUs mL ⁻¹) of <i>B. subtilis</i> ET-1 at the steady growth phase and on the inhibition of <i>P. digitatum</i> conidia germination, expressed as the highest serial dilution of the cell-free supernatant causing ≥95% inhibition.	107
Table 23. Control efficacy of powdery mildew in field experiments on melon plants treated with cell-free supernatant and crude lipopeptide extract (100 ppm iturin A) produced by <i>B. subtilis</i> ET-1. Values followed by different letters are significantly different according to statistical analysis ($p \leq 0.05$).	109
Table 24. Percentage of wounds infected by <i>P. digitatum</i> on clementine fruits following treatment with liquid CFS, stabilised CFS, chemical fungicide, and water.	110
Table 25 shows data relating to the chlorophyll content index (CCI) recorded for the apical (F1-F2) and median (F3-F4) leaves of basil plants treated with microbial biomass (B), spring water (C) and ammonium sulphate (S).	119
Table 26 shows data relating to the chlorophyll content index (CCI) recorded on the front and back of leaf blades for the apical (F1A-F3A) and median (F2M-F4M) leaves of basil plants (P1, P2, P3).	120

Table 27. Number of germinated seeds and germination percentages obtained 13 days after sowing for seeds coated with microbial biomass (B), coated with pectin (C) and uncoated (N).....	123
Table 28. Number of germinated seeds and germination percentages obtained 19 days after sowing for seeds coated with microbial biomass (B), coated with pectin (C) and uncoated (N).....	123
Table 29 shows data relating to the chlorophyll content index (CCI) recorded for the apical (F1-F2) and median (F3-F4) leaves of basil plants derived from seeds coated with biomass and pectin (B), with pectin only (C) and uncoated (N).	129
Table 30 of average Fv/Fm values obtained for plants treated with <i>P. granadensis</i> CT364 (PG1A, PG2B, PG3D) and for control plants treated only with magnesium sulphate (MS1D, MS2C, MS3A).....	133
Table 31. Summary of sterilisation procedures carried out on Cochise wheat seeds and respective results.....	137
Figure 1. Examples of <i>B. subtilis</i> application. Created by the author.	10
Figure 2. Schematic representation of the life cycle of <i>B. subtilis</i> . Image created by the author using graphic components designed in BioRender.com.....	12
Figure 3. Mechanisms of action of <i>Bacillus</i> spp. lipopeptides on the plasma membrane of plant pathogens. Image created by the author using graphic components designed in BioRender.com.	16
Figure 4. Characteristic structures of iturin, fengycin and surfactin. Image created by the author based on data from the PubChem Compound Database (PubChem, n.d.).....	17
Figure 5. Housing for cylinders containing basil seedlings.	53
Figure 6. Orientation of the cultivation system and the distribution of the different treatments. ‘C’ (negative control, water), ‘B’ (plants treated with microbial biomass), ‘S’ (plants treated with ammonium sulphate).	54
Figure 7. Orientation of holes for basil treatments.....	55
Figure 8. Cylinder housing at the time of potato transplanting.	61
Figure 9. Orientation of the cultivation system and the distribution of the different treatments. ‘C’ (negative control, water), ‘B’ (plants treated with microbial biomass), ‘S’ (plants treated with ammonium sulphate).	61

Figure 10. Orientation of holes for potato treatments.	62
Figure 11. Housing for cylinders containing basil seedlings. Housing for cylinders containing basil seedlings.	66
Figure 12. Orientation of the cultivation system and the distribution of the different treatments. ‘C’ (negative control, water), ‘B’ (plants treated with microbial biomass), ‘S’ (plants treated with ammonium sulphate).	67
Figure 13. Basil treatment schedule.	68
Figure 14. Orientation of holes for basil treatments.	68
Figure 15. Post-treatment crop setting up at T1	69
Figure 16. Measurement of photosynthetically active photon flux.	71
Figure 17. Details of the 3 basil plants.	73
Figure 18. Steps in the freeze-drying process.	75
Figure 19. Diagram showing the arrangement of basil seeds in a pot.	77
Figure 20. Pots at the end of basil sowing.	78
Figure 21. Diagram showing the arrangement of basil seeds in a Petri dish.	78
Figure 22. Petri dishes at the end of basil sowing.	79
Figure 23. Orientation of the cultivation system and the distribution of the different treatments. ‘C’ (coating with pectin), ‘B’ (coating with pectin and microbial biomass), ‘N’ (uncoated seeds).	84
Figure 24. Measurement of photosynthetically active photon flux.	89
Figure 25. Arrangement of samples in Petri dishes for chlorophyll fluorescence analysis using Fluorcam equipment. PG: plant treated with <i>P. granadensis</i> CT364; MS: plants treated with magnesium sulfate.	98
Figure 26. Effect of the antimicrobial activity of <i>B. subtilis</i> ET-1 on the growth of <i>P. digitatum</i> hyphae (left) compared to normal growth (right).	104
Figure 27. Response Surface Methodology (RSM) based on a two-level full factorial design showing that iturin A production increases with sucrose concentration up to 20 g/L, while prickly pear extract does not significantly influence production	105
Figure 28. Amount of iturin A (g/L) produced by <i>B. subtilis</i> ET-1 when grown on different substrate formulations.	106
Figure 29. Time-course of iturin A production (mg/L) by <i>B. subtilis</i> ET-1 grown on substrate 28 at 24, 48, 72, and 96 h post-inoculation.	106

Figure 30. Figure 30. Effect of increasing dilutions of the cell-free supernatant obtained from <i>B. subtilis</i> ET-1 grown in substrate 14 on the growth of <i>P. digitatum</i> colonies.....	108
Figure 31. Figure 31. Inhibitory effect on <i>P. digitatum</i> conidia germination observed in serial dilutions of the cell-free supernatant obtained from <i>B. subtilis</i> ET-1 grown in substrate 28.	109
Figure 32. Clementine fruits infected with <i>P. digitatum</i> and treated with liquid CFS, stabilised CFS, imazalil (chemical control), and water (negative control).	111
Figure 33. Microbial biomass containing spores of <i>B. subtilis</i> ET-1 obtained through fermentation and spray-drying processes.	112
Figure 34. Details of basil roots treated with microbial biomass.	113
Figure 35. Details of the early stage of floral bud development on the B2 thesis basil. ...	114
Figure 36. Details of early floral bud development on the B4 and S2 basil specimens. ...	114
Figure 37. Figure 37. Details of the early floral bud on Basil of the C1, C3 and B3 theses.	115
Figure 38. Detailed comparison between C4 and S1 theses 48 days after transplantation.	115
Figure 39. Details of the anthesis on Basil from the B2 thesis.....	116
Figure 40. Graph showing the average height of plants treated with microbial biomass (B), spring water (C) and ammonium sulphate (S). The values were rounded to one decimal place to simplify presentation, in accordance with the instrument's precision.	117
Figure 41. Graph showing the total fresh biomass (leaves, flowers and stems) of plants treated with microbial biomass (B), spring water (C) and ammonium sulphate (S). The values were rounded to two decimal places to simplify presentation, in accordance with the instrument's precision.	118
Figure 42. Graph showing the total dry biomass (leaves, flowers and stems) of plants treated with microbial biomass (B), spring water (C) and ammonium sulphate (S). The values were rounded to two decimal places to simplify presentation, in accordance with the instrument's precision.	118
Figure 43. Graph showing the Chlorophyll Content Index (CCI) of plants treated with microbial biomass (B), spring water (C) and ammonium sulphate (S).	119
Figure 44. Graph relating to the normal distribution of chlorophyll content indices obtained on Basil plants. It is noticeable that a large number of measurements are required to achieve	

a normal distribution, although even in this case, there are values that deviate significantly from the mean.	121
Figure 45. Graph showing the 10 SPAD measurements taken on the 3 plants (P1-P2-P3) on apical leaves (1A-3A) and median leaves (2M-4M).	122
Figure 46. Details of the emergence of the first true leaves 19 days after sowing.	124
Figure 47. Side A before (on the left) and after (on the right) standardising the number of seedlings to 4 per cylinder.	125
Figure 48. Details of the emergence of the fifth and sixth true leaves on Basil Prospera F1 35 days after sowing.	125
Figure 49. Detail of the floral scape emission on Basilico Prospera F1 60 days after sowing.	126
Figure 50. Details of the root branching on Basilico Prospera F1 60 days after sowing. .	126
Figure 51. Graph showing the height differences between plants grown from seeds coated with microbial biomass and pectin (B), pectin only (C), and uncoated (N). The Y-axis does not start at zero to improve the readability of the differences between treatments. The values were rounded to one decimal place to simplify presentation, in accordance with the instrument's precision.	127
Figure 52. Graph showing the differences in fresh biomass between plants grown from seeds coated with microbial biomass and pectin (B), with pectin only (C) and uncoated (N). The Y-axis does not start at zero to improve the readability of the differences between treatments. The values were rounded to two decimal places to simplify presentation, in accordance with the instrument's precision.	128
Figure 53. Graph showing the differences in dry biomass between plants grown from seeds coated with microbial biomass and pectin (B), with pectin only (C) and uncoated (N). The Y-axis does not start at zero to improve the readability of the differences between treatments. The values were rounded to two decimal places to simplify presentation, in accordance with the instrument's precision.	129
Figure 54. Graph showing the Chlorophyll Content Index (CCI) of plants derived from seeds coated with microbial biomass and pectin (B), with pectin only (C) and uncoated (N). ..	130
Figure 55. Differences in root development and growth between Micro-Tom tomato seedlings treated with <i>P. granadensis</i> CT364 (left) and magnesium sulphate (right). Plants	

treated with the bacterium have greater root branching and root architecture development in the direction of the bacterial inoculum.....	131
Figure 56. Differences in root development and growth between Micro-Tom tomato seedlings treated with <i>P. granadensis</i> CT364 (left) and magnesium sulphate (right). Plants treated with the bacterium have more expanded leaves.	131
Figure 57. Differences in the colonisation of Micro-Tom tomato root tissues by <i>P. granadensis</i> CT364 after 10 (left) and 14 days (right) from treatment.	132
Figure 58. Three days after replanting the shoots into soil, it was observed that the shoots treated with the bacterium had coped better with the transplant shock, appearing more vigorous and with more expansive leaves than the control shoots.....	132
Figure 59. Details of burns and necrosis affecting the leaf blades of Micro-Tom tomatoes during anthesis.....	133
Figure 60. Comparison between the average heights of plants treated with <i>P. granadensis</i> CT364 (PG) and the control plants (MS). The Y-axis does not start at zero to improve the readability of the differences between treatments. The values were rounded to one decimal place to simplify presentation, in accordance with the instrument's precision.	134
Figure 61. Comparison between the fresh biomass (stems, leaves and flowers) of plants treated with <i>P. granadensis</i> CT364 (PG) and control plants (MS). The Y-axis does not start at zero to improve the readability of the differences between treatments. The values were rounded to two decimal places to simplify presentation, in accordance with the instrument's precision.	135
Figure 62. Comparison between the fresh biomass (stems, leaves and flowers) of plants treated with <i>P. granadensis</i> CT364 (PG) and control plants (MS). The Y-axis does not start at zero to improve the readability of the differences between treatments. The values were rounded to two decimal places to simplify presentation, in accordance with the instrument's precision.	135
Figure 63. Details of the bacterial outgrowth and fluorescence expressed by <i>P. granadensis</i> CT364 in the stems of the PG13A plant.....	136
Figure 64. Details of the fluorescence expressed by <i>P. granadensis</i> CT364 in a stem of the PG2B3 plant.	137

Figure 65. Details of the germination and contamination of Cochise wheat seeds sterilised with 3% sodium hypochlorite and placed in square Petri dishes filled with 1/2 MS supplemented with 1% sucrose.....	139
Figure 66. Details of the germination (at the top), the fungal contamination (at the bottom left) and the rot (at the bottom right) of Cochise wheat seeds sterilised with 3% sodium hypochlorite and placed in Petri dishes filled with Whatman filter paper wetted with sterile distilled water.	140
Figure 67. Details of the germination and contamination of Cochise wheat seeds sterilised with 3% sodium hypochlorite (left) and 3% sodium hypochlorite + 70% ethanol. and placed in square Petri dishes filled with 1/2 MS supplemented with 1% sucrose.....	141
Figure 68. Details of the germination of Cochise wheat seeds exposed to chlorine gas for 3 hours and 30 minutes and placed in square Petri dishes filled with 1/2 MS supplemented with 3% sucrose.....	142
Figure 69. Details of the germination and contamination of Cochise wheat seeds 17 days after sowing, following exposure to chlorine gas for 3 hours and 30 minutes and subsequent incubation in square Petri dishes containing 1/2 MS medium supplemented with 3% sucrose.	143

Abstract

There is an increasing need to enhance crop productivity while reducing agrochemical inputs to support more sustainable agricultural systems. Microorganisms represent a promising alternative to chemical pesticides and fertilisers, offering both plant protection and plant growth-promoting functions. This thesis investigates two complementary microbial systems with distinct scientific relevance: *Bacillus subtilis* ET-1 and *Pseudomonas granadensis* CT364.

The work conducted on *B. subtilis* ET-1 introduces a novel approach in the field of microbial bioproducts. Agro-industrial waste materials were successfully valorised as fermentation substrates for the production of bioactive lipopeptides, and the process was scaled up to an industrially relevant level. This optimisation yielded two functional outputs: (i) antimicrobial preparations rich in lipopeptides such as iturin effective against key phytopathogens such as *Penicillium digitatum* and *Podosphaera xanthii*; and (ii) a stable microbial biomass suitable for use as a plant biostimulant, demonstrating positive effects on basil growth.

During an international research period at Newcastle University, the colonisation ability and plant interaction of *Pseudomonas granadensis* CT364—a recently identified bacterial species—were investigated using tomato as a model system. CT364 efficiently colonised roots and aerial tissues, exhibited endophytic behaviour, and promoted favourable trends in plant growth and stress tolerance, highlighting its potential as an emerging plant-associated beneficial bacterium.

Together, these findings advance current knowledge on sustainable microbial-based strategies and demonstrate how waste valorisation, industrial-scale fermentation and multifunctional microbial traits can converge to support the development of next-generation bioinputs for environmentally friendly agriculture.

Abstract in italiano

La crescente necessità di aumentare la produttività delle colture riducendo al contempo l'impiego di agrofarmaci richiede sistemi agricoli più sostenibili. I microrganismi rappresentano un'alternativa promettente ai pesticidi e ai fertilizzanti chimici, offrendo sia funzioni di protezione delle piante sia proprietà promotrici della crescita. Questa tesi indaga due sistemi microbici complementari, caratterizzati da una distinta rilevanza scientifica: *Bacillus subtilis* ET 1 e *Pseudomonas granadensis* CT364.

Il lavoro svolto su *B. subtilis* ET 1 introduce un approccio innovativo nel campo dei bioprodotto microbici. Scarti agro-industriali sono stati efficacemente valorizzati come substrati di fermentazione per la produzione di lipopeptidi bioattivi, e il processo è stato scalato fino a un livello rilevante dal punto di vista industriale. Questa ottimizzazione ha generato due output funzionali: (i) preparati antimicrobici ricchi in lipopeptidi, come l'iturina, efficaci contro rilevanti microrganismi fitopatogeni quali *Penicillium digitatum* e *Podosphaera xanthii*; e (ii) una biomassa microbica stabile, idonea all'uso come biostimolante, che ha mostrato effetti positivi sulla crescita del basilico.

Durante un periodo di ricerca internazionale presso la Newcastle University, sono state studiate la capacità di colonizzazione e l'interazione con la pianta di *Pseudomonas granadensis* CT364—una specie batterica recentemente identificata—utilizzando il pomodoro come sistema modello. CT364 ha colonizzato in modo efficiente radici e tessuti aerei, ha mostrato un comportamento endofitico e ha favorito tendenze positive nella crescita e nella tolleranza allo stress, evidenziando il suo potenziale come nuovo batterio benefico associato alle piante.

Nel complesso, questi risultati avanzano le conoscenze sulle strategie microbiche sostenibili e dimostrano come la valorizzazione degli scarti, la fermentazione su scala industriale e i tratti microbici multifunzionali possano convergere per supportare lo sviluppo di bioinput di nuova generazione per un'agricoltura più rispettosa dell'ambiente.

1. Introduction

1.1 Reference agronomic context

Issues related to the protection of the environment, as well as human and animal health, have become increasingly important in recent decades. Groundwater pollution, soil degradation, biodiversity loss, and rising global temperatures represent a pressing and growing threat to the health of our planet (DeClerck et al., 2023; FAO, 2019). Human activities and agricultural practices, particularly the excessive exploitation of soils, remain major drivers of natural ecosystem alteration.

The onset of such problems occurred in the post-World War II period between 1940 and 1960, when the Green Revolution, an innovative approach to issues in the primary sector, developed.

Through the creation of high-yield plant varieties via genetic improvement programmes and the extensive use of chemical fertilisers and synthetic plant protection products, it was possible to increase agricultural production to feed the growing global population significantly.

However, over time, it has become evident that the agricultural practices promoted during the Green Revolution have also generated high environmental costs, with negative consequences for both human and animal health. For example, the extensive use of chemical products has caused groundwater pollution, soil degradation and the development of resistance in phytopathogenic microorganisms. Furthermore, the increase in monoculture in response to the need to raise production has led to a reduction in biological and genetic variability.

In the 1960s, thanks to a growing awareness of environmental protection and health issues, an environmentalist movement developed, among whose proponents was Rachel Carson, who in 1962 wrote the essay *Silent Spring*. This is a pioneering manifesto of the environmentalist movement, highlighting the irreversible damage caused by the use of DDT (dichloro-diphenyl-trichloroethane, a chlorinated organic compound with insecticidal action) and pesticides, both to the environment and to humans.

According to the FAO report “The State of the World’s Land and Water Resources for Food and Agriculture – Systems at Breaking Point” (FAO, 2021), soil degradation caused by

human activity already affects 34% of agricultural land worldwide, threatening food security, given that approximately 95% of food production depends on soil.

More recently, the FAO flagship report “The State of the World’s Land and Water Resources for Food and Agriculture 2025” (FAO, 2025) further emphasises that meeting the food demand of a global population expected to reach nearly 10 billion by 2050 will require a substantial increase in agricultural productivity, while simultaneously reducing pressure on soil and water resources. This dual challenge highlights the urgent need for innovative and sustainable agronomic strategies capable of reconciling productivity, environmental protection, and long-term ecosystem resilience.

The agricultural sector is threatened by ongoing climate change and the increasing incidence of extreme weather events, which will have negative effects on production and the availability of water resources (Anwar et al., 2013).

While the Green Revolution successfully addressed food shortages through genetic improvement and chemical inputs, its long-term environmental and ecological costs have become increasingly evident. As a consequence, contemporary agriculture is now moving towards a “Green Revolution 2.0”, in which productivity gains must be achieved through environmentally sustainable practices that safeguard human and ecosystem health. Within this paradigm shift, Nature-based Solutions are gaining increasing attention as viable alternatives to input-intensive conventional agriculture (Seddon et al., 2021).

This transition towards more sustainable agricultural systems is strongly reflected in European Union policies, which aim to reduce the environmental impact of crop protection practices while maintaining crop productivity and food safety.

Directive 2009/128/EC of the European Commission (EU, 2009/128/EC.) establishes a regulatory framework for the sustainable use of pesticides by promoting integrated pest management (IPM) and encouraging the adoption of alternative, non-chemical control strategies, thereby reducing reliance on synthetic chemical products. Within this framework, biological control represents a core IPM principle, aiming to maintain harmful organisms below economic and ecological damage thresholds while minimising the use of synthetic plant protection products.

The application of biological control in agriculture dates back to the second half of the seventeenth century, when early studies by naturalists such as Redi and Vallisnieri revealed interactions between entomophagous and phytophagous insects (Roncalli Amici, 2001). In Italy, biological control developed substantially in the early twentieth century through the work of Antonio Berlese and Filippo Silvestri, notably on *Rodolia cardinalis* (Mulsant, 1850) for the control of *Icerya purchasi* (Maskell, 1878) and on the identification of natural enemies of the olive fly *Bactrocera oleae* (Rossi, 1790) (Vacante, 2011). From the 1980s onward, growing attention to biodiversity and ecosystem conservation has further reinforced the relevance of biological control strategies. Among the most widely adopted biological control agents is *Bacillus thuringiensis* (Berliner, 1915), a soil bacterium producing δ -endotoxins (Cry toxins) that disrupt the digestive tract of target insect pests, particularly Diptera and Lepidoptera.

1.2 BCAs and BAs as key factors for biological control

Biological control can also be useful against plant diseases caused by phytopathogens. Disease is defined as an alteration of normal physiological and productive functions caused by biotic and abiotic factors. Its development results from the interaction among the host plant, the environment—including both abiotic conditions and cultivation practices—and the pathogen, collectively known as the disease triangle (Francl, 2001). Crop protection strategies aim to prevent or reduce economic losses by targeting one or more components of this interaction. Biological control encompasses a set of predominantly preventive approaches designed to limit pathogen populations by exploiting naturally occurring antagonistic interactions or by modifying environmental conditions and/or host plant responses.

Within this regulatory framework, Integrated Pest Management (IPM) represents a cornerstone approach, promoting the rational use of plant protection products and prioritising preventive and non-chemical strategies whenever possible.

In line with this objective, the European Commission promotes the use of Plant Protection Products (PPPs), defined as formulations containing one or more active substances designed to protect plants from damage caused by weeds, insects, and pathogens; these active substances may include microorganisms or compounds derived from them (European Commission, 2009).

More specifically, the European legislation (Article 14 of Directive 2009/128/EC) recognises not only biological control agents (BCAs), but also biostimulants (BAs) as key tools to reduce dependence on synthetic chemical inputs while supporting plant health and productivity (“Directive 2009/128/EC,” n.d.).

BCAs, including fungi from the genera *Trichoderma*, *Penicillium* and *Phoma*, integrate into the host–pathogen–environment system and influence disease development (Burpee, 1990) by reducing plant susceptibility to diseases through multiple mechanisms, such as parasitism, antibiosis, and competition for space and nutrients with pathogenic organisms, thereby limiting pathogen colonisation of plant tissues. Additionally, BCAs may boost plant defence by activating induced resistance mechanisms (Elnahal et al., 2022; Harman et al., 2004; Wei et al., 2020).

Among these, Induced Systemic Resistance (ISR) is triggered by the recognition between the host plant and beneficial microorganisms and is mainly mediated by jasmonic acid and ethylene signalling pathways, resulting in a systemic defensive state against non-pathogenic organisms. Plants can also activate Systemic Acquired Resistance (SAR), a salicylic acid–dependent response induced by pathogen attack and associated elicitors, which provides long-lasting, broad-spectrum resistance and decreases disease susceptibility upon subsequent infections. Although ISR and SAR depend on different signalling pathways, they are not mutually exclusive and may coexist due to crosstalk between their underlying hormonal networks.

On the other hand, Regulation (EU) 2019/1009 defines a biostimulant as any product that stimulates plant nutritional processes independently of its nutrient content, aiming to improve nutrient use efficiency, tolerance to abiotic stress, qualitative traits, or nutrient availability in the soil or rhizosphere.

BA are organisms that stimulate the nutritional processes of the plant while improving nutrient use efficiency, tolerance to abiotic stress, qualitative characteristics, and availability of nutrients confined to the soil or rhizosphere.

Among the wide range of biological inputs compatible with IPM principles, Plant Growth Promoting Rhizobacteria (PGPR), such as *Pseudomonas* spp., *Bacillus* spp., and *Arthrobacter* spp. (Fira et al., 2018; Ju et al., 2019; Woo et al., 2020), are of particular interest

due to their dual functionality. These microorganisms can simultaneously enhance plant growth and nutrient use efficiency while contributing to disease suppression and stress tolerance, thereby integrating biostimulant and biocontrol functions within a single biological strategy.

1.3 PGPR for plant health and environmental protection

From this perspective, PGPR are particularly interesting as they can, through direct application or via their secondary metabolites, exert multiple beneficial effects on plant health, making them viable alternatives to pesticides and synthetic fertilisers. PGPR colonise plant roots and establish mutualistic relationships with their hosts, contributing to plant growth, nutrition and resilience to stress (Elnahal et al., 2022; Fira et al., 2018; Khan et al., 2021; Stamenković et al., 2018).

The colonisation of the rhizosphere by beneficial microorganisms is a crucial process for improving plant performance and health (Ruiz-Muñoz et al., 2025). The rhizosphere, defined as the soil zone directly influenced by root exudates, is a highly dynamic and competitive environment shaped by carbon- and nitrogen-rich compounds released by plant roots, which structure the rhizomicrobiome and mediate diverse interactions ranging from mutualistic to pathogenic. Many rhizosphere-associated microorganisms positively affect plant health by improving nutrient acquisition, suppressing pathogens, and inducing plant defence responses (Guan et al., 2024; Pranav et al., 2024; Ruiz-Muñoz et al., 2025).

Plant–microbe interactions have evolved over millions of years within complex environments, resulting in highly specific relationships influenced by soil characteristics, plant developmental stage, and host genotype. These interactions are often mediated by specialised metabolites that function as signalling molecules or defensive compounds, facilitating close microbial associations with plant roots (Pranav et al., 2024). Among these interactions, some microorganisms can overcome plant surface barriers and establish stable, asymptomatic colonisation within internal tissues (Guan et al., 2024). While most PGPR exert their beneficial effects in the rhizosphere, a subset of these microorganisms can form more intimate associations with the host by colonising internal plant tissues. Such microorganisms are referred to as endophytes—ubiquitous endosymbiotic organisms transmitted either vertically or horizontally that inhabit plant tissues for most of their life cycle without causing disease. By establishing mutualistic

relationships with their host plants, many endophytes enhance plant growth and nutritional status and reduce susceptibility to biotic and abiotic stresses, thereby exerting both biostimulant and biocontrol functions. This interaction is based on reciprocal benefits, whereby endophytes acquire carbon compounds from the host, while plants gain improved stress tolerance and nutrient availability. However, endophyte–plant relationships are context-dependent, and endophytes may shift towards pathogenic or saprophytic behaviour under host stress conditions (Barra-Bucarei et al., 2020; Tall and Meyling, 2018).

1.4 Effects of PGPR on Plant Growth and Health

Experimental research has consistently demonstrated that PGPR can positively influence plant health both by enhancing growth and by suppressing pathogens under controlled and field conditions. For instance, native PGPR isolates, including *Pseudomonas* spp., *Enterobacter* spp., *Acinetobacter* spp., *Stenotrophomonas* spp., *Lysinibacillus* spp., and *Bacillus* spp. species isolated from alfalfa (*Medicago sativa* L., 1753) rhizospheres significantly increased plant height, stem diameter, leaf area, shoot dry weight and root fresh weight in tomato (*Solanum lycopersicum* L.) and watermelon (*Citrullus lanatus* (Thunb.) Matsum. and Nakai) compared to non-inoculated controls, indicating direct growth-promoting effects of PGPR application on horticultural crops. These effects were associated with the presence of multiple plant-growth traits such as phosphate solubilisation, indole-3-acetic acid (IAA) synthesis, siderophore production, and ACC deaminase activity, which facilitate nutrient uptake and stress mitigation in plants (Ünlü et al., 2024).

In perennial crops, field applications of a consortium of *Bacillus subtilis* (Ehrenberg, 1835) Cohn, 1872, *Bacillus amyloliquefaciens* (Priest et al., 1987), and *Pseudomonas monteilii* (Elomari, et al. 1997) improved strawberry (*Fragaria × ananassa* cultivar Hood) quality traits, including total soluble solids and volatile compound profiles, and reshaped the rhizosphere microbiome in ways consistent with enhanced nutrient cycling and plant metabolic activity, further highlighting the biostimulant potential of PGPR under real agricultural conditions (Nam et al., 2023).

In addition to biostimulation, PGPR have been shown to modulate plant defence responses. In basil (*Ocimum basilicum* L.), inoculation with *Bacillus amyloliquefaciens* GB03 altered phenolic biosynthesis pathways and increased defence-associated hormone levels in plants exposed to herbivory by *Spodoptera frugiperda*, indicating that PGPR can enhance

secondary metabolism and defence signalling, which may contribute to reduced pest damage and improved resilience to biotic stressors (Palermo et al., 2025).

Despite the increasing evidence supporting PGPR effectiveness, there are still few comparative studies examining their dual roles as biostimulants and biocontrol agents under controlled conditions.

1.5 Application Methods of PGPR

PGPR can be delivered to crops through various practical application methods aimed at ensuring effective colonisation of the rhizosphere and maximising their beneficial effects. A common approach is seed inoculation or seed coating, where seeds are treated with a PGPR suspension before sowing, promoting early root colonisation and enhancing seedling vigour and nutrient uptake throughout plant development (seed inoculation promotes early microbiome establishment) (Yang et al., 2024).

Soil inoculation or soil drenching involves introducing PGPR directly into the growing medium at sowing or transplanting; this method enhances nutrient availability, supports root development, and can increase biomass and nutrient uptake under field conditions (Yang et al., 2024).

In environments where immediate microbial action is needed, foliar sprays of PGPR suspensions can induce systemic responses in the plant and contribute to disease suppression, as demonstrated in pea, where foliar application of *Pseudomonas* strains increased phenolic compounds and reduced powdery mildew development (Bahadur et al., 2007).

Root dips, where seedlings' roots are immersed in PGPR solutions before planting, are another effective delivery method that can improve root colonisation and subsequent plant growth, particularly in transplant systems (Yang et al., 2024). The choice of application technique depends on crop type, environmental conditions, and the target outcomes—whether enhancing growth, increasing nutrient uptake, or improving resilience to biotic and abiotic stressors.

Currently, most commercialised PGPR are from the Gram-positive *Bacillus* genus or the Gram-negative *Pseudomonas* genus. Notable biocontrol species of *Bacillus* include *Bacillus velezensis* (Ruiz-García et al., 2005), *Bacillus amyloliquefaciens*, and *Bacillus subtilis*, while important *Pseudomonas* species include *Pseudomonas fluorescens*, *Pseudomonas putida*

(Trevisan, 1889) (Wang et al., 2024), and the recently identified rhizobacterium *Pseudomonas granadensis* (Carro et al., 2016).

In this framework, the present PhD thesis aims to investigate selected PGPR strains, such as *Bacillus subtilis* and *Pseudomonas granadensis* as multifunctional biological inputs, evaluating their biostimulant and biocontrol potential in improving resistance to biotic stress and plant growth under controlled experimental conditions.

1.6 *Bacillus subtilis* for plant health

Bacillus subtilis is a long-term studied and generally recognised as safe microorganism (Errington and van der Aa, 2020; Su et al., 2020). Due to its strong metabolism, which enables it to grow easily on low-cost substrates, *B. subtilis* has a wide range of industrial applications (Figure 1). These include the production of biosurfactants and biopolymers, as well as their use in the food industry for the processing of food waste (Al-Dhabi et al., 2020; Ciurko et al., 2022; Das and Kumar, 2018; Hassan et al., 2019; Mok et al., 2019; Peña-Jurado et al., 2019; Rathika et al., 2019).

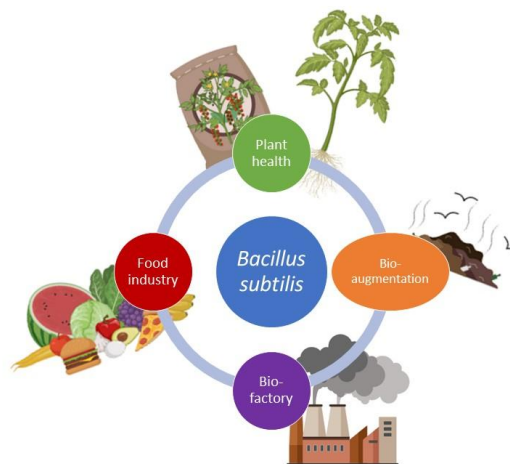


Figure 1. Examples of *B. subtilis* application. Created by the author.

Moreover, *B. subtilis* is useful for bio-augmentation of nitrogen removal and degradation of tannery effluents in wastewater treatment, as confirmed by Rahimi et al. (2020) and Arasu and Al-Dhabi (2024), respectively.

From an agricultural point of view, *B. subtilis* is particularly interesting because of its ability to be both a BCA and a BA. For instance, the lipopeptides (especially iturin, fengycin and surfactin) produced by *Bacillus* spp. Showed antagonistic activity against several agronomically important pathogens (Ambrico and Trupo, 2017; Li et al., 2019; Trupo et al., 2023; Wang et al., 2020.). Also, the bacterium can solubilise soil phosphorus, promote nitrogen fixation, and enhance biotic and abiotic stress tolerance in plant hosts (Hashem et al., 2019).

1.6.1 *Bacillus subtilis* features

B. subtilis is a non-pathogenic, rod-shaped (2-6 μm in length and just under 1 μm in diameter), endospore-forming, gram-positive bacterium belonging to the Firmicutes phylum. The bacterium has an aerobic or facultatively anaerobic metabolism and it is exceptionally ubiquitous, since it can inhabit a large variety of ecological niches, such as soil, water, and air, as well as plants surfaces and rhizosphere, and the gastrointestinal tract of animals. Also, *B. subtilis* can live in many extreme environments.

As proof of its great adaptability, *B. subtilis* strain ZB was isolated from a Tamil Nadu saltpan by Arasu and Al-Dhabi in 2024, from marine soil sediment in Saudi Arabia by Al-Dhabi et al. in 2020 (Al-Dhabi et al., 2020) and from a hydrocarbon-contaminated soil near the Tunisian Chemical Group of Gabes by Minif et al. in 2022. Moreover, *B. subtilis* strains have been found in the plant rhizosphere in various locations across the Qinghai-Tibetan Plateau by Wu et al. (2019). This plateau is the highest in the world, with an average altitude of 4000 m above sea level, and an annual average temperature range of 1.7°C to 9.8°C.

The ideal temperature for the growth of the *B. subtilis* cells is between 30-35°C, which allows them to double their population in as little as 20 minutes. In conditions of nutrient shortage (Figure 2), the cells undergo a complex two-cell differentiation process, leading to the formation of an endospore that is released by the lysis of the mother cell. The vegetative cells are capable of movement and can also form biofilms and "fruiting bodies" that contain spores.

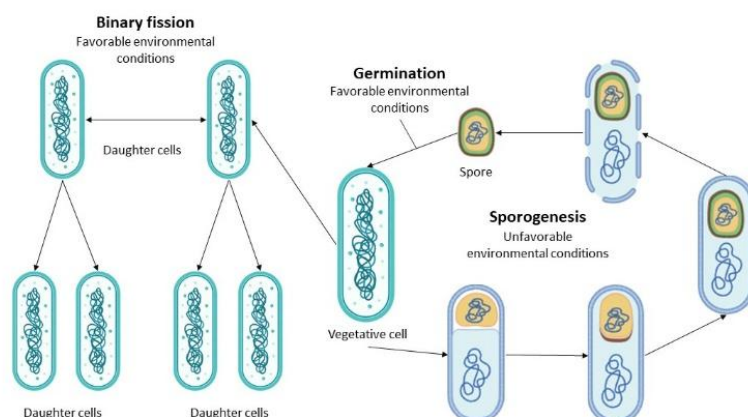


Figure 2. Schematic representation of the life cycle of *B. subtilis*. Image created by the author using graphic components designed in BioRender.com.

The spore structure consists of multiple layers that protect the central core which contains spore DNA, ribosomes, metabolic and biosynthetic enzymes, and several spore-specific components. It has low water content, accounting for only 35% of wet weight. *B. subtilis* spores are easy to purify and shaped like an ellipse, with a length of 0.8 to 1.2 μm (Zhang et al., 2020).

Spores are metabolically inactive, do not express any genes, and are highly resistant to various environmental stresses, such as high temperature, radiation, desiccation, toxic chemicals, and extreme pH levels. Suppose the necessary nutrients, specifically L-alanine, are available. In that case, the spores of *B. subtilis* can awaken from their dormant state through a process called germination and resume their vegetative growth through a process called outgrowth (Cho and Chung, 2020; Su et al., 2020).

Vegetative cells can exhibit survival or adapting strategies by forming morphologically distinct colonies, as observed by Ambrico et al. (2019). The study demonstrated that the *B. subtilis* strain ET-1 displays at least three different colony morphologies, referred to as Rough, Smooth, and Mucoid morphotypes (R-, S-, and M-form). The phenotypic heterogeneity of these morphotypes has advantageous properties for the survival of microbial populations under various stress conditions.

1.6.2 B. subtilis- plants interaction

Thanks to *B. subtilis* ability to live and to thrive with plants, the interest in the application of the microorganism in the primary sector is increasing. In fact, it can be found either on the surface of plants (as an epiphyte) or in the rhizosphere, and it is usually isolated from decaying plant matter such as hay (Errington and van der Aa, 2020).

For instance, strains of *B. subtilis* have been isolated from winter wheat (*Triticum aestivum* L.) (Sidorova et al., 2020) and banana plant (*Musa* AAA cv. Valery) rhizosphere (Franco-Sierra et al., 2020) and from hot pepper (*Capsicum frutescens* L.) leaves (Wang et al., 2020.).

The rhizosphere is a thin layer of soil surrounding plant roots where crucial biological, physiological, and chemical activities occur. Bacteria in the rhizosphere are the most representative microorganisms, with a density of around 10^9 cells per gram of plant root tissue. The plant actively recruits beneficial bacteria through root exudates (Elnahal et al., 2022; Hashem et al., 2019; Nordgaard et al., 2022).

Usually, the colonisation of plant roots by bacteria is a crucial step in the relationship between microbes and plants. The success of this process depends on several factors, including the characteristics of the bacteria, their motility, and the formation of biofilms. Chemotaxis is crucial for *B. subtilis* to locate roots, while biofilm production is helpful for long-term colonisation of the rhizosphere (Figure 3) (Blake et al., 2021; Hashem et al., 2019).

In particular, the bacterium can colonise plant roots thanks to its chemoreceptors McpB, McpC, and TlpC which sense plant signals during attraction. Intercellular signalling during attachment involves the cyclic di- di-adenylate monophosphate (c-di-AMP) permeases YcnB and YhcA. Kinases KinC and KinD detect plant polysaccharides and l-malic acid produced by plants, which leads to matrix production. The binding of plant cell wall polysaccharides to an unknown receptor also results in the upregulation of galactan (gan operon), which can lead to exopolysaccharide production. Biofilm formation occurs with the digestion of galactan and the production of matrix components (Arnaouteli et al., 2021).

B. subtilis colonising the roots of plants is beneficial for both the bacterium and the host plant. The bacterium receives complex carbohydrates that are essential for its nutrition, while

the host plant receives bacterial compounds and activities that promote its growth and protect it from biotic and abiotic stress (Hashem et al., 2019).

Bacillus spp. strains can suppress and inhibit the growth of plant pathogens. This happens either indirectly, by competing with the pathogens for a niche or nutrient requirements, or directly by producing various lipopeptide compounds like iturin, surfactin and fengycin, which are effective against many plant pathogens. Additionally, they are capable of inducing systemic resistance in plants by producing volatile substances such as alcohols, aldehydes, aromatics, sulfides and ketones. These lipopeptides and volatiles can stimulate the expression of genes coding for pathogenesis-related proteins and other defence-related proteins in the plant hosts by activating jasmonic acid, salicylic acid or ethylene signalling pathways (Dimkić et al., 2022).

Evidence of these abilities is given by Franco-Sierra et al. (2020) study. The scientists sequenced the genome of *B. subtilis* strain EA-CB0575 and identified genes involved in the production of various compounds such as indoles, siderophores, lipopeptides, volatile compounds, phytase, bacilibactin, and nitrogenase. Furthermore, they evaluated that this bacterium was capable of increasing the total dry weight of tomato plants (*Solanum lycopersicum* L.) by 34.60% when compared to non-inoculated plants in a greenhouse environment.

In a 2022 experiment on cucumber (*Cucumis sativus* L.) roots, Samaras et al. (2022) discovered that the *B. subtilis* strain MBI600 activates genes that are critical to ISR and SAR signalling. Additionally, plant genes linked to phytohormone production and nutrient availability exhibited an upregulation pattern, which explains the growth promotion.

In a study conducted by Jabborova et al. in 2021 on ginger (*Zingiber officinale* Roscoe, 1807), it was found that *B. subtilis* strain L2 inoculation had a positive effect on the plant health. The study revealed that the inoculation increased the plant height, leaf length, number of leaves per plant, leaf width, and chlorophyll content.

Furthermore, *B. subtilis* has been found to improve plants' ability to resist abiotic stress, according to a study by Gowtham et al. in 2018. The study revealed that tomato plants (*Solanum lycopersicum* L.) treated with the *B. subtilis* strain Rhizo SF 48 exhibited significantly improved growth even when exposed to varying levels of drought stress,

compared to plants in the control group that were exposed to stress. Moreover, as reported by Woo et al. in a 2020 study (Woo et al., 2020), the application of *B. subtilis* strain GOT9, led to the enhancement of drought and salt stress tolerance and improved lateral root growth in *Arabidopsis thaliana* (L.) Heynh. Finally, *B. subtilis* GOT9 enhanced tolerance against drought and salt stresses and up-regulation of drought-inducible genes in *Brassica campestris* L., a closely related crop to *Arabidopsis*.

1.6.3 *B. subtilis*: a source of antimicrobial lipopeptides

Bacteria belonging to the *Bacillus* genus exhibit antimicrobial activity by producing metabolites, which are composed mainly of molecules from the polypeptide and aminoglycoside series. These metabolites are classified as antibiotics since they can impede the growth and development of harmful organisms. The number of biologically active substances produced by *Bacillus* spp. bacteria can vary depending on the specific strain, ranging from 50 to 200 (Iqbal et al., 2023; Sidorova et al., 2020).

In fact, *B. subtilis* has approximately 4 to 5% of its whole genome dedicated to the synthesis of secondary metabolites. As the plant microbiome is a highly competitive niche, these metabolites allow bacteria to compete against other microorganisms in their natural environment and establish beneficial host-associated communities (Dimkić et al., 2022; Fira et al., 2018; Iqbal et al., 2023; Maan et al., 2021).

In particular, some of the best-known biologically active plant protection compounds are non-ribosomally synthesised lipopeptides, which are structurally composed of cyclic peptides linked to a fatty acid chain (Yaseen et al., 2017). The synthesis of different lipopeptides involves shared regulatory and cross-linked components among synthetic pathways. However, it includes three key steps: synthesis of side chain fatty acids, activation and loading of fatty acids, and extension of the peptide chain (Ongena and Jacques, 2008).

The antimicrobial activity of lipopeptides is determined by their amphiphilic nature and their capacity to interact with the cell membrane of target organisms (Fira et al., 2018). Lipopeptides action (Figure 3) involves physical damage to the cell envelope of pathogens, resulting in permeability due to disruption and formation of pores on the plasma membrane with cytoplasm leakage, hyphae death or inhibition of spore germination inhibition (Crouzet et al., 2020; Dimkić et al., 2022; Tran et al., 2022).

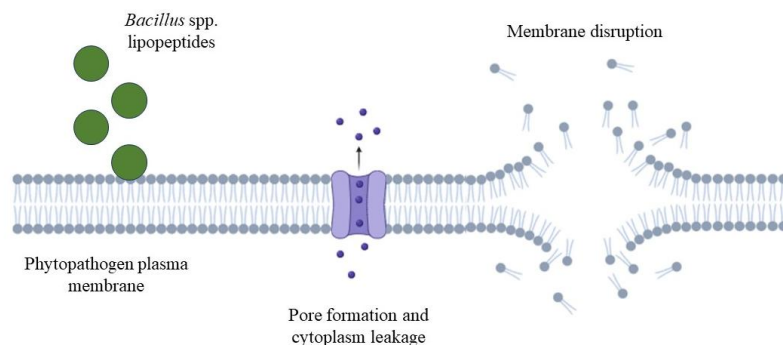


Figure 3. Mechanisms of action of *Bacillus* spp. lipopeptides on the plasma membrane of plant pathogens. Image created by the author using graphic components designed in BioRender.com.

Lipopeptides not only have an antimicrobial activity, but they also induce many other effects such as tumour inhibition, oil recovery and bioremediation of heavy metals, etc. (Pilz et al., 2023; Yang et al., n.d.). Like other biosurfactants, lipopeptides show various desirable characteristics such as biodegradability, low toxicity, high selectivity, high activity under extreme temperature, pH and salinity conditions (Bouassida et al., 2023a; Domínguez Rivera et al., 2019; Venkataraman et al., 2022). In 2021, Umar et al. (Umar et al., 2021) produced lipopeptides from *B. subtilis* SNW3 that showed excellent surfactant properties and high stability across a wide range of pH (1–11), salinity (1–8%), temperature (20–121°C), and even after autoclaving (Bouassida et al., 2023a).

Most of the cyclic lipopeptides from *Bacillus* are classified into three families based on their peptide scaffold - surfactin, iturin, and fengycin (Figure 4). Surfactins contain a β -hydroxy fatty acid in their ring structure, while iturins have a β -amino fatty acid, and fengycins are characterised by a terminal amide-linked β -hydroxy fatty acid (Iqbal et al., 2023; Kaspar et al., 2019).

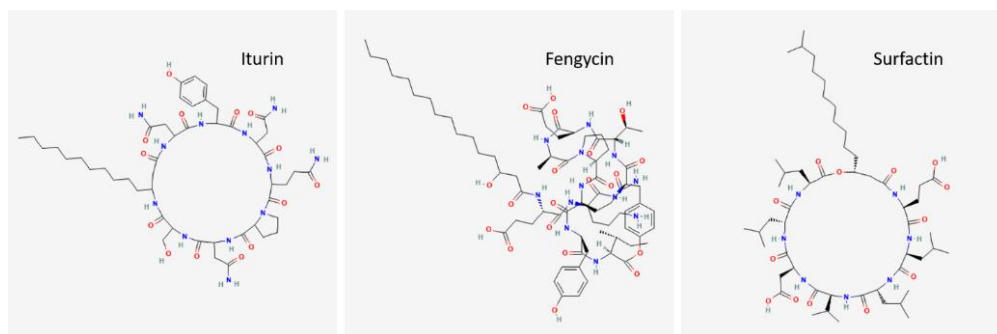


Figure 4. Characteristic structures of iturin, fengycin and surfactin. Image created by the author based on data from the PubChem Compound Database (PubChem, n.d.).

Scientific interest in the *Bacillus*-derived lipopeptides iturin, fengycin and surfactin has markedly increased over the last decade. Bibliographic surveys conducted on Scopus (Elsevier, accessed January 2026), indicate a steady growth in publications since the mid-2010s, reflecting the expanding relevance of these metabolites in agricultural, biological and biomedical research.

The majority of studies fall within the subject areas of Biochemistry, Genetics and Molecular Biology, Agricultural and Biological Sciences, and Microbiology, with China, India and the United States emerging as the most active contributors. Among the three compounds, surfactin consistently appears as the most extensively investigated lipopeptide, likely due to its broad spectrum of physicochemical and biological activities extending beyond plant–microbe interactions.

Several studies have demonstrated that the biosynthesis of *Bacillus* lipopeptides is closely associated with the onset of sporulation and nutrient limitation. In particular, Ambrico and Trupo 2017 study showed that in *Bacillus subtilis* strain ET-1, the production of Iturin A coincides with the late exponential phase of growth, under conditions of nutrient depletion in batch culture, highlighting the tight regulatory link between secondary metabolism and sporulation.

In agriculture field, various reports have shown that lipopeptides produced by *B. subtilis* could represent a valid alternative to agrochemicals because of their antagonistic activity against several agronomically-important fungal pathogens, such as *Botrytis cinerea* (Pers., 1794) and *Penicillium digitatum* ((Pers.) Sacc., 1881), *Phytophthora infestans* ((Mont.) de

Bary), and *Alternaria alternata* (Fr.) Keissl., 1912 (Ambrico and Trupo, 2017; Malik et al., 2024; Wang et al. 2020).

Table 1 presents a list of the most noteworthy studies conducted over the last 5 years that examine the effectiveness of lipopeptides in fighting off pathogens. As can be seen, there are only a limited number of articles that focus on the antibiotic capabilities of lipopeptides, compared to all the literature on the three lipopeptides. While most studies on the anti-pathogenic effects of lipopeptides are conducted in a laboratory, some experiments performed in a glasshouse or open-field setting have demonstrated their effectiveness in combating significant plant pathogens. Li et al. conducted a study in 2019 which demonstrated that fengycin and surfactin produced by *B. subtilis* GLB191 were effective against the biotrophic oomycete *Plasmopara viticola* (Berk. and M.A. Curtis) Berl. and De Toni, 1888, the causal agent of grapevine downy mildew. The study also showed that the activity was due to both a direct effect against the pathogen and stimulation of the grapevine plant defences.

Table 1. Summary of the studies carried out on the antipathogenic action of lipopeptides produced by different strains of *B. subtilis* and other microorganisms on different plant hosts.

Lipopeptide	Microorganism	Phytopathogen	Host plant	Sperimentation level	Authors
Fengycin	<i>B. subtilis</i> ZD01	<i>Alternaria solani</i>	<i>Solanum tuberosum</i> L.	Laboratory and greenhouse	Zhang et al. (2022)
Fengycin/surfactin and mycosubtilin/surfactin mixtures	<i>B. subtilis</i> ATCC 21332	<i>Venturia inaequalis</i>	<i>Malus domestica</i> (Suckow) Borkh., 1803	Open-field	Leconte et al. (2022)
Fengycin and Surfactin	<i>B. subtilis</i> GLB191 mutant	<i>Plasmopara viticola</i>	<i>Vitis vinifera</i> L. cv. Marselan (Cabernet sau-vignon × Grenache)	Greenhouse	Li et al. (2019)

Gageopeptides A–D and gageotetrin B	<i>B. subtilis</i> 109GGC020	<i>Magnaporthe oryzae</i> <i>Triticum</i>	-	Laboratory	Chakrab orty et al. (2020)
Generic lipopeptides	<i>B. subtilis</i> XZ16- 1	<i>Blumeria graminis</i> f. sp. <i>tritici</i>	<i>Triticum</i> aestivum L. cv. Yangmai 23	Laboratory	(Yi et al. (2022)
Iturin A	<i>B. subtilis</i> ET-1	<i>Podosphaera xanthii</i>	<i>Cucumis</i> <i>melo</i> L. cv. Amarillo Oro	Greenhouse and open-field	Trupo et al. (2023)
Iturin A	<i>Bacillus</i> <i>velezensis</i>	<i>Aspergillus fumigatus</i>	-	Laboratory	Xiong et al. (2022)
Iturin A	<i>Bacillus</i> <i>amyloliquefaciens</i> LZ-5	<i>Rhizopus stolonifer</i>	<i>Solanum</i> <i>lycopersic</i> <i>um</i> L. var. cerasif orme	Laboratory	Jiang et al. (2021)
Iturin A	<i>B. subtilis</i> WL-2	<i>Phytophthora</i> <i>infestans</i>	<i>Solanum</i> <i>tuberosum</i> L. cv. Bintje	Laboratory	Wang et al. (2020)
Iturin A	<i>B. subtilis</i> ET-1	<i>Botrytis cinerea</i> and <i>Penicillium digitatum</i>	<i>Fragaria</i> L. cv. Sabrosa and <i>Citrus</i> <i>limon</i> cv. Zagara Bianca	Laboratory	Ambrico and Trupo, (2017)
Iturin, fengycin, surfactin	<i>Bacillus</i> <i>altitudinis</i> TM22A	<i>Alternaria alternata</i>	<i>S.</i> <i>lycopersic</i> <i>um</i> L.	Laboratory	Malik et al. (2024)
Iturin, fengycin, surfactin	<i>B. subtilis</i> T3, T4, T5, and T6	<i>A. alternata</i>	-	Laboratory	Harish et al., (2023)

Iturin, fengycin, surfactin	<i>B. subtilis</i> UL-1	<i>Fusarium solani</i>	-	Laboratory	(Santos- Lima et al., 2023)
Iturin, fengycin, surfactin	<i>B. subtilis</i> CtpxS2-1	<i>Colletotrichum</i> <i>acutatum</i>	<i>Lupinus</i> <i>mutabilis</i> (Sweet)	Laboratory	(Yáñez- Mendizá bal et al., 2023)
Iturin, fengycin, surfactin	<i>B. subtilis</i> AKP	<i>Colletotrichum</i> <i>capsici</i>	<i>Capsicum</i> <i>annuum</i> L	Laboratory	(Kumar et al., 2021)
Surfactin	<i>B. subtilis</i> KLP2015	<i>Mucor</i> spp. and <i>Aspergillus niger</i>	<i>C. annuum</i> L.	Laboratory	(Meena et al., 2020)

Leconte et al. (2022) demonstrated that lipopeptides can work synergistically against phytopathogens. *In vivo* open field tests revealed that mixtures of fengycin/surfactin and mycosubtilin/surfactin are effective at reducing the incidence of apple scab caused by *Venturia inaequalis* ((Cooke) Wint). In fact, both mixtures showed a 70% reduction in apple scab incidence.

1.6.4 Industrial lipopeptides production

To utilise lipopeptides in industrial, medical, pharmaceutical and agricultural applications, they need to be produced through fermentation, followed by downstream isolation and purification. However, these steps pose significant challenges. Therefore, considerable efforts have been directed towards improving the fermentation process, which is a crucial step in the overall production (Beltran-Gracia et al., 2017).

As shown in Table 2, lipopeptides can be produced industrially through two methods: submerged fermentation (SmF) and solid-state fermentation (SSF). SmF is used for producing a variety of products, such as wine, beer, and even the cultivation of animal and plant cell cultures for biomedical applications. This technique is generally used in the synthesis of yeast and bacterial biosurfactants in controlled bioreactors (Sundaram et al., 2024).

Table 2. Summary of the fermentation processes applied for the production of compounds using *B. subtilis* and other microorganisms.

Production process	Substrate	Microorganism	Product	Yields converted in mg/L	Auathors
SSF	Cow dung	<i>B. subtilis</i> ZB	Protease	-	Arasu and Al-Dhabi (2024)
SSF over SmF	Aleppo pine waste and confectionery effluent	<i>B. subtilis</i> SPB1	Biosurfactants	SSF: 27590 ± 1.63 mg/L SmF: 17160 ± 0.91 mg/L	Bouassida et al. (2023b)
SmF	High Medium Broth	<i>B. subtilis</i> ET-1	Iturin A	396.86 mg/L	Trupo et al. (2023)
SmF	Defatted soy flour and molasses	<i>B. subtilis</i> CtpxS2-1	Iturin, fengycin, and surfactin	-	Yáñez-Mendizábal et al. (2023)
SmF	Sunflower and rapeseed cakes	<i>B. subtilis</i> #309	Surfactin	1190 ± 0.03 and 1450 ± 0.09 mg/L	Ciurko et al. (2022)
SSF	Chickpeas	<i>B. subtilis</i> lwo	Protease	-	Li and Wang, (2021)
SSF	Corn cobs, olive mill, wheat bran, rice straw, rice bran and sorghum	<i>Aspergillus pseudocaelatus</i> MG772677 and <i>Trichoderma gamsii</i> KX685665	Antioxidants and antimicrobial agents	-	Sadik et al. (2021)
SmF	White beans powder, waste frying oil and urea	<i>B. subtilis</i> SNW3	Lipopeptides	1170 mg/L	Umar et al. (2021)

SSF	Date molasses	<i>B. subtilis</i> Al-Dhabi-130	Biosurfactant	-	Al-Dhabi et al. (2020)
SSF	Wheat bran, starch and yeast	<i>B. subtilis</i> D19	Amylase	-	Almana et al. (2020)
SSF	Corn gluten meal	<i>B. subtilis</i> MTCC5480	Bioactive peptides	369400 mg/L	Jiang et al. (2020)
SmF	Bio surfactant production medium	<i>Bacillus amyloliquefaciens</i> SAS-1 and <i>B. subtilis</i> BR-15	Lipopeptides	2080 and 2400 mg/L respectively	Sharma et al. (2020)
SmF	Rice bran	<i>B. subtilis</i> Azhar	Polyhydroxybutyrate	310 mg/L	Hassan et al. (2019)
SmF	Cheese whey and urea	<i>B. subtilis</i> EPAH18	Poly (3-hydroxybutyrate)	540 mg/L	Peña-Jurado et al. (2019)
SmF	Bagasse and potato peels	<i>Pseudomonas azotoformans</i> AJ15	Biosurfactant	-	Das and Kumar (2018)
SmF	Pre-treated sugarcane molasses	<i>B. subtilis</i> RS1	Polyhydroxyalkanoates	2010 ± 0.09 mg/L	Rathika et al. (2018)
SmF	Landy medium	<i>B. subtilis</i> BBG208 genetically modified	Fengycin and Surfactin	768 mg/L	Yaseen et al. (2017)
SmF:	Enhanced Cooper medium	<i>B. subtilis</i> DSM 10T	Surfactin	1100 mg/L	Willenbacher et al. (2015)
SSF	Olive leaf residue flour and olive cake flour	<i>B. subtilis</i> SPB1	Biosurfactant	30670 mg/L	Zouari et al. (2014)

SSF, which is traditionally used in the production of various Asian fermented foods and for fungal biosurfactants (Sundaram et al., 2024), is a newer method that is gaining popularity due to its lower investment requirements, shorter production times, and higher yields of secondary metabolites (Beltran-Gracia et al., 2017; Bouassida et al., 2023b; Venkataraman et al., 2022).

Numerous studies have been conducted under SmF and SSF conditions for the production of various compounds, including bioactive peptides, amylase, and lipopeptides, using *B. subtilis* or other microorganisms, as summarised in Table 2. In some cases, the microorganisms were reared on agro-industrial waste such as molasses and waste frying oil as a production medium (Al-Dhabi et al., 2020; Umar et al., 2021; Yáñez-Mendizábal et al., 2023). Both techniques have proven to be useful in producing lipopeptides.

However, one particularly interesting study is the 2023 research conducted by Bouassida et al. (2023b). The study compared the use of SmF and SSF techniques to produce biosurfactants using Aleppo pine waste and confectionery effluent as a medium for breeding *B. subtilis* SPB1. According to the study, SSF was found to be more efficient than SmF, with a production of $27,590 \pm 1.63$ mg/L and $17,160 \pm 0.91$ mg/L, respectively.

The production of biologically active metabolites by fermentation processes is dependent on the microbial strain characteristics and on the abiotic breeding factors such as medium composition, temperature, pH values, mixing speed and concentration of oxygen (Sidorova et al., 2020; Stamenković et al., 2018).

To produce lipopeptides efficiently through fermentation, the following steps should be taken: (1) Choose a suitable culture and isolate an effective microorganism, (2) characterize the chosen microorganisms on an optimum medium with appropriate growth conditions, (3) multiply microbial mass, (4) find and provide optimal conditions for lipopeptides production, (5) conduct laboratory efficacy tests, (6) conduct field and (7) large-scale studies and production at the industrial level, (8) establish a quality control and storage system (Stamenković et al., 2018).

It has been verified that optimal conditions for producing *B. subtilis* lipopeptides include good oxygenation, temperatures ranging from 25 to 30°C, and pH values between 6-8 (Al-Dhabi et al., 2020; Sidorova et al., 2020; Yaseen et al., 2017).

The composition of the production medium plays a crucial role in achieving an efficient lipopeptide production. First, because it has to be suitable for the bacterium's metabolism and for its target product and last, because the medium represents a significant cost percentage in the overall production process (Arasu and Al-Dhabi, 2024; Nurfarahin et al., 2018).

There is a direct correlation between lipopeptide production and biomass yield. For these reasons there is a need for an optimal carbon to nitrogen (C/N) ratio in the substrate. Since lipopeptide production occurs during the stationary growth stage of bacteria, a production medium with a high C/N ratio can be useful because it promotes cell metabolism for metabolite production (Umar et al., 2021).

Simple sugar, starch, and plant sugar-based carbohydrates are the main types of carbon sources used in biosurfactant production among the carbohydrate group. Glucose is the most commonly used carbon source, which can be easily metabolized by microorganisms through the glycolysis pathway to produce energy and a higher yield of the final product (Nurfarahin et al., 2018).

Furthermore, oil presence in the substrate can improve lipopeptides production as verified by Yaseen et al. in a 2017 study. In fact, surfactin production was implemented by the presence of paraffin oil and silicon oil (Yaseen et al., 2017).

Organic nitrogen contains both nitrogen and carbon components. It has been found to significantly aid in cell growth and polysaccharide formation in comparison to inorganic nitrogen. Organic nitrogen comes in the form of molecules such as yeast extract, meat extract, tryptone, or peptone. Out of all these, yeast extract is the most preferable substrate for significant biosurfactant production (Umar et al., 2021).

There are various techniques for lipopeptides extraction, including acid precipitation (using HCl 6N), solvent extraction (using chloroform, ethyl acetate, dichloromethane or mixtures of chloroform and methanol), ammonium sulphate precipitation with dialysis to remove small molecules and salts, and foam fractionation (which is used for continuous retention process and high purity) (Beltran-Gracia et al., 2017; Biniarz et al., 2020; Singh et al., 2022).

Different levels of lipopeptide purity are required depending on their intended application. For instance, crude lipopeptides are suitable for bioremediation applications where process

economy is the primary concern. Partially purified fractions, which are about 60-80% pure, are suitable for applications in microemulsion-based nanoparticle synthesis, laundry, and food industries. However, ultrahigh purity is essential for pharmaceuticals and human healthcare (Beltran-Gracia et al., 2017). For purification, a valid downstream process includes multiple steps of ultrafiltration, diafiltration, and evaporation (Kourmentza et al., 2021; Vassaux et al., 2021).

The isolation and identification of lipopeptides can be achieved through various techniques, such as liquid chromatography coupled to mass spectrometry (LC-MS) and MALDI-TOF mass spectrometry. These methods are considered the fastest and most efficient for identifying lipopeptides in mixtures and sequencing peptides, respectively. They are also useful for identifying novel lipopeptides and even small changes in the sequence of amino acids that can affect their properties (Beltran-Gracia et al., 2017; Biniarz et al., 2020).

The last step in producing lipopeptides involves transforming them into powder form in order to concentrate the product and facilitate the storage for longer periods of time. It also reduces the risk of product degradation and increases its shelf-life. To achieve this, surfactin, iturin, and fengycin are conventionally changed from a liquid to a solid state through a process called freeze-drying. However, good results have also been achieved through the process of spray-drying (Kourmentza et al., 2021; Vassaux et al., 2021).

While industrial fermentation is primarily optimised for the large-scale production of specific bioactive metabolites, the same bioprocessing platforms can be adapted for the generation of whole-cell microbial biomass. In this alternative application, downstream processing is simplified, and the final product consists of viable or spore-based formulations intended for direct application to soil. This approach broadens the agronomic potential of *Bacillus*-based bioinputs, shifting from metabolite-centred products to multifunctional microbial fertiliser alternatives, as discussed in Section 1.6.6.

1.6.5 Limits and potential for a large-scale *B. subtilis* utilisation

To enable large-scale and field applications of *B. subtilis* and its lipopeptides, certain issues need to be addressed. These issues pertain to the bacterium's persistence in the rhizosphere, its ability to produce lipopeptides, the industrial production process, and legislation.

In open-field conditions, *B. subtilis* cannot persist on plants or in the rhizosphere without extensive introduction. The complexity of the interactions between bacteria and plants, as well as between bacteria and microorganisms, is the reason for this (Blake et al., 2021; Earl et al., 2008).

In fact, the interactions between *B. subtilis* and the plant microbiome can be both cooperative and competitive. For example, *Pseudomonas protegens* (Flügge 1886), another widely used PGPR, can inhibit the formation of *B. subtilis* biofilms in co-culture, as verified by Powers et al. in 2015 (Powers et al., 2015).

Wild types of *B. subtilis* have a low capacity to produce lipopeptides, typically. So, it may be necessary to resort to genetic engineering to lower production costs by enhancing the bacteria's performance and increasing their ability to produce lipopeptides (Jimoh et al., 2021).

When it comes to the production process, both SmF and SSF have constraints that hinder the scaling up of lipopeptides. For instance, SmF requires large volumes of water (with a moisture content of about 80–95%) compared to the low yield (Saadoun et al., 2021).

This is a significant concern because, on an industrial level, the production expense can be quite high, with around 30-40% of the cost going towards the production medium (Arasu and Al-Dhabi, 2024; Nurfarahin et al., 2018). Furthermore, a low yield can make the separation and purification of lipopeptides difficult (Zhao et al., 2017).

In SmF fermentation, control can be challenging because of the presence of surfactin that often causes foam production. The intense foaming during aerobic liquid fermentation is a significant hindrance to commercialisation, as it makes the recovery and purification of lipopeptides difficult. Moreover, it increases the cost of purification up to 60% of the total production cost (Beltran-Gracia et al., 2017; Zhao et al., 2017).

SSF has gained attention due to its low operating cost, reduced water consumption (moisture content between 40–80%), and the lack of requirement for sophisticated bioreactors. However, the limitations of this technique are the limited control of the environment within the bioreactor and the high costs for end-product recovery and downstream processing (Hadj Saadoun et al., 2021).

To succeed in using SSF, it is important to choose the most suitable media and microorganisms for optimisation and planning of downstream processing steps. Agro-industrial waste can be used as a potential substrate with both economic and environmental advantages (Al-Dhabi et al., 2020; Arasu and Al-Dhabi, 2024).

The challenge is to create a production process that is efficient, economical, and environmentally friendly. The valorisation and utilisation of agro-industrial waste in both SSF and SmF are in line with the Sustainable Development Goals of the United Nations and the European Green Deal. In Europe, the Farm to Fork Strategy, which is an essential aspect of this deal, encourages the use of renewable resources and agro-industrial waste for food, energy, and chemical production (Duque-Acevedo et al., 2020; Sadik et al., 2021).

From a legislative perspective, it is essential to note that, currently, only four strains of *B. subtilis* are listed in the "EU Pesticides Database" (European Commission, 2026). Only *B. subtilis* strain IAB/BS03 and RTI477 are approved for biological control. Pending approval is *B. subtilis* strain FMCH002, while *B. subtilis* strain IBE 711 is not approved. In particular, *B. subtilis* IAB/BS03 is present only in fungicides with both curative and preventive effects, useful for controlling powdery mildew, apple scab, downy mildew, grey mould, and leaf spot through foliar application on various crops, including both vegetables and trees, in greenhouses and open fields (Ministry of Agriculture, Food Sovereignty and Forestry, 2026) and no products containing its lipopeptides are commercialised.

In the EU Pesticides Database (European Commission, 2026) section "Active substances, safeners, and synergists," searching for the keywords "lipopeptides", "iturin", "fengycin", and "surfactin" yields no results. This is indicative of the embryonic state of studies concerning the application of these metabolites in large-scale agriculture. In addition, this means that it will take additional time for these substances to become legal and their use to be regulated.

In fact, the majority of research studies conducted on *B. subtilis* and its metabolites have been on a laboratory or greenhouse scale. However, it is crucial to investigate how *B. subtilis* and its metabolites perform in open field conditions on different plants that are of agricultural interest and against various phytopathogens.

Although there are many obstacles to the large-scale use of *B. subtilis* and its lipopeptides, there is much potential to be considered and exploited. *B. subtilis* possesses several properties that make it an attractive candidate for the development of novel pest management and biostimulation technologies. Its unique characteristics enable it to be a vital component in producing multi-active products that can provide various useful actions for crop health simultaneously (Su et al., 2020). For this particular ability, the bacterium could be an effective tool for the reduction and substitution. Also, the bacterium itself can act as a BCA and a BA simultaneously (Table 3).

Table 3. Recent studies on the BA and BCA attitudes of *B. subtilis*.

Microorganism	Host Plant	Action on Plant Health	Controlled Phytopathogen	Authors
<i>B. subtilis</i> SPB1	<i>Solanum lycopersicum</i> L., 1753	-	<i>Agrobacterium tumefaciens</i>	Bouassida et al. (2023b)
<i>B. subtilis</i> J3 and <i>Pseudomonas fluorescens</i> J8	<i>S. lycopersicum</i>	-	<i>Alternaria solani</i>	Jia et al. (2023)
<i>Bacillus pumilus</i> PTB180 and <i>B. subtilis</i> PTB185	<i>S. lycopersicum</i> cv. Microtom	-	<i>Botrytis cinerea</i>	Bouchard- Rochette et al. (2022)
<i>B. subtilis</i> MBI600	<i>Cucumis sativus</i> L., 1753	Induction of genes involved in ISR and SAR signaling and upregulation of genes involved in phytohormone production and nutrient availability	-	Samaras et al. (2022)

			justifying the plant growth promotion.		
<i>B. subtilis</i> YB-04	<i>C. sativus</i>		Pronounced growth promotion of cucumber seedlings and increased cucumber defense-related enzyme activities.	<i>Fusarium oxysporum</i> f.sp. <i>cucumerinum</i>	Xu et al. (2022b)
<i>B. subtilis</i> YB-15	<i>Triticum aestivum</i> L.		Induction of defense-related enzyme activities in wheat seedlings. Promotion of plant growth through the production of indole acetic acid, siderophores, and phosphorus solubilization.	<i>Fusarium pseudograminearum</i>	Xu et al. (2022a)
<i>B. subtilis</i> L2	<i>Zingiber officinale</i> Roscoe, 1807		Improved plants' resistance to biotic and abiotic stresses and enhanced	-	Jaborova et al. (2021)

		physiological parameters (plant height, leaf length, number of leaves per plant and leaf width).		
<i>B. subtilis</i> PM32	<i>Solanum tuberosum</i> L., 1753	Enhanced potato plant growth by measuring biomass accumulation, chlorophyll a, b, and carotenoid contents.	<i>Rhizoctonia solani</i>	Mehmood et al. (2021)
<i>B. subtilis</i> PTA-271 and <i>Trichoderma atroviride</i> SC1	<i>Vitis vinifera</i> L. cv. Tempranillo (clone RJ-26) and cv Chardonnay (clone 7535)	-	<i>Neofusicoccum parvum</i> Bt67	Leal et al. (2021)
<i>B. subtilis</i> MBI600	<i>S. lycopersicum</i> cv. Belladonna	Signaling for ISR and SAR induction occurred. Genes involved in promoting plant growth, phytohormone production, and nutrient availability	<i>R. solani</i> , <i>Pythium ultimum</i> , <i>F. oxysporum</i> f.sp. <i>radicis-lycopersici</i>	Samaras et al. (2021)

		were upregulated.		
	<i>S. Lycopersicum</i> L., <i>Pisum sativum</i> L., <i>Capsicum annuum</i> L., and <i>Lactuca sativa</i> L.	Promotion of seed germination and plant growth.	-	Umar et al. (2021)
<i>B. subtilis</i> SNW3				
<i>B. subtilis</i> MK-252	<i>Allium cepa</i> L.	-	<i>F. oxysporum</i> f. sp. <i>cepae</i>	Bektas and Kusek (2020)
<i>B. subtilis</i> QST 713	<i>Castanea sativa</i> (Miller, 1768)	-	<i>Cryphonectria parasitica</i>	Murolo et al. (2019)
<i>B. subtilis</i> 713	<i>Phaseolus vulgaris</i> L., 1758	-	<i>B. cinerea</i> wild types and mutants	Samaras et al. (2019)

According to studies by Mehmood et al. (2021); Samaras et al. (2022) and Xu et al. (2022b) on cucumber and potato (*Solanum tuberosum* L.), *B. subtilis* exhibits both BCA and BA attitudes. These studies confirm that the presence of *B. subtilis* improves the plants' resistance to biotic and abiotic stresses and enhances their physiological parameters.

It is also documented that *Bacillus* spp. lipopeptides can produce positive effects not only in phytopathogens control but also on plant health. Umar et al. (2021) found that lipopeptides produced by *B. subtilis* strain SNW3 promoted seed germination and growth of tomato (*Solanum lycopersicum* L.), pea (*Pisum sativum* L.), chilli pepper (*Capsicum annuum* L.),

and lettuce (*Lactuca sativa* L.). Also, as verified by Wang et al. (2020), Iturin A and Fengycin A from *Bacillus megaterium* (De Bary, 1884) were able to promote plant photosynthetic efficiency, plant growth, and potato yield, especially when the two lipopeptides were combined.

B. subtilis can successfully cooperate with other BCA (Table 3), such as *Trichoderma atroviride* and *Pseudomonas fluorescens* (Flügge) Migula, 1895, as demonstrated by Jia et al. (2023) and Leal et al. (2021) for the control of *Neofusicoccum parvum* (Pennycook and Samuels) Crous, Slippers and Phillips and *Alternaria solani* (Sorauer, 1896) respectively. This feature has the potential to be quite useful in the creation of new microbial consortia.

The utilisation of microorganisms and their metabolites can provide multiple benefits for crops, both economically and environmentally. In agriculture, the excessive use of synthetic plant protection products is still one of the main risk factors for the environment, biodiversity and health. For instance, cupric compounds are generally used as fungicides, also authorised in organic farming, but their massive and continuous use results in negative effects on the plant-soil-microorganism system. In plants, the presence of toxic heavy metals that interact with membrane proteins causes lipid peroxidation and oxidative stress, with increased production of reactive oxygen species. Heavy metal pollution can also decrease metabolic activity, biomass, and the diversity of microorganisms in the rhizosphere, resulting in altered nutrient availability for plant uptake (Ju et al., 2019). For these reasons, viable alternatives are sought.

Compared to agrochemicals, lipopeptides are an environmentally friendly resource for disease management due to their high biodegradability (Crouzet et al., 2020). In addition, lipopeptides can be effective in fighting pathogens even at lower doses compared to traditional synthetic plant protection products. For instance, Cupravit 35 WG®, a cupric fungicide authorised in organic farming, is typically applied at kilogram-per-hectare rates depending on the crop, whereas Trupo et al. in 2023 demonstrated that a supernatant containing only 400 mg/L of iturin A achieved 100% control of cucurbit powdery mildew.

In a study conducted by Jiang et al. in 2021) 512 mg/L of iturin A could effectively inhibit the incidence of soft rot of cherry tomato fruit caused by *Rhizopus stolonifer* (Ehrenb.) Vuill., 1903. Additionally, Ambrico and Trupo (2017) reported that the minimum concentration of iturin A required to inhibit *P. digitatum* and *B. cinerea* was 6.60 and 3.30 mg/L, respectively.

It was also observed by Santos- Lima et al. (2023) that a lipopeptides concentration of ≥ 2 mg/L was adequate to inhibit the metabolic activity of *Fusarium solani* (Mart.) Sacc., 1881.

Last but not least, lipopeptides can help overcome the spread and persistence of the antibiotic-resistance issue caused by the excessive use of antibiotics in human health, hygiene, veterinary and agricultural practices. Pathogens can develop different mechanisms to resist antibiotics from entering their cells. One of the most common ways that microbes become drug-resistant is by decreasing or regulating the expression of outer membrane channels, such as porins (Khare et al., 2021; Yu et al., 2020). Cyclic lipopeptides and their fatty acid moiety offer a viable alternative to traditional antibiotics, as they can pass through the cell wall and target phytopathogens' plasma membrane, causing cytoplasmic leakage, membrane disruption and cell death (Crouzet et al., 2020; Dimkić et al., 2022; Fira et al., 2018; Tran et al., 2022).

1.6.6 Microbial biomass and whole-cell formulations as sustainable alternatives to chemical fertilisers

Beyond the production of specific bioactive metabolites, plant growth-promoting bacteria such as *Bacillus subtilis* can be exploited in agriculture through the application of whole-cell biomass formulations. These microbial inoculants represent a complementary strategy to metabolite-based biostimulants and biocontrol agents, aiming primarily at enhancing soil fertility, nutrient availability, and long-term agroecosystem resilience (Aloo et al., 2025).

Whole-cell microbial formulations act through multiple, synergistic mechanisms. Living bacterial cells contribute directly to nutrient cycling by solubilising inorganic phosphate, mobilising micronutrients such as iron and zinc, and participating in nitrogen transformation processes. In addition, microbial biomass can stimulate soil enzymatic activity and increase soil organic carbon turnover, indirectly improving soil structure, water retention, and root penetration. Unlike synthetic fertilisers, which deliver nutrients in a readily available but transient form, microbial biomass promotes a gradual and biologically mediated nutrient release, better aligned with plant demand (Singh and Pujari, 2022).

Experimental evidence from greenhouse and field studies has demonstrated that inoculation with PGPR can partially substitute mineral fertilisers while maintaining or even enhancing crop productivity. For instance, Shahzad et al. (2017) demonstrated that the combined application of PGPR and reduced nitrogen fertilisation significantly improved growth, yield

and nitrogen use efficiency in *Brassica napus*, confirming the potential of PGPR to optimise fertiliser use efficiency. Similarly, the application of a *Bacillus subtilis*-based biofertiliser in citrus orchards resulted in improved fruit quality and yield, enabling a substantial reduction in chemical fertilisation without compromising crop performance (Qiu et al., 2021).

Bacillus subtilis-based biomass formulations are particularly attractive due to the species' robustness, spore-forming ability, and high survival rates during storage and field application. Spores can withstand desiccation, temperature fluctuations, and UV radiation, ensuring persistence in the soil after inoculation (Nicholson et al., 2000; Ongena and Jacques, 2008). Once activated in the rhizosphere, vegetative cells can colonise root surfaces and interact dynamically with plant hosts, thereby combining nutritional functions with growth promotion and stress mitigation (Idris et al., 2007; Radhakrishnan et al., 2017).

From an agronomic perspective, whole-cell microbial inoculants are increasingly viewed as partial substitutes or complements to chemical fertilisers, especially in low-input and sustainable farming systems. Numerous greenhouse and field studies have demonstrated that microbial biomass applications can reduce the need for mineral fertilisers while maintaining or improving crop yield and nutrient use efficiency (Adesemoye et al., 2009; Vessey, 2003; Calvo et al., 2014). However, the magnitude of these effects remains highly context-dependent, influenced by soil physicochemical properties, crop species, native microbial communities, and environmental conditions (Bashan et al., 2014; Backer et al., 2018).

Despite their promise, the large-scale adoption of microbial biomass-based fertilisers faces several challenges. Variability in field performance, difficulties in ensuring consistent colonisation, and limited shelf life of some formulations remain significant constraints (Herrmann and Lesueur, 2013; Malusá et al., 2016). Moreover, the efficacy of whole-cell inoculants is often lower in soils with high native microbial diversity, where introduced strains must compete for ecological niches (van Veen et al., 1997; Compant et al., 2010). These limitations underscore the importance of formulation strategies, carrier materials, and application timing in maximising inoculant effectiveness (Bashan et al., 2014; Malusá and Vassilev, 2014).

In this context, integrated approaches combining whole-cell biomass with microbial metabolites or biocontrol compounds are emerging as particularly promising. Such strategies aim to harness the immediate effects of microbial secondary metabolites alongside the longer-term benefits of living microbial populations (Ongena and Jacques, 2008; Backer et al., 2018). This dual functionality aligns with current efforts to develop multifunctional bioinputs capable of simultaneously improving crop nutrition, enhancing stress tolerance, and suppressing plant pathogens, thereby contributing to the transition toward more sustainable and resilient agricultural systems (Berg et al., 2020; Mishra et al., 2021).

1.6.7 Seed coating with beneficial microorganisms

Seed coating represents one of the most effective delivery strategies for beneficial microorganisms in sustainable agriculture, as it enables precise control over seed properties while ensuring the targeted application of growth-promoting agents, micronutrients, and microbial inoculants. By localising bioactive compounds and living microorganisms directly at the seed–soil interface, coating technologies enhance early root–microbe interactions, protect seeds from biotic stresses, and promote uniform germination and seedling establishment (Tu et al., 2016; Hussain et al., 2020; Paravar et al., 2023).

From a formulation perspective, seed coatings are complex systems composed of binders, fillers, carriers, and active ingredients, each playing a distinct role in determining coating performance and microbial viability.

Binders, typically natural or synthetic polymers such as gum arabic or xanthan, ensure adhesion of the coating matrix to the seed surface while contributing to the physical stability of the formulation and the preservation of microbial vitality (Ehteshamul-Haque et al., 2007; Singh et al., 2014; Paravar et al., 2023).

Fillers, including materials such as bentonite, calcium carbonate, talc, biochar, or chitosan, are primarily used to modify seed size, weight, and shape, thereby improving handling and sowing precision (Tu et al., 2016; Paravar et al., 2023).

Carriers, such as vermiculite or perlite, are particularly critical for microbial inoculants, as they provide a supportive microenvironment by retaining moisture and buffering environmental stresses without exerting phytotoxic effects.

The active ingredients incorporated into seed coatings may include macronutrients and micronutrients, protective agents, and beneficial microorganisms (Tu et al., 2016; Paravar et al., 2023). In the case of microbial seed coatings, particular attention must be paid to the compatibility between microbial cells and other formulation components, as certain chemical protectants may negatively affect seed germination or microbial survival. Symbiotic and associative microorganisms, such as rhizobia and other PGPR, must also exhibit sufficient tolerance to desiccation and storage conditions to remain viable until sowing.

Several coating techniques are currently employed, ranging from dry coating and seed dressing to film coating, encrusting, and pelleting. These approaches differ in the thickness of the applied layer, the degree of modification of seed morphology, and the quantity of active ingredients delivered. Film coating and encrusting are particularly suitable for microbial inoculation, as they allow uniform distribution of inoculants without substantially altering seed size, while pelleting is often used for small or irregular seeds to improve sowing efficiency (Paravar et al., 2023).

The formulation of microbial seed coatings is a critical determinant of inoculation success, as inappropriate combinations of carriers, binders, or additives can severely compromise microbial viability and reduce seed shelf life. Consequently, the rational selection of formulation components and coating methods is essential to ensure the stability and efficacy of microbial inoculants.

Inoculation through seed coating with beneficial microorganisms enhances plant growth and fitness through multiple mechanisms, including improved nutrient bioavailability via nitrogen fixation and phosphate solubilisation, stimulation of plant development through phytohormone production, and suppression of plant pathogens through competition, antibiotic production, and the induction of systemic resistance. In addition, coated beneficial microorganisms can increase plant tolerance to abiotic stresses, such as salinity and drought, further supporting crop establishment under suboptimal environmental conditions (Hussain et al., 2020; Song et al., 2023).

The microorganisms most commonly employed in microbial seed coatings belong to the group of plant growth-promoting rhizobacteria, including species of the genera *Rhizobium*, *Pseudomonas*, and *Bacillus*. Their successful application through coating technologies

provides a direct link between whole-cell microbial formulations and early-stage plant development, reinforcing the role of microbial biomass-based bioinputs as viable complements or alternatives to conventional agrochemicals (Junges et al., 2013; Teymouri et al., 2016; Ahmad et al., 2021; Gupta et al., 2021; Gupta et al., 2022).

1.7 *Pseudomonas granadensis* and its role in the Rhizosphere

1.7.1 Overview of the Genus *Pseudomonas*

The genus *Pseudomonas* (Migula, 1894) represents one of the most diverse and ecologically versatile bacterial groups currently described. Members of this genus are Gram-negative, non-spore-forming, aerobic rods belonging to the class Gammaproteobacteria and are characterised by remarkable metabolic plasticity, which enables their colonisation of a wide range of environments, including soil, water, plant-associated niches, and animal hosts (Palleroni, 2015).

Among plant-associated pseudomonads, the *Pseudomonas fluorescens* complex has attracted particular attention due to its prominent role in plant growth promotion and biological control biocontrol (Pranav et al., 2024).

Soil- and rhizosphere-dwelling *Pseudomonas* spp. are widely recognised for their ability to enhance plant health by suppressing phytopathogens and promoting plant growth through multiple, often complementary mechanisms (Tienda et al., 2024).

These mechanisms include the production of phytohormones such as indole-3-acetic acid (IAA), cytokinins and gibberellins; modulation of plant ethylene levels via ACC deaminase activity; solubilisation of phosphate and micronutrients (e.g. Fe and Zn); secretion of siderophores, cyclic lipopeptides and other antimicrobial metabolites; emission of volatile organic compounds (VOCs); and activation of plant defence responses, including induced systemic resistance (ISR). Collectively, these traits enable *Pseudomonas* spp. to function as effective plant growth-promoting rhizobacteria (PGPR) and biocontrol agents (Guan et al., 2024).

Although numerous in vitro and greenhouse studies have demonstrated positive effects of *Pseudomonas* spp. on seed germination, root development, biomass accumulation and yield, the translation of these findings into consistent field-level performance remains a key

challenge, largely due to environmental variability and complex soil microbial interactions (Guan et al., 2024).

1.7.2 Taxonomy and Discovery of *P. granadensis*

Pseudomonas granadensis was first described as a distinct species by López-Caballero et al. (2009) following its isolation from the rhizosphere of cultivated soil in Granada (Spain). Phylogenetic analyses place this species within the *P. fluorescens* lineage, specifically in the *P. lutea* group.

The taxonomic classification of *P. granadensis* was achieved through a polyphasic approach combining phenotypic characterisation with molecular analyses, including 16S rRNA gene sequencing and multilocus sequence analysis (MLSA) of housekeeping genes such as *gyrB*, *rpoD* and *rpoB*. Although *P. granadensis* shares phenotypic similarities with closely related species such as *P. moraviensis* and *P. koreensis*, it exhibits a distinct genetic profile and fatty acid composition, supporting its recognition as a separate species (López-Caballero et al., 2009).

1.7.3. Morphological and Physiological Characteristics

Cells of *P. granadensis* are Gram-negative rods, approximately 0.3–0.7 µm in width and 1.1–2.2 µm in length. The species displays several phenotypic traits typical of the *P. fluorescens* group, including motility mediated by one or more polar flagella and the production of the fluorescent siderophore pyoverdine, which plays a key role in iron acquisition under iron-limited conditions.

P. granadensis is oxidase- and catalase-positive and grows optimally at temperatures between 25 °C and 30 °C, consistent with adaptation to temperate soil environments. Growth has been observed in laboratory conditions between 4 °C and 37 °C, with an optimum around 28 °C. After 48 h of incubation at 28 °C on tryptic soy agar (TSA), colonies appear white to yellowish, circular, convex, mucoid, and approximately 3–5 mm in diameter (Pascual et al., 2015).

1.7.4 Genomic Architecture and Rhizosphere Competence

Whole-genome sequencing of *P. granadensis* strains, including CT364 and R4-79, has provided valuable insights into the genetic basis of its ecological fitness and rhizosphere

competence. The genome typically consists of a single circular chromosome of approximately 6.2 Mbp, with a G+C content of around 60% (Cea-Torrescassana et al., 2024).

Functional annotation has revealed a substantial repertoire of genes associated with plant colonisation and survival in the rhizosphere. These include genes encoding advanced secretion systems (Type II, IV and VI), which are involved in protein delivery, microbial competition and interaction with host organisms; genes related to exopolysaccharide synthesis and adhesins, supporting biofilm formation and stable attachment to the rhizoplane; and a complex chemotaxis and motility network that enables the bacterium to sense and migrate toward plant-derived signals, such as root exudates.

1.7.5 Ecological Significance and Plant-Microbe Interactions

The agronomic interest in *P. granadensis* primarily derives from its classification as a PGPR and its ability to colonise the rhizosphere, the narrow zone of soil influenced by root exudates (Montero-Calasanz et al., 2013). Within this niche, *P. granadensis* exhibits several plant-beneficial activities, including siderophore-mediated iron sequestration, which can limit the availability of iron to soil-borne phytopathogens; phosphate solubilisation, enhancing plant phosphorus nutrition; and modulation of phytohormone balance through mechanisms such as ACC deaminase activity, contributing to improved tolerance to abiotic stresses.

The strain *P. granadensis* CT364, isolated from the rhizosphere of olive trees (*Olea europaea* L.) in Mairena del Aljarafe (Seville, Spain), has been shown to promote plant growth in multiple hosts. Phenotypic characterisation demonstrated its ability to enhance the growth of olive cuttings, induce root elongation in rapeseed (*Brassica napus*), and stimulate root development in mung bean (*Vigna radiata* L.) and cowpea (*V. unguiculata*) (Montero-Calasanz et al., 2013).

1.7.6 The Endophytic Lifestyle of *P. granadensis*

Although *Pseudomonas granadensis* is primarily described as a rhizosphere-associated bacterium, evidence from studies on closely related *Pseudomonas* species suggests that, under favourable conditions, it may establish a more intimate association with the host plant by adopting an endophytic lifestyle (Bajpai and Johri, 2019). The transition from a free-living soil bacterium to an endophyte is a multistep process involving chemotactic recognition of root exudates, attachment to the rhizoplane, biofilm formation mediated by

exopolysaccharides, and subsequent entry into plant tissues through natural openings or sites of lateral root emergence (Santoyo et al., 2021; Yang et al., 2024).

Once internalised, *P. granadensis* is thought to preferentially colonise intercellular spaces within root tissues and, as reported for other endophytic *Pseudomonas* species, may occasionally translocate to aerial organs (Ahmed et al., 2025). This internal niche offers several ecological advantages, including reduced competition with other microorganisms, access to plant-derived carbon sources, and prolonged persistence within the host (Bajpai and Johri, 2019).

1.7.7 Mechanisms of Biocontrol and Stress Resilience

One of the most relevant benefits associated with the endophytic and rhizosphere-associated lifestyles of beneficial *Pseudomonas* spp. is their capacity to enhance plant resistance to both biotic and abiotic stresses. *P. granadensis* possesses biosynthetic gene clusters encoding a range of secondary metabolites, including antimicrobial compounds such as hydrogen cyanide, phenazines and specialised lipopeptides, which contribute to the suppression of fungal and bacterial pathogens.

In addition, colonisation by *Pseudomonas* spp. is known to prime plant immune responses through the activation of induced systemic resistance (ISR). This primed state, typically mediated by jasmonic acid and ethylene signalling pathways, allows plants to respond more rapidly and effectively to subsequent pathogen attacks without the metabolic costs associated with constitutive defence activation. Beyond biotic stress protection, *P. granadensis* has also been associated with enhanced tolerance to abiotic stresses such as salinity and osmotic stress, likely through phytohormonal regulation and the production of stress-mitigating enzymes (Alghanmi et al., 2025).

1.7.8 Current State of the Literature

Research on *Pseudomonas granadensis* remains relatively limited but is steadily increasing, reflecting its recent taxonomic description and emerging relevance in agricultural microbiology (Pascual et al., 2015). To date, fewer than 50 primary research articles have focused specifically on this species, although it is frequently detected in broader metagenomic surveys of soil and crop-associated microbiomes.

Early studies primarily addressed taxonomy and phylogenetic placement within the *P. fluorescens* complex, whereas more recent work has shifted toward functional genomics, rhizosphere competence and potential applications as a bioinoculant, particularly in olive and cereal cropping systems. These emerging findings highlight *P. granadensis* as a promising candidate for sustainable agriculture, warranting further investigation under controlled and field conditions.

Aim of the thesis

The experiment conducted as part of the CN Agritech Project (National Centre for New Technologies in Agriculture) (AGRITECH National Research Centre, 2022), whose aim is to create a national HUB to help preserve natural capital stocks and achieve climate neutrality by 2050, with particular reference to the agricultural sector, in line with the European Green Deal (European Commission, 2019), is part of the “New circular economy models through the valorisation and recycling of waste” (Spoke 8) strand.

This research concerns the “Recovery of nutrients and organic matter from waste to reduce the use of agrochemicals and close the waste cycle” (Working Package 8.3) and, more precisely, the line of “Production of organic fertilisers from waste to improve soil fertility” (Task 8.3.3).

The objective of the experiment was to find alternatives to agrochemicals by selecting useful microorganisms and agro-industrial waste suitable for their cultivation in fermentation and downstream processes aimed at obtaining one or more products that can have various beneficial effects on plant health, from biocontrol to biostimulation, with a view to the circular economy.

The experimental activity focused on the cultivation of plant growth-promoting rhizobacterium *B. subtilis* ET-1 on a substrate containing spent yeast and potato peel extract to obtain lipopeptides with antimicrobial activity, in particular iturin A, and biomass containing the spores of the bacterium, useful for the biostimulation of plants of agronomic interest.

The antimicrobial activity of the biological preparations containing iturin A obtained was tested *in vitro* and *in vivo* against relevant phytopathogenic fungi such as *Penicillium digitatum* and *Podosphaera xanthii* (Castagne) U. Braun and Shishkoff, 2000.

Basil (*Ocimum basilicum* L.) was chosen as the plant species to be used as a model for the evaluation of the microbial biomass biostimulation activity, as it is a species of great global interest and is cultivated at various levels, from professional cultivation for industrial production to amateur cultivation for domestic use.

This experiment, therefore, aimed to verify whether *B. subtilis* biomass produced by fermentation in a bioreactor can promote plant growth and enhance soil fertility without

causing any adverse effects, using standard potting soil under controlled ventilation and lighting conditions through fertirrigation and seed coating.

Furthermore, at the laboratories of the School of Natural and Environmental Sciences at Newcastle University, the ability of the recently identified *P. granadensis* CT364 to colonise the tissues of plants of great agricultural interest, such as tomatoes and wheat, and to improve their fitness was tested.

In particular, the Tomato Micro-Tom (*Solanum lycopersicum* L.) was selected as a model plant because it is a dwarf, determinate variety and a well-recognised model organism in scientific research. Its small size and short life cycle of just 60 to 70 days make it an excellent candidate for a variety of studies, including genetics, plant physiology, and molecular biology.

On the other hand, Cochise wheat was chosen because it is a high-yielding spring wheat variety recognised for its exceptional performance in both spring and late autumn sowing periods with good grain quality.

It is tall but stiff-strawed with a solid disease profile, including resistance against the predominant pest of wheat crops in the UK, like orange wheat blossom midge (*Sitodiplosis mosellana* (Géhin, 1857)) and to *Furovirus tritici*, the causal agent of Soil Borne Wheat Mosaic Virus.

However, experimental work on Cochise wheat could not be completed due to persistent seed sterilisation issues, a well-known constraint in cereal microbiome studies.

2. Materials and Methods

2.1. Production of biological preparations containing iturin A with antimicrobial action

In this study, two different types of microbial preparations were produced: the cell-free supernatant and the crude lipopeptide extract.

The cell-free supernatant is the liquid part of the culture that has been separated from the bacterial cells and contains the entire range of extracellular metabolites naturally released into the medium.

Conversely, the crude lipopeptide extract is a more concentrated preparation enriched with lipophilic bioactive compounds, including iturin A, obtained through a process that enables the comprehensive isolation of lipopeptide molecules.

The combined use of both preparations allows for a comparative assessment of the antimicrobial potential associated with the total extracellular metabolome versus the concentrated lipopeptide fraction.

To obtain these bioactive preparations, the selected microorganism was cultivated on agro-industrial waste. In addition, the scaling up of these fermentation processes was fine-tuned, while evaluating the iturin A content and antimicrobial activity against various phytopathogenic microorganisms.

2.1.1 General Workflow for Microbial Cultivation and Iturin A Production

Young colonies of the selected microorganism grown on nutrient agar (NA) were collected and cultured in nutrient broth (NB). After 72 hours of inoculation, the microbial biomass pellet was resuspended in PBS (Phosphate Buffered Saline) buffer and pasteurised for 10 minutes at 75°C.

This spore suspension was then inoculated into the different bioreactors on the previously sterilised selected substrate by autoclaving at 121°C for 15 minutes.

The substrate pH (pH=7) was kept constant by automatically adding sodium hydroxide (NaOH 1M) and sulphuric acid (H₂SO₄ 0.25 M).

Broth aliquots were taken for microscopic analysis to ensure the absence of contaminants and abnormalities in the growth of the selected microorganism.

After 96 hours, at the onset of bacterial spore formation, a portion of the pellet was dried to determine the biomass yield per litre of substrate, while an aliquot of the supernatant was analysed using liquid chromatography to evaluate the content of iturin A.

Usually, during bacterial growth, 4 supernatant samples were taken at 24-hour intervals.

Subsequently, the effectiveness of iturin A against various phytopathogenic organisms was tested.

2.1.2 Microorganism selection

To select the most suitable microorganism for the experimental activity, the ability of three species belonging to the genus *Bacillus* spp. (*Bacillus subtilis* ET – 1, *Bacillus* spp. and *Bacillus licheniformis* (Weigmann 1898) Chester 1901) to inhibit the growth of phytopathogenic organisms such as *Botrytis cinerea* (Pers., 1794) and *Penicillium digitatum* (Pers.) Sacc. was evaluated *in vitro*.

In particular, the Percentage of Mycelial Growth Inhibition (MGI %) was calculated using the following formula:

$$\text{MGI}(\%) = \frac{\text{AWD} - \text{ATD}}{\text{AWD}} \times 100$$

- MGI: Mycelial Growth Inhibition
- AWD: Average Witness Diameter
- ATD: Average Thesis Diameter

2.1.3 Selected bacterial strain

B. subtilis ET-1 strain was previously isolated from soil and stored at –80 °C in 20% glycerol (Ambrico et al., 2010). It was activated before any experimental use and cultured on nutrient agar (NA) at 25 °C.

2.1.4 Fungal pathogens

The pathogenic fungi used throughout the present study were provided by ENEA Trisaia Research Centre.

In particular, the pathogens used in this work were *Botrytis cinerea*, the causal agent of grey mould; *Penicillium digitatum* and *Penicillium italicum* Wehmer, 1894, the causal agents of

green and blue mold; *Monilinia laxa* (Aderh. and Ruhland) Honey, 1928, the causal agent of stone fruit monilia; and *Podosphaera xanthii*, the causal agent of powdery mildew disease.

Except *P. xanthii*, the pathogens were grown on potato dextrose agar (PDA) at 25°C.

The inoculum of *P. xanthii* was prepared by spreading fungal conidia obtained by diseased melon leaves in sterilised physiological water. Then, they were counted using a Burker chamber in order to adjust the suspension to 5×10^5 conidia/mL.

2.1.5 Agro-industrial waste selection for breeding the chosen microorganism

To select the most suitable substrate for cultivating the previously chosen microorganism, various combinations of ingredients were evaluated, both those traditionally used for cultivating bacteria in the laboratory and those derived from agro-industrial processes, proceeding from bench-scale cultivation in flasks, moving to cultivation in Biostat® C fermenters with steel vessels of 5 L and 21 L, and reaching the industrial scale.

In particular, 28 substrates resulting from the combination of agro-industrial waste and ingredients normally used for the cultivation of microorganisms in the lab at various concentrations were tested.

The amount of iturin A produced and the antimicrobial activity against various phytopathogens of the cell-free supernatant and crude lipopeptide extract were considered in selecting the best substrate.

To define the optimal concentration of crucial components, an experimental scheme was implemented using the Response Surface Methodology (RSM) with a two-level Full-factorial design.

The effect of sucrose concentration (X1: 20 – 80 g L⁻¹) and *Opuntia ficus-indica* (L.) Mill., 1768) extract concentration (X2: 0-130 ml L⁻¹) on iturin yield was analysed using a two-level full factorial design. The design matrix showing the independent variables is presented in Table 4.

Table 4. Design matrix generated with the Design of Experiments (DOE) software Modde 13.0.2

Run Order	Independent Variables	
	Sucrose	<i>Opuntia ficus-indica</i> extract

	X1	Sac (g L⁻¹)	X2	Opu (ml L⁻¹)
1	0	50	0	65
2	0	80	+1	130
3	-1	20	+1	130
4	+1	80	-1	0
5	0	50	0	65
6	-1	20	-1	0
7	0	50	0	65

2.1.6 Determination of the quantity of iturin A

The amount of iturin A produced was checked during the fermentation at 24 h intervals, through an Agilent 1200 series High Performance Liquid Chromatography (HPLC) instrument (Agilent Technologies) consisting of an in-line degasser (G1379B), binary pump (G1312B), auto-sampler (G1367B), column temperature controller (G1316A) and UV-Vis detector (G1314B)

Before analysis, 1 mL samples of CFS were filtered through a 0.22 µm Millipore filter and transferred into 2 mL vials. Analyses used a Zorbax RX-C18 column (4.6 × 250 mm, 5 µm) with a mobile phase of acetonitrile and 3.8 mM trifluoroacetic acid (30:70, v/v).

Conducted under isocratic conditions at 30 °C with a flow rate of 1.5 mL/min for 50 minutes, a 20 µl injection volume was used, and elution was monitored at 210 nm.

HPLC peaks were identified by comparing retention times to those of the external Iturin A standard (Sigma-Aldrich, St Louis, MO). A calibration curve over at least five concentrations (10- 800 mg/l) showed excellent linearity ($R^2 \geq 0.9997$).

Data were collected and analysed with OpenLAB CDS Chemstation Edition Rev. C.01.10(201).

Analyses were performed at different sampling times in triplicate, with results expressed as mean ± standard deviation (mg/l).

2.1.7 Preparation of cell-free supernatant and crude lipopeptide extract

At the end of the culture, broth medium was centrifuged in an Avanti™ J- 25 centrifugation unit (Beckman Coulter, U.S.A.) at 9.000 g for 10 min at 10 °C and the bacterial cells were discarded. The CFS was stored at 4°C.

To obtain the crude lipopeptide extract, 6M HCl was added to 2 L of CFS (pH 2).

The acidified suspension was kept at 4 °C overnight, and then it was centrifuged at 12.000 g for 10 min at 4 °C. The resulting pellet was re-suspended in 2 L of 50 mM phosphate buffer (PBS) (pH 7.0) and the content of Iturin A was determined by chromatographic analysis.

Based on the Iturin A amount, the PBS solution was appropriately diluted with water before its application in trials. In addition, 100 mL of CFS was subjected at the same acid precipitation method, and the recovered pellet was dried and weighed for quantification.

The purity of Iturin A in the crude lipopeptide extract was calculated by following the formula:

$$\text{Purity (\%)} = \left(\frac{\text{Iturin amount in 100 mL}}{\text{weight of dried extract}} \right) \times 100$$

2.1.8 Antimicrobial activity evaluation during the scaling-up and optimisation process

During the scaling-up of the fermentation processes and the optimisation of the culture substrate formulation, *in vitro* and *in vivo* assays were performed to evaluate the biocontrol activity of the cell-free supernatant and the crude lipopeptide extract. *In vitro* and *in vivo* tests were conducted against *P. digitatum*, while an *in vivo* assay was performed on *Cucumis melo* L. (cv. Amarillo Oro) against *P. xanthii*.

Additional antimicrobial screening was performed against *B. cinerea*, *P. italicum*, and *M. laxa* (data not shown), as part of routine laboratory tests aimed at confirming the broad-spectrum activity of the strain.

Below are the assays used to evaluate the antimicrobial activity of the preparations obtained from the cultivation of the microorganism on the selected substrates (substrates 14 and 28).

In vitro tests

To assess the effect of secondary metabolites contained in the cell-free supernatant of substrates 14 and 28, plate tests with the addition of PDA were carried out. In particular, serial dilutions of the cell-free supernatant with the addition of PDA were sterilised at 100 °C for 15 minutes.

Each plate was inoculated with 100 µl of a 1.3×10^3 conidia/mL suspension of *P. digitatum*, and the suspension was then evenly spread over the surface by spreading.

After 3-4 days of incubation at 26 °C, the number of colony-forming units (CFU) was counted on the plates with the serial dilutions of the supernatant and on the control plates.

In vivo test

Some of the procedures and results reported in this section derive from preliminary activities carried out by the research group. They are reported to provide a comprehensive overview of the effectiveness of the product tested.

Biological preparations containing iturin A against *P. xanthii* on melon plants

The artificial inoculation of *P. xanthii* was performed by nebulising the conidia suspension (5×10^5 conidia mL⁻¹) uniformly on all 48 plants. The treatments were carried out at 2 and 12 days from the inoculation by spraying uniformly on the foliage of melon plants.

To use as treatments, the CFS and the crude lipopeptide extract were diluted to reach an Iturin A content of about 100 mgL⁻¹ (or 100 ppm).

Treatments with physiological water and a conventional fungicide (INDAR™ 5 EW, Sumitomo Chemical Italia, Fenbuconazole 50 g L⁻¹) were used as negative and chemical controls, respectively, with spraying at 5 mL plant⁻¹ for both.

For all treatments, a range of 300–500 L ha⁻¹ was used, depending on the plants' phenological phase.

To estimate the disease, the leaf area covered by fungus was measured after 15 days from the observation of the first symptoms on the control.

To estimate the spreading of the disease, the disease severity (DS) was evaluated adopting a visual scale from 0 to 5 based on symptoms leaves as follows: 0 = no symptom; 1 = up to

5% infected leaf area; 2 = 6–10% infected leaf area; 3 = 11–25% infected leaf area; 4 = 26–50% infected leaf area; 5 = 51–100% infected leaf area.

DS describes the damage caused by the diseases on plants and was analysed according to Gullino et al. (2009) by the following formula:

$$DS = \sum \frac{(n^{\circ} \text{ leaves} \times X_0 - 5)}{(\text{total of leaves recorded})}$$

(2)

with $X_0-5 = (X_0 = 0; X_1 = 3\%; X_2 = 8\%; X_3 = 18\%; X_4 = 38\%; X_5 = 75.5\%)$.

The efficacy of each treatment was compared with the control and calculated by following formula:

$$\text{Control efficacy (\%)} = \left[\frac{(\text{DS in control} - \text{DS in treatment})}{\text{DS in treatment}} \right] \times 100$$

(3)

For the experiment, a randomised complete block design with 3 blocks was adopted. For each block, four different treatments were conducted, and each treatment consisted of four plants.

Dried cell-free supernatant against *P. digitatum* on clementine fruits

To produce a cell-free supernatant (CFS) rich in iturin A, useful for phytopathogens control, *B. subtilis* ET-1 was bred at 25°C for 96 hours with a working volume of 10 L of the previously selected substrate in a 21 L stirred-tank bioreactor (Biostat® C unit).

The supernatant was clarified by centrifugation, and the CFS was added with skim milk and stabilised by a drying process using an APTSol®-2.0 Spray Dryer.

The antimicrobial activity of the dried cell-free supernatant has been tested *in vivo* against *P. digitatum* on clementine (*Citrus × clementina* Yu. Tanaka, 1954) fruits.

Previously sanitised fruits have been injured and inoculated with 20 µL of *P. digitatum* suspension at a concentration of 10⁴ conidia/mL.

As positive and chemical controls, fruit were treated by dipping in distilled water and Imazalil (emulsifiable concentrate 500 g/L), a post-harvest fungicide active ingredient for citrus fruit treatments, respectively.

The action of liquid CFS and CFS stabilised with skimmed milk was also compared.

After treatments, clementines have been incubated at room temperature for 7 days.

The percentage of infected wounds was then assessed as follows:

$$\text{Disease Incidence (\%)} = \left(\frac{IW}{W} \right) \times 100$$

where W is the number of wounds and IW is the number of infected wounds.

2.2 Microbial biomass production for plant biostimulation

B. subtilis ET-1 was cultivated in a 500 L Biostat® industrial fermenter in 250 L of substrate containing ammonium nitrate (NH₄NO₃), potato peel extract, spent yeast and sucrose.

This substrate was chosen for the cultivation of the bacterium because previous experimental tests showed it to be the most suitable for the production of iturin A (2,450 mg/L), a lipopeptide useful for the biocontrol of phytopathogenic organisms.

The biomass resulting from this process was removed from the supernatant by centrifugation at 9630 RPM with a Seital® centrifuge and processed with APTSol® spray dry in the presence of skimmed milk to encapsulate the cells and make the process more efficient until the biomass was obtained in powder form.

The viability of the biomass obtained was assessed by determining the colony-forming units (cfu) four days after inoculation of plates containing Nutrient Agar, following serial dilutions of the bacterial suspension (0.025 g/mL).

2.3 Evaluation of the microbial biomass biostimulant activity

2.3.1 Pilot trials

To determine the experimental setup and identify the model plant for evaluating the biostimulant effect of the microbial biomass obtained as described above, two pilot tests were carried out simultaneously.

The model plants compared were basil and potatoes, both grown under ventilated lamps.

The data obtained from these trials are reported in Annex B. They will not be considered for statistical purposes due to the number of replicates (2 plants/thesis), determined by the availability of the cultivation facility.

In any case, these data were useful for choosing the model plant, designing the microbial biomass administration protocol and determining the setup of the cultivation system.

Pilot trial on Basilico

Rationale

Two different types of treatment were compared, under identical growing conditions, on the growth and development of basil grown in the laboratory on conventional substrate and under precision lighting.

The choice of “Genovese” basil (*Ocimum basilicum* L.) as the model plant was made taking into account the widespread cultivation of the species, the economic importance of its cultivation and the supply chain derived from it, the susceptibility of the crop to pollution and contamination during the cultivation phases, and the potential risk to consumers from direct consumption of the edible parts of the plant.

The theses correspond to:

- ‘C’ (negative control), in which plants are grown using irrigation with laboratory source water.
- ‘B’ (plants treated with microbial biomass), in which plants are grown using fertigation with 10^6 cfu/mL of *B. subtilis* strain ET-1.
- ‘S’ (plants treated with ammonium sulphate), in which plants are grown using fertigation with 1g/l of $(\text{NH}_4)_2\text{SO}_4$.

Microbial biomass

B. subtilis was cultivated in a 500 L Biostat® industrial fermenter in 250 L of substrate containing ammonium nitrate (NH_4NO_3), potato peel extract, spent yeast and sucrose.

This substrate was chosen for the cultivation of the bacterium because previous experimental tests showed it to be the most suitable for the production of iturin A (2,450 mg L⁻¹), a lipopeptide useful for the biocontrol of phytopathogenic organisms.

The biomass resulting from this process was removed from the supernatant by centrifugation at 9630 RPM with a Seital® centrifuge and processed with APTSol® spray dry in the presence of skimmed milk to encapsulate the cells and make the process more efficient until the biomass was obtained in powder form.

The viability of the biomass obtained was assessed by determining the colony-forming units (cfu) four days after inoculation of plates containing Nutrient Agar, following serial dilutions of the bacterial suspension (0.025 g/mL).

Equipment for plant cultivation

For plant cultivation purposes, transparent polycarbonate cylinders with open bases were used, placed on plastic saucers of appropriate dimensions (Figure 5).

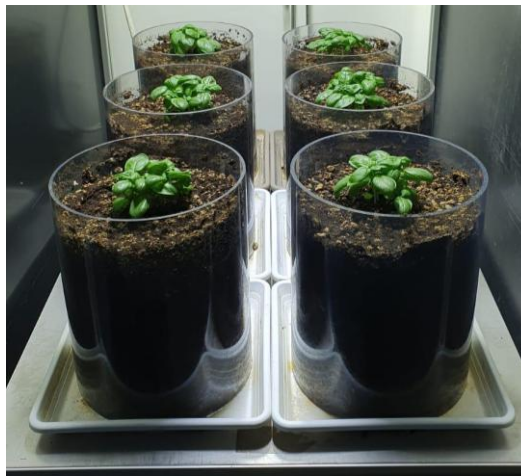


Figure 5. Housing for cylinders containing basil seedlings.

The cultivation system consisting of cylinders and saucers was placed under “ventilating lamps” designed by ENEA, conceived, designed and manufactured as part of the PON ISAAC Project - Innovative Lighting System for Indoor Plant Cultivation to improve human well-being (CUP B88I17000590008), capable of providing light with a spectrum and intensity suitable for plant cultivation in the laboratory, combined with ventilation calibrated to the needs of indoor plants.

The orientation of the cultivation system and the distribution of the different treatments are shown below (Figure 6).

The window side of the laboratory	Back		Laboratory door side
	Basil		
	C2	S2	
	B2	S1	
	C1	B1	
Front			

Figure 6. Orientation of the cultivation system and the distribution of the different treatments. ‘C’ (negative control, water), ‘B’ (plants treated with microbial biomass), ‘S’ (plants treated with ammonium sulphate).

In practice, after the first irrigation carried out at transplanting, performed for all plants with spring water, the treatments were differentiated as follows:

- Cylinders C irrigation with spring water only.
- Cylinders B fertigation with spring water containing microbial biomass 2 g/L (7.2×10^8 cfu *B. subtilis*/g).
- Cylinders S fertigation with spring water containing ammonium sulphate 1 g/L.

Taking the plant collar as a reference, all treatments are administered in each cylinder through holes in the soil to a depth of approximately 1/3 of the soil height.

The holes are oriented according to the four cardinal points as shown below, and 50 mL of water, water containing biomass or water containing ammonium sulphate is administered to each hole (Figure 7).

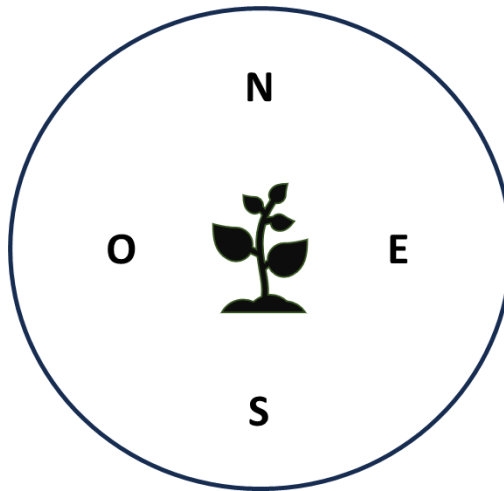


Figure 7. Orientation of holes for basil treatments.

Reference time stamp

The trial followed the growth cycle of basil seedlings and lasted approximately three and a half months.

The reference timetable used to track the different phenological stages of the plants, as well as the timing of watering and treatments, is shown below (Table 5).

Table 5. Timetable of the pilot experimental activity for evaluating the biostimulant effect of microbial biomass containing *B. subtilis* on basil.

March – April 2024									
25	26	27	28	29	30	31	01	02	03
00	01	02	03	05	05	06	07	08	09
April 2024									
04	05	06	07	08	09	10	10	11	12
10	11	12	13	14	15	16	17	18	19
13	14	15	16	17	18	19	20	21	22
20	21	22	23	24	25	26	27	28	29
April – May 2024									
23	24	25	26	27	28	29	30	1	2
30	31	32	33	34	35	36	37	38	39
May 2024									
3	4	5	6	7	8	9	10	11	12
40	41	42	43	44	45	46	47	48	49
13	14	15	16	17	18	19	20	21	22
50	51	52	53	54	55	56	57	58	59
May – June 2024									
23	24	25	26	27	28	29	30	31	01

60	61	62	63	64	65	66	67	68	69
June2024									
02	03	04	05	06	07	08	09	10	11
70	71	72	73	74	75	76	77	78	79
June – July 2024									
12	13	14	15	16	17	18	19	20	21
80	81	82	83	84	85	86	87	88	89
July 2024									
02	03	04	05	06	07	08	09	10	11
90	91	92	93	94	95	96	97	98	99
100	101	102	103	104	105	106	107	108	109

Day “0” is considered to be the day on which the plants were transplanted.

The trial was concluded when the flower stalks appeared.

Growing conditions

The trolley as a whole was equipped with four square lighting panels with LEDs supplied by Becar.

Only the LEDs emitting Cool White light were activated in the lamps, with 85% of the maximum value emitted.

The emission values of the lighting system were set to emit a photosynthetically active photon flux of approximately 220 $\mu\text{mol}\cdot\text{m}^{-2}\cdot\text{s}^{-1}$ when measured in the centre of the platform at plant level, approximately 90 cm from the lamp diffuser.

The measurement was carried out using the LI-190/R (LI-COR) sensor and the LI-1500 (LI-COR) measurement processor.

The photoperiod was 16 hours of light and 8 hours of darkness per day, with the lamps switching on at 5:00 a.m. and switching off at 9:00 p.m.

Forty-three days after transplanting, the lamps were set to turn on at 6:00 a.m. and turn off at 9:00 p.m.

Ventilation was directed from the bottom upwards and was active 24 hours a day.

The thermoperiod was that of the laboratory, approximately 23-24°C.

Growing medium

To create the substrate columns, each cylinder was filled with Primavita (Terflor®) soil, supplemented with monopotassium phosphate + dipotassium phosphate + potassium sulphate + magnesium sulphate + iron sulphate.

Each of these salts was administered in a quantity of 0.5 g per cylinder.

Germplasm

The germplasm used was Genovese basil.

The starting material consisted of seedlings in the fifth and sixth true leaf stage, previously sown directly in pots and grown in a greenhouse before being transplanted under ventilated lamps.

Plant cultivation

The basil was transplanted into cylinders with an internal diameter of 19 cm and a height of 25 cm.

Ten days after transplanting, the weakest seedlings were removed, leaving four seedlings per cylinder.

The association between plants and cylinders is shown above.

For the first watering after transplanting, spring water was used and administered on the surface.

The amounts per seedling and per cylinder are shown below in Table 6.

Table 6. Water supply, treatments and fertilisation for the plants of the 3 considered trials (water, microbial biomass and ammonium sulphate). Fertiactyl GZ (an organomineral NK fertiliser) was used in fertigation towards the end of the crop cycle for the plants in all trials.

Time	Treatment					
	Water		Microbial biomass		Ammonium sulphate	
	Cylinder 1	Cylinder 2	Cylinder 1	Cylinder 2	Cylinder 1	Cylinder 2

00	Water 1.000 mL	Water 1.000 mL	Water 1.000 mL	Water 1.000 mL	Water 1.000 mL	Water 1.000 mL
+ 3	Water 500 mL	Water 500 mL	Water 500 mL	Water 500 mL	Water 500 mL	Water 500 mL
+ 16	Water 200 mL	Water 200 mL	Water 200 mL + 0,400 g microbial biomass	Water 200 mL + 0,400 g microbial biomass	Water 200 mL + 0,200 g ammonium sulphate	Water 200 mL + 0,200 g ammonium sulphate
+ 22	Water 200 mL	Water 200 mL	Water 200 mL	Water 200 mL	Water 200 mL	Water 200 mL
+ 26	Water 200 mL	Water 200 mL	Water 200 mL + 0,400 g microbial biomass	Water 200 mL + 0,400 g microbial biomass	Water 200 mL + 0,200 g ammonium sulphate	Water 200 mL + 0,200 g ammonium sulphate
+ 31	Water 400 mL	Water 400 mL	Water 400 mL	Water 400 mL	Water 400 mL	Water 400 mL
+ 34	Water 300 mL	Water 300 mL	Water 300 mL	Water 300 mL	Water 300 mL	Water 300 mL
+ 36	Water 200 mL	Water 200 mL	Water 200 mL	Water 200 mL	Water 200 mL	Water 200 mL
+ 40	Water 400 mL	Water 400 mL	Water 400 mL	Water 400 mL	Water 400 mL	Water 400 mL
+ 45	Water 300 mL	Water 300 mL	Water 300 mL	Water 300 mL	Water 300 mL	Water 300 mL
+ 47	Water 400 mL + 2 mL Fertiactyl GZ	Water 400 mL + 2 mL Fertiactyl GZ	Water 400 mL + 2 mL Fertiactyl GZ	Water 400 mL + 2 mL Fertiactyl GZ	Water 400 mL + 2 mL Fertiactyl GZ	Water 400 mL + 2 mL Fertiactyl GZ

Phenotypic observations and biometric measurements

Throughout the cultivation period, observations were made on the condition of the plants and, at the end of the trial, various biometric parameters were measured.

The height of the plants and the number of nodes for each replicate were considered.

The height was determined on the tallest stem of the tallest plant in the group of plants present in the given cylinder, measured from the collar to the point of intersection of the floral axis, even straightening the stem along the metre.

The number of nodes was determined by counting the recognisable nodes on the main stem of the tallest plant in the group of plants in the given cylinder, starting from the first node above the cotyledons and ending at the last node before the floral scape.

To determine the biomass yield, 57 days after transplanting, the fresh weights were determined, then the leaves, flower scapes and stems collected were left to dry in the air in the laboratory until a constant weight was reached.

The plants were cut at the collar and the leaves and flower scapes were separated from the stems.

For the survey, leaves that had fallen into the cylinders and completely withered or dry biomass were not taken into account.

After 71 days, a constant weight was reached and the dry weight of leaves, stems and flower stalks was determined for all samples. The samples were then placed in a freezer at a temperature of -20°C.

Measurement of Chlorophyll Content Index

Forty-five days after transplanting, the chlorophyll content index (CCI) was measured using a SPAD-502 Plus meter (Konica Minolta).

The measurements were taken as if there were only one plant per cylinder, measuring four leaves per cylinder, two apical and two median, proceeding from the apical leaves towards the median ones.

Pilot trial on Potato

Rationale

Two different types of treatment were compared, under identical growing conditions, on the growth and development of potatoes (*Solanum tuberosum* L.) grown in the laboratory on conventional substrate and under precision lighting.

Potatoes were chosen as the model plant because of the widespread cultivation of the species, the economic importance of its cultivation and the supply chain derived from it, the susceptibility of the crop to pollution and contamination during the cultivation phases, and the potential risk to consumers from direct consumption of the edible parts of the plants.

The theses correspond to:

- ‘C’ (negative control), in which the plants are grown using irrigation with laboratory source water.
- ‘B’ (plants treated with microbial biomass), in which the plants are grown using fertigation with 10^6 cfu/mL of *B. subtilis*.
- ‘S’ (plants treated with ammonium sulphate), in which the plants are grown using fertigation with 1g/l of $(\text{NH}_4)_2\text{SO}_4$.

Microbial biomass

The microbial mass was obtained as reported in the basil experiment.

Equipment for plant cultivation

The set-up conditions are similar to those reported for the basil experiment, using taller cylinders (Figure 8).



Figure 8. Cylinder housing at the time of potato transplanting.

The orientation of the farming system and the distribution of the different treatments are shown below (Figure 9).

The window side of the laboratory	Back		Laboratory door side
	Potatoes		
	C2	S2	
	B2	S1	
	C1	B1	
Front			

Figure 9. Orientation of the cultivation system and the distribution of the different treatments. ‘C’ (negative control, water), ‘B’ (plants treated with microbial biomass), ‘S’ (plants treated with ammonium sulphate).

In practice, after the first irrigation carried out at transplanting, performed for all plants with spring water, the treatments were differentiated as follows:

- Cylinders C irrigation with spring water only.

- Cylinders B fertigation with spring water containing microbial biomass 2 g/L (7.2×10^8 cfu *B. subtilis*/g).
- Cylinders S fertigation with spring water containing ammonium sulphate 1 g/L.

Taking the plant collar as a reference, all treatments are administered in each cylinder through holes in the soil to a depth of approximately 1/3 of the soil height.

The holes are oriented to the east and west as shown below, and 250 mL of water, water containing biomass or water containing ammonium sulphate is administered to each hole (Figure 10).

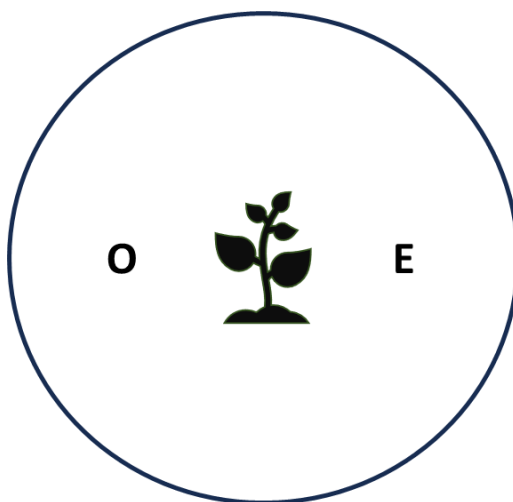


Figure 10. Orientation of holes for potato treatments.

Reference time stamp

The trial followed the growth cycle of potatoes plants and lasted approximately two months.

The reference timetable used to track the different phenological stages of the plants, as well as the timing of watering and treatments, is shown below (Table 7).

Table 7. Timetable of the pilot experimental activity for evaluating the biostimulant effect of microbial biomass containing *B. subtilis* on potatoes plants.

March - April 2024									
25	26	27	28	29	30	31	01	02	03
00	01	02	03	05	05	06	07	08	09
April 2024									
04	05	06	07	08	09	10	10	11	12

10	11	12	13	14	15	16	17	18	19
13	14	15	16	17	18	19	20	21	22
20	21	22	23	24	25	26	27	28	29
April – May 2024									
23	24	25	26	27	28	29	30	1	2
30	31	32	33	34	35	36	37	38	39
May 2024									
3	4	5	6	7	8	9	10	11	12
40	41	42	43	44	45	46	47	48	49
13	14	15	16	17	18	19	20	21	22
50	51	52	53	54	55	56	57	58	59

Day “0” is considered to be the day on which the plants were transplanted.

The trial was concluded when the flower stalks appeared.

Growing conditions

The growing conditions are similar to those reported in the basil experiment.

Growing substrate

To create the substrate columns, each cylinder was filled with Primavita soil (Terflor®), supplemented with monopotassium phosphate + dipotassium phosphate + potassium sulphate + magnesium sulphate + iron sulphate.

Each of these salts was administered in a quantity of 1 g per cylinder.

Germplasm

The germplasm used was the ‘Riccione di Napoli’ potato variety.

Six sprouted tubers were used, four of which were cut lengthwise and two left whole.

Plant cultivation

The potatoes were placed in cylinders with an internal diameter of 19 cm and a height of 61 cm.

Each cylinder contained one tuber.

The association between plants and cylinders is shown above.

For the first irrigation after transplanting, spring water was used and administered on the surface.

The water inputs per thesis and per cylinder are shown below (Table 8).

Table 8. Water supply and treatments for the plants of the 3 considered trials (water, microbial biomass and ammonium sulphate).

Time	Thesis					
	Water		Microbial biomass		Ammonium sulphate	
	Cylinder1	Cylinder 2	Cylinder 1	Cylinder 2	Cylinder 1	Cylinder 2
00	Water 1.500 mL	Water 1.500 mL	Water 1.500 mL	Water 1.500 mL	Water 1.500 mL	Water 1.500 mL
+ 3	Water 1.000 mL	Water 1.000 mL	Water 1.000 mL	Water 1.000 mL	Water 1.000 mL	Water 1.000 mL
+ 10	Water 1.000 mL	Water 1.000 mL	Water 1.000 mL	Water 1.000 mL	Water 1.000 mL	Water 1.000 mL
+ 16	Water 500 mL	Water 500 mL	Water 500 mL + 1,000 g microbial biomass	Water 500 mL + 1,000 g microbial biomass	Water 500 mL + 0,500 g ammonium sulphate	Water 500 mL + 0,500 g ammonium sulphate
+ 22	Water 500 mL	Water 500 mL	Water 500 mL	Water 500 mL	Water 500 mL	Water 500 mL
+ 26	Water 500 mL	Water 500 mL	Water 500 mL + 1,000 g microbial biomass	Water 500 mL + 1,000 g microbial biomass	Water 500 mL + 0,500 g ammonium sulphate	Water 500 mL + 0,500 g ammonium sulphate
+ 31	Water 500 mL	Water 500 mL	Water 500 mL	Water 500 mL	Water 500 mL	Water 500 mL
+ 34	Water 500 mL	Water 500 mL	Water 500 mL	Water 500 mL	Water 500 mL	Water 500 mL
+ 36	Water 300 mL	Water 300 mL	Water 300 mL	Water 300 mL	Water 300 mL	Water 300 mL
+ 40	Water 600 mL	Water 600 mL	Water 600 mL	Water 600 mL	Water 600 mL	Water 600 mL
+ 45	Water 600 mL	Water 600 mL	Water 600 mL	Water 600 mL	Water 600 mL	Water 600 mL
+ 47	Water 400 mL	Water 400 mL	Water 400 mL	Water 400 mL	Water 400 mL	Water 400 mL

Phenotypic observations and biometric measurements

Throughout the growing period, observations were made on the condition of the plants and, at the end of the trial, various biometric parameters were measured.

Parameters such as shape, appearance, weight, size and ripeness of the tubers were considered [26].

2.3.2 Biostimulant test on Basil

Rationale

Three theses were considered to evaluate the effectiveness of the microbial biomass in promoting the growth of important crops and improving soil fertility without any negative effect, in standard soil under controlled ventilation and lightning conditions.

The theses correspond to:

- ‘C’ (untreated control), in which plants are grown using irrigation with laboratory source water.
- ‘B’ (plants treated with microbial biomass), in which plants are grown using fertigation with the microbial biomass containing *B. subtilis* ET-1 spores.
- ‘S’ (treated control), in which plants are grown using fertigation with ammonium sulphate ((NH₄)₂SO₄).

To evaluate results, biometric parameters such as plant height, number of nodes, fresh and dry weights, were considered, such as Chlorophyll Content Index (CCI) and phenotypic observations.

Microbial biomass

The microbial biomass containing *B. subtilis* ET-1 spores was obtained using the same methods described for the pilot test on basil.

Germoplasm

The germplasm used was Fenix basil.

The starting material consisted of seedlings in the third and fourth true leaf stage, previously sown directly in pots and grown in a greenhouse before being transplanted under ventilated lamps.

Cultivation substrate

To create the substrate columns, each cylinder was filled with Completo® (Vigor Plant®) soil, supplemented with monopotassium phosphate + dipotassium phosphate + potassium sulphate + magnesium sulphate + iron sulphate.

Each of these salts was administered in a quantity of 0.2 g per cylinder.

Equipment for plant cultivation

For the purpose of growing the plants, transparent polycarbonate cylinders with open bases were used, placed on plastic saucers of appropriate dimensions (Figure 11).



Figure 11. Housing for cylinders containing basil seedlings. Housing for cylinders containing basil seedlings.

The cultivation system consisting of cylinders and saucers was placed under “ventilating lamps” designed by ENEA, conceived, designed and manufactured as part of the PON ISAAC Project - Innovative Lighting System for Indoor Plant Cultivation to Improve Human Wellbeing (CUP B88I17000590008), capable of providing light with a spectrum and intensity suitable for plant cultivation in the laboratory, combined with ventilation calibrated to the needs of indoor plants.

The orientation of the farming system and the distribution of the different treatments are shown below (Figure 12).

Window side of the laboratory	Back				Laboratory door side
	C1	C2	B3	S3	
	S2	B2	C3	B4	
	B1	S1	S4	C4	
	Front				

Figure 12. Orientation of the cultivation system and the distribution of the different treatments. 'C' (negative control, water), 'B' (plants treated with microbial biomass), 'S' (plants treated with ammonium sulphate).

In practice, the treatments were differentiated as follows:

- Cylinders C irrigation with spring water only.
- Cylinders B fertigation with spring water containing 0.2 g microbial biomass (7.2×10^8 cfu *B. subtilis*/g).
- Cylinders S fertigation with spring water containing 0.4 g and 0.2 g of ammonium sulphate.

After basal fertilisation with a mixture of salts for all cylinders, the treatments with microbial biomass were carried out at two different times: at transplanting (T0) and 10 days after transplanting (T1) (Figure 13).

Ammonium sulphate was administered in a single treatment 10 days after transplanting.

Spring water was administered at the time of treatment and whenever the plants' water requirements demanded it.

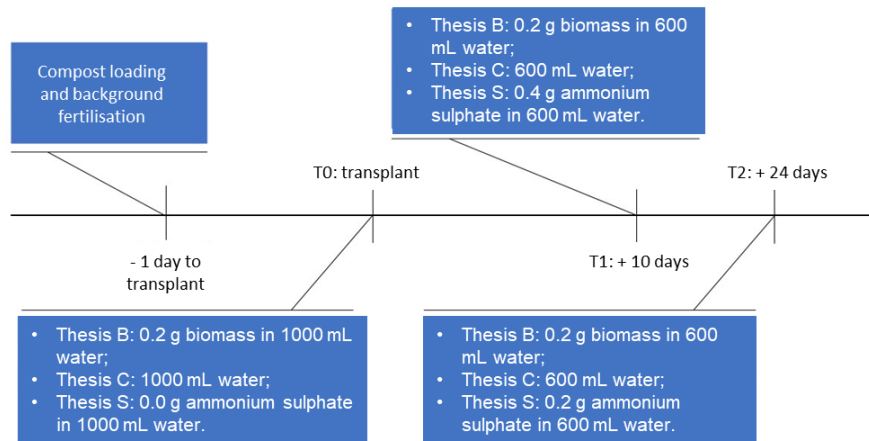


Figure 13. Basil treatment schedule.

At T0, biomass treatment was carried out by simple irrigation.

At T1, taking the plant collar as a reference, biomass and ammonium sulphate treatments were administered in each cylinder through holes in the soil to a depth of approximately 1/3 of the soil height (- 7 cm).

The holes were oriented according to the four cardinal points as shown below, and 50 mL of water containing biomass or water containing ammonium sulphate was administered to each hole, for a total of 200 mL per cylinder (Figure 14).

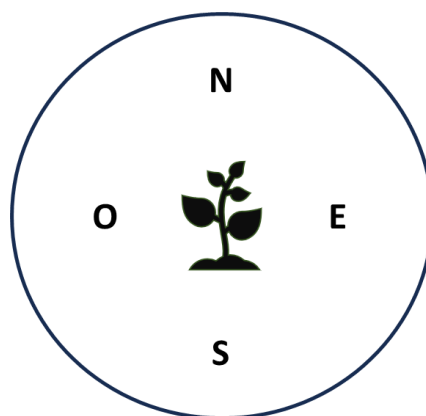


Figure 14. Orientation of holes for basil treatments.

An additional 400 mL of water was administered for normal irrigation to meet water requirements and promote better distribution of the treatments.

In thesis C, 600 mL of water was administered for simple irrigation.

A total of 600 mL of water was administered for each thesis at T1 (Figure 15).



Figure 15. Post-treatment crop setting up at T1

At T2, taking the plant collar as a reference, the biomass and ammonium sulphate treatments, as well as the water in the control plants, were administered into each cylinder through holes in the soil to a depth of approximately 15 cm.

The holes were oriented according to the four cardinal points as previously shown, and 100 mL of water, water containing biomass or water containing ammonium sulphate was administered to each hole, for a total of 400 mL per cylinder.

An additional 200 mL of water was administered through normal irrigation in order to meet water requirements and promote better distribution of the treatments.

A total of 600 mL of water was administered for each thesis at T2.

Reference time stamp

Day 0 corresponds to the transplanting of the seedlings (Table 9).

Table 9. Timetable of the pilot experimental activity for evaluating the biostimulant effect of microbial biomass containing *B. subtilis* on basil plants.

June 2024									
04	05	06	07	08	09	10	11	12	13
00	01	02	03	05	05	06	07	08	09
14	15	16	17	18	19	20	21	22	23
10	11	12	13	14	15	16	17	18	19
June – July 2024									
24	25	26	27	28	29	30	01	02	03
20	21	22	23	24	25	26	27	28	29
July 2024									
04	05	06	07	08	09	10	11	12	13
30	31	32	33	34	35	36	37	38	39
14	15	16	17	18	19	20	21	22	23
40	41	42	43	44	45	46	47	48	49
July – August 2024									
24	25	26	27	28	29	30	31	01	02
50	51	52	53	54	55	56	57	58	59
August 2024									
03	04	05	06	07	08	09	10	11	12
60	61	62	63	64	65	66	67	68	69
13	14	15	16	17	18	19	20	21	22
70	71	72	73	74	75	76	77	78	79
August - September 2024									
23	24	25	26	27	28	29	30	31	01
80	81	82	83	84	85	86	87	88	89
September 2024									
02	03	04	05	06	07	08	09	10	11
90	91	92	93	94	95	96	97	98	99
12	13	14	15	16	17	18	19	20	21
100	101	102	103	104	105	106	107	108	109
September – October 2024									
22	23	24	25	26	27	28	29	30	01
110	111	112	113	114	115	116	117	118	119
02	03	04	05	06	07	08	09	10	11
120	121	122	123	124	125	126	127	128	129

Forty-one and fifty-one days after transplanting, respectively, chlorophyll content index measurements and biometric surveys were carried out. Dry weights were determined fifty-seven days after transplanting.

Breeding conditions

The trolley as a whole was fitted with four square lighting panels equipped with LEDs supplied by Becar.

Only the LEDs emitting Cool White light were activated in the lamps, with 75% of the maximum value emitted.

The emission values of the lighting system were set to emit a photosynthetically active photon flux of approximately $205 \mu\text{mol}\cdot\text{m}^{-2}\cdot\text{s}^{-1}$ when measured in the centre of the platform at plant level, approximately 90 cm from the lamp diffuser.

The measurement was carried out using a system consisting of the LI-190/R sensor (LI-COR) and the LI-1500 measurement processor (LI-COR) (Figure 16).

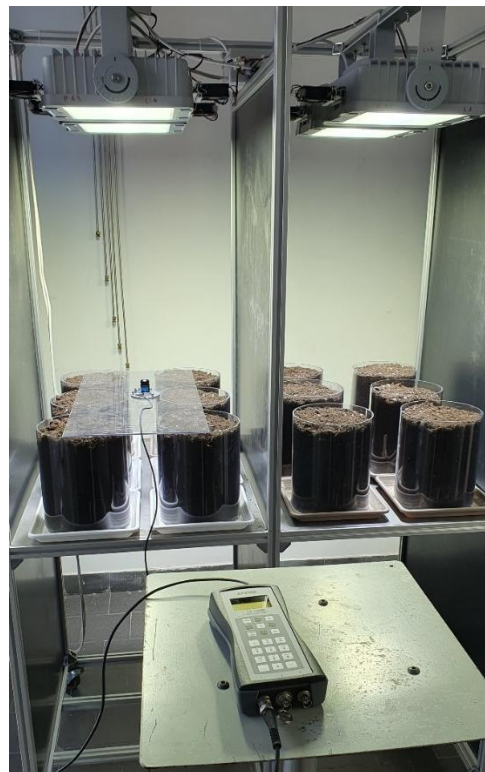


Figure 16. Measurement of photosynthetically active photon flux.

The photoperiod was 14 hours of light and 10 hours of darkness per day, with the lamps switching on at 06:00 and switching off at 20:00.

Ventilation was directed from the bottom upwards and was active 24 hours a day.

The thermoperiod was that of the laboratory and is shown below (Table 10):

Table 10. Maximum and minimum temperatures recorded in the laboratory during the growing cycle of basil plants.

Time	Temperature (°C)	
	Minimum degree	Maximum degree
00	24	27
+ 10	25	30
+ 13	26	29
+ 17	26	29
+ 20	26	31
+ 21	26	29
+ 22	26	30
+ 24	26	29
+ 27	26	31
+ 31	26	31
+ 34	28	31
+ 37	28	29
+ 41	28	33
+ 44	29	31
+ 48	29	29
+ 51	29	31

Plant cultivation

The Basil was transplanted into cylinders with an internal diameter of 19 cm and a height of 25 cm.

Three days after transplanting, the weakest seedlings were removed, leaving three seedlings per cylinder (Figure 17).



Figure 17. Details of the 3 basil plants.

For the first irrigation after treatment, spring water supplied to the surface was used.

The water inputs per thesis and per cylinder are shown below (Table 11).

Table 11. Water supply and treatments for the plants of the 3 considered trials (water, microbial biomass and ammonium sulphate).

Time	Thesis											
	Water (C)				Biomass (B)				Ammonium sulphate (S)			
	1	2	3	4	1	2	3	4	1	2	3	4
00	1.000 mL	1.000 mL	1.000 mL	1.000 mL	1.000 mL + 0,2 g B	1.000 mL + 0,2 g B	1.000 mL + 0,2 g B	1.000 mL + 0,2 g B	1.000 mL	1.000 mL	1.000 mL	1.000 mL
+ 10	600 mL	600 mL	600 mL	600 mL	600 mL + 0,2 g B	600 mL + 0,2 g B	600 mL + 0,2 g B	600 mL + 0,2 g B	600 mL + 0,4 g S	600 mL + 0,4 g S	600 mL + 0,4 g S	600 mL + 0,4 g S
+ 17	150 mL	150 mL	150 mL	150 mL	150 mL	150 mL	150 mL	150 mL	150 mL	150 mL	150 mL	150 mL
+ 24	600 mL	600 mL	600 mL	600 mL	600 mL + 0,2 g B	600 mL + 0,2 g B	600 mL + 0,2 g B	600 mL + 0,2 g B	600 mL + 0,2 g S	600 mL + 0,2 g S	600 mL + 0,2 g S	600 mL + 0,2 g S
+ 31	200 mL	200 mL	200 mL	200 mL	200 mL	200 mL	200 mL	200 mL	200 mL	200 mL	200 mL	200 mL
+ 34	500 mL	500 mL	500 mL	500 mL	500 mL	500 mL	500 mL	500 mL	500 mL	500 mL	500 mL	500 mL

+ 37	500 mL	500 mL	500 mL	500 mL	500 mL	500 mL	500 mL	500 mL	500 mL	500 mL	500 mL	500 mL
+ 41	300 mL	300 mL	300 mL	300 mL	300 mL	300 mL	300 mL	300 mL	300 mL	300 mL	300 mL	300 mL
+ 44	700 mL	700 mL	700 mL	700 mL	700 mL	700 mL	700 mL	700 mL	700 mL	700 mL	700 mL	700 mL
+ 48	200 mL	200 mL	200 mL	200 mL	200 mL	200 mL	200 mL	200 mL	200 mL	200 mL	200 mL	200 mL
+ 51	500 mL	500 mL	500 mL	500 mL	500 mL	500 mL	500 mL	500 mL	500 mL	500 mL	500 mL	500 mL

Phenotypic observations and biometric measurements

Throughout the cultivation period, observations were made on the condition of the plants and, at the end of the trial, various biometric parameters were recorded.

The height of the plants and the number of nodes for each replicate were considered.

The height was determined on the tallest stem of the tallest plant in the group of plants present in the given cylinder, measured from the collar to the point of intersection of the floral axis, even straightening the stem along the metre.

The number of nodes was determined by counting the recognisable nodes on the main stem of the tallest plant in the group of plants in the given cylinder, starting from the first node above the cotyledons and ending at the last node before the floral scape.

To determine the biomass yield, 51 days after transplanting, the fresh weights were determined, then the leaves, flower scapes and stems collected were left to dry in the air in the laboratory until they reached a constant weight.

The plants were cut at the collar and the leaves and flower scapes were separated from the stems.

For the survey, fallen leaves in the cylinders and completely withered or dry biomass were not taken into account.

After 57 days, a constant weight was reached and the dry weight of leaves, stems and flower stalks was determined for all samples. The samples were then placed in paper bags and stored in a cool, dry place.

Measurement of Chlorophyll Content Index

Forty-one days after transplantation, the Chlorophyll Content Index (CCI) was measured using a SPAD-502 Plus meter (Konica Minolta).

The measurements were taken as if there were only one plant per cylinder, measuring four leaves per cylinder, two apical and two medians, proceeding from the apical to the median leaves.

Freeze-drying of plant samples

118 days after transplantation, the samples, previously stored in paper bags, were taken to the ENEA Trisaia Research Centre for freeze-drying using a CHRIST ALPHA 1 - 4 bench-top freeze dryer.

The samples were crushed in a mortar (leaves), cut with scissors (stems) or left as they were (flower stalks), placed in 100 mL and 250 mL Lenz Laborglasinstrumente™ flasks and treated with liquid nitrogen before the flasks were attached to the freeze dryer (Figure 18).



Figure 18. Steps in the freeze-drying process.

The freeze-drying cycles were considered complete when the pressure reached 0.08 mbar.

The first freeze-drying cycle, which involved samples 1 to 11, lasted approximately 18 hours.

The second freeze-drying cycle involved samples 1A to 13A and lasted approximately 21 hours.

The third freeze-drying cycle involved samples 1B to 10B and lasted approximately 22 hours.

At the end of each cycle, the samples were placed in plastic bags and vacuum sealed.

2.3.3 Coating basil seeds with microbial biomass containing *B. subtilis* ET-1

It was decided to coat basil seeds (*Ocimum basilicum* L.) with microbial biomass containing the selected strain of *B. subtilis* to assess not only the suitability of this biomass for coating seeds, but also to ensure that the coating did not adversely affect seed germination and seedling development and, therefore, the production cycle.

Basil was chosen as the model plant because of the widespread cultivation of the species, the economic importance of its cultivation and the supply chain derived from it.

Chitosan coating test

A coating test with chitosan was performed to determine the best polysaccharide for seed coating. To assess basil germination and growth, the following hypotheses were proposed:

- 1) Seeds coated with chitosan.
- 2) Uncoated seeds.

For each hypothesis, sowing will be carried out both in pots filled with soil and in Petri dishes lined with absorbent paper.

Specifically, six pots were used for each hypothesis, and each pot contained six seeds, for a total of 36 seeds per hypothesis.

In addition, a Petri dish containing 36 seeds was used for each hypothesis.

The test results were not considered for statistical analysis and are reported in Annex B.

Seed coating protocol

Seeds were coated with a chitosan-based formulation using an immersion treatment. The procedure consisted of soaking the seeds in a chitosan solution and subsequently air-drying them until they returned to their initial moisture content. Specific operational parameters

(e.g., soaking time, solution-to-seed ratio) followed the internal laboratory protocol routinely adopted for seed coating.

Seeding equipment

Plastic pots filled with soil and Petri dishes lined with absorbent paper were used for plant cultivation.

Each pot contained 6 seeds, and each dish contained 36 seeds.

The pots were square, with sides measuring 6 cm and a height of approximately 7 cm.

Six pots filled with Primavita (Terflor®) soil were used for both theses.

Each pot contained 6 basil seeds arranged in 2 rows of 3 seeds (Figure 19).

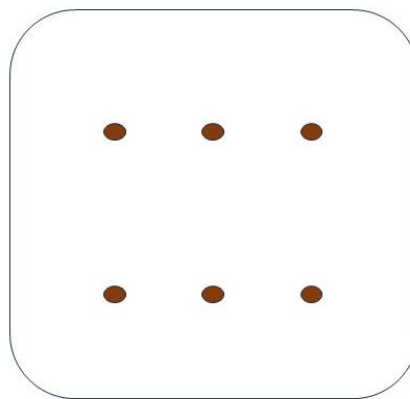


Figure 19. Diagram showing the arrangement of basil seeds in a pot.

Once the seeds had been planted, 100 mL of spring water was administered per pot (Figure 20).

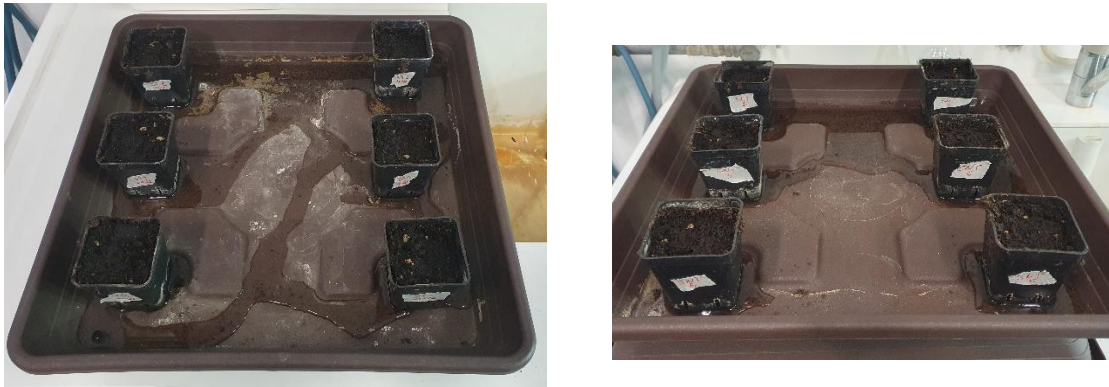


Figure 20. Pots at the end of basil sowing.

The pots were covered with square saucers to create the darkness necessary for germination.

Two Petri dishes with an internal diameter of 9 cm were also used for plant cultivation, one per thesis.

Two overlapping discs of absorbent paper were placed at the bottom of each dish.

The basil seeds were placed on these discs with the aid of tweezers.

Each dish contained 36 seeds arranged in 6 rows of 6 seeds to form a square.

The arrangement is shown below (Figure 21).

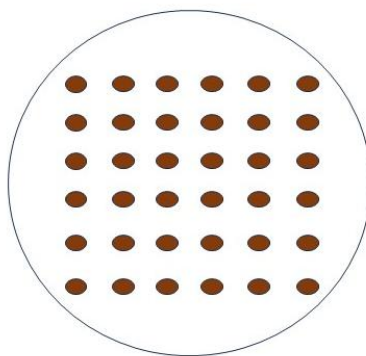


Figure 21. Diagram showing the arrangement of basil seeds in a Petri dish.

Once the seeds had been arranged, the paper discs on all the plates were moistened with 4 mL of spring water using a disposable pipette (Figure 22).

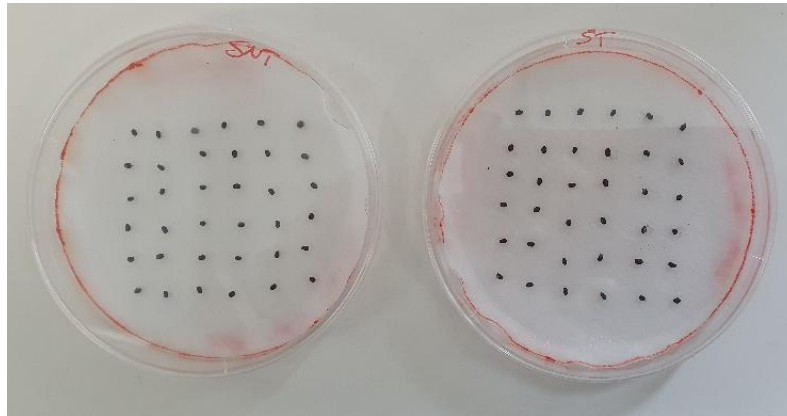


Figure 22. Petri dishes at the end of basil sowing.

The plates, once assembled and sealed, were covered with aluminium foil to create the darkness necessary for germination.

Reference time stamp

Day 0 corresponds to the moment of sowing. The test has been considered complete at the end of the germination process (Table 12).

Table 12. Timetable of the pilot experimental activity for evaluating the effect of coating with chitosan on basil seeds.

November 2024									
20	21	22	23	24	25	26	27	28	29
00	01	02	03	04	05	06	07	08	09
November - December 2024									
30	01	02	03	04	05	06	07	08	09
10	11	12	13	14	15	16	17	18	19
December 2024									
10	11	12	13	14	15	16	17	18	19
20	21	22	23	24	25	26	27	28	29
20	21	22	23	24	25	26	27	28	29
30	31	32	33	34	35	36	37	38	39

Rearing conditions

The thermoperiod was that used in the laboratory and is shown below (Table 13).

Table 13. Maximum and minimum temperatures recorded in the laboratory during the basil seed coating test with chitosan.

Time	Temperature (°C)	
	Minimum degree	Maximum degree
00	18	23
+ 01	21	23
+ 05	16	23
+ 07	19	24
+ 09	23	24
+ 16	19	24

Germplasm

Seeds of “classic Italian” basil (*Ocimum basilicum* L.) were used.

The starting material consisted of 72 seeds coated with chitosan and 72 uncoated seeds.

Cultivation

Spring water was used for the first irrigation after sowing.

The water supplies for each pot and tray are shown below (Tables 14 and 15).

Table 14. Water supply for chitosan-coated and uncoated basil seeds.

Time	Pots											
	Coated seeds						Uncoated seeds					
	1	2	3	4	5	6	1	2	3	4	5	6
00	100 mL	100 mL	100 mL	100 mL	100 mL	100 mL	100 mL	100 mL	100 mL	100 mL	100 mL	100 mL
+ 09	50 mL	50 mL	50 mL	50 mL	50 mL	50 mL	50 mL	50 mL	50 mL	50 mL	50 mL	50 mL

Table 15. Water supply for chitosan-coated and uncoated basil seeds.

Time	Petri dishes	
	Coated seeds	Uncoated seeds
00	4 mL	4 mL

Germination percentage

The germination percentage was also determined for both the seeds placed in Petri dishes and those placed in pots:

$$GP = \frac{Nr. \text{ germinated seeds}}{Nr. \text{ total seeds}} \times 100$$

GP = germination percentage.

Nr. germinated seeds = number of seeds that have sprouted roots.

Nr. total seeds = number of seeds present in the plate.

The seeds were therefore found to be suitable for the coating test.

In particular, the germination percentage was determined at the moment of root emergence for seeds placed in Petri dishes and at the moment of shoot emergence for seeds placed in pots.

Phenotypic observations

Throughout the cultivation period, observations were made on the condition of the seeds and seedlings, assessing the growth of the rootlets in terms of length and branching for the seeds planted in Petri dishes.

Evaluation of the biostimulant activity of microbial biomass through coating of Basil seeds

Rationale

It was decided to coat Prospera F1 basil seeds (*Ocimum basilicum* L.) with pectin and microbial biomass to assess not only the ability of this biomass to promote germination and biostimulation, but also to ensure that the coating did not negatively affect seed germination, seedling development and, therefore, the production cycle.

Basil was chosen as the model plant due to its widespread cultivation, the economic importance of its cultivation, and the supply chain derived from it.

Pectin was chosen as the coating polymer instead of chitosan, which was used in previous germination tests, because pectin has greater solubility in water and moist soils, making it particularly suitable for applications where rapid release (within a few days) is required.

To evaluate the germination and development of basil, the following hypotheses were considered:

1. Seeds coated with pectin.
2. Uncoated seeds.
3. Seeds coated with pectin and microbial biomass.

For each hypothesis, sowing was carried out in polycarbonate cylinders filled with soil and placed under a ventilated lamp.

Each cylinder contained 20 seeds, totalling 240 seeds.

Four replicates were considered for each hypothesis, for a total of 80 seeds per hypothesis.

The data obtained are reported in full in Annex 1.

Microbial biomass

Microbial biomass was obtained using the same methods previously described for biostimulation tests.

Germoplasm

The germplasm used was Basil Prospera F1 from Fenix S.r.l.

To assess the germination capacity of the seeds, and therefore their suitability for the coating test, an *in vitro* germination test was carried out.

The seeds were placed in a Petri dish lined with two discs of absorbent paper soaked in 4 mL of water and covered with aluminium foil to create the darkness necessary for germination.

The dish contained 20 seeds arranged in five rows of four seeds each.

Germination began 4 days after sowing on 07/01/2025, affecting 9 out of 20 seeds.

Five days after sowing, 18 out of 20 seeds had germinated, with a germination rate of 90%.

The germination percentage was calculated as follows:

$$GP = \frac{\text{No. of germinated seeds}}{\text{Total no. of seeds}} \times 100$$

- GP = germination percentage.

- No. of germinated seeds = number of seeds that have sprouted a root.
- Total no. of seeds = number of seeds present in the plate.

The seeds were therefore found to be suitable for the coating test.

Seed coating protocol

To coat the Prospera F1 basil seeds, 50 mL of an aqueous solution containing 2% by weight of pectin (AGLUPECTIN LC-S12P, SilvaTeam Ingredients) were prepared by dissolving the polymer in double-distilled water and stirring at 70°C until completely dissolved, thus obtaining a homogeneous solution.

1% by weight of Tween® 80 (P1754, Sigma Aldrich) was added to the polymer solution to improve the interaction between the pectin and the solvent, as well as to promote better dispersion and stability of the solution. Tween® 80 acts as a surfactant, reducing surface tension and facilitating the solubilisation of the polymer. The solution was then stirred at room temperature until the surfactant was completely dissolved.

The solution was divided into two aliquots of equal volume (5 mL), one of which was used as is for coating the seeds in the “pectin coating” thesis.

Then 0.05 g of microbial biomass containing *B. subtilis* was added to the second 5 mL aliquot. The final concentration of microbial biomass in the solution was 10 mg/mL.

The basil seeds were immersed in the solution (with or without microbial biomass) for 60 seconds.

Finally, the seeds were then drained and left to air dry for 24 hours on nets.

On 17/02/2025, the weight was determined using an analytical balance for an aliquot of 20 seeds for each thesis in order to determine the amount of pectin and biomass present per seed. The data are reported below (Table 16):

Table 16. Weights of seeds of the thesis coated with pectin (C), coated with microbial biomass and pectin (B) and uncoated (N).

Thesis	Weight of 20 seeds (g)	Weight of the coating only for 20 seeds (g)	Coating weight per single seed (g)
C	0,0323	0,0034	0,00017
B	0,0578	0,0289	0,00145
N	0,0289	-	-

Equipment for plant cultivation

For sowing and growing the plants, transparent polycarbonate cylinders with open bases were used, placed on plastic saucers of appropriate sizes.

The cultivation system consisting of cylinders and saucers was placed under “ventilating lamps” designed by ENEA, conceived, designed and manufactured as part of the PON ISAAC Project - Innovative Lighting System for Indoor Plant Cultivation to Improve Human Wellbeing (CUP B88I17000590008), capable of providing light with a spectrum and intensity suitable for plant cultivation in the laboratory, combined with ventilation calibrated to the needs of indoor plants.

The orientation of the breeding system and the distribution of the theses are shown below (Figure 23).

Window side of the laboratory	Back				Door side of the laboratory
	Thesis C1	Thesis C2	Thesis B3	Thesis N4	
	Thesis N1	Thesis B2	Thesis C3	Thesis B4	
	Thesis B1	Thesis N2	Thesis N3	Thesis C4	
	Front				

Figure 23. Orientation of the cultivation system and the distribution of the different treatments. ‘C’ (coating with pectin), ‘B’ (coating with pectin and microbial biomass), ‘N’ (uncoated seeds).

In practice, the theses were differentiated as follows:

- 1) Thesis C: cylinders seed coated with pectin.
- 2) Thesis B: cylinders seeds coated with 10 mg of microbial biomass/mL of aqueous pectin solution (7.2×10^8 cfu *B. subtilis*/g).
- 3) Thesis N: uncoated seeds.

Spring water was administered at the time of sowing and whenever the plants' water requirements demanded it.

Reference time stamp

Day zero corresponds to the moment of sowing (Table 17).

Table 17. Timetable of the experimental activity to evaluate the effects of coating with pectin and microbial biomass on basil seeds compared to seeds coated only with pectin and uncoated seeds.

January - February 2025									
24	25	26	27	28	29	30	31	01	02
00	01	02	03	04	05	06	07	08	09
February 2025									
03	04	05	06	07	08	09	10	11	12
10	11	12	13	14	15	16	17	18	19
13	14	15	16	17	18	19	20	21	22
20	21	22	23	24	25	26	27	28	29
February – March 2025									
23	24	25	26	27	28	01	02	03	04
30	31	32	33	34	35	36	37	38	39
March 2025									
05	06	07	08	09	10	11	12	13	14
40	41	42	43	44	45	46	47	48	49
15	16	17	18	19	20	21	22	23	24
50	51	52	53	54	55	56	57	58	59
March - April 2025									
25	26	27	28	29	30	31	01	02	03
60	61	62	63	64	65	66	67	68	69
April 2025									
04	05	06	07	08	09	10	11	12	13
70	71	72	73	74	75	76	77	78	79
14	15	16	17	18	19	20	21	22	23
80	81	82	83	84	85	86	87	88	89
April - May 2025									
24	25	26	27	28	29	30	01	02	03
90	91	92	93	94	95	96	97	98	99

Thirteen days after sowing, the germination percentage was calculated.

Sixty days after sowing, the chlorophyll content index was measured and biometric measurements were taken. This marked the end of the trial.

Dry weights were determined 95 days after sowing.

Growing medium

To create the substrate columns, each cylinder was filled with Completo® (Vigor Plant®) soil, supplemented with monopotassium phosphate + dipotassium phosphate + potassium sulphate + magnesium sulphate + iron sulphate.

Each of these salts was administered in a quantity of 0.2 g per cylinder.

In addition, 0.2 g of naturally occurring cohesive soil from Piacenza was added to the soil in each cylinder at the time of basal fertilisation.

Germination percentage

The germination percentage was determined thirteen days after sowing, at the time of sprouting, using the following formula:

$$GP = \frac{\text{No. germinated seeds}}{\text{Total no seeds}} \times 100$$

- GP = germination percentage.
- No. of germinated seeds = number of seeds that have produced cotyledons.
- Total no. of seeds = number of seeds present in each cylinder.

Plant cultivation

When the cylinders were filled with soil on 17/01/2025, 2 L of spring water were added to each cylinder.

The basil seeds were arranged in 5 rows of 4 seeds in cylinders with an internal diameter of 19 cm and a height of 25 cm.

Thirty-one days after sowing, the number of seedlings was standardised to four in each cylinder.

For the first irrigation after sowing, spring water was used and administered on the surface.

The water inputs per thesis and per cylinder are shown below (Table 18).

Table 18. Water supply for pectin-coated, biomass-coated and uncoated basil seeds.

Time	Thesis											
	Pectin (C)				Biomass (B)				Uncoated (N)			
	1	2	3	4	1	2	3	4	1	2	3	4
00	700 mL	700 mL	700 mL	700 mL	700 mL	700 mL	700 mL	700 mL	700 mL	700 mL	700 mL	700 mL
+ 06	250 mL	250 mL	250 mL	250 mL	250 mL	250 mL	250 mL	250 mL	250 mL	250 mL	250 mL	250 mL
+ 10	100 mL	100 mL	100 mL	100 mL	100 mL	100 mL	100 mL	100 mL	100 mL	100 mL	100 mL	100 mL
+ 13	500 mL	500 mL	500 mL	500 mL	500 mL	500 mL	500 mL	500 mL	500 mL	500 mL	500 mL	500 mL
+ 21	200 mL	200 mL	200 mL	200 mL	200 mL	200 mL	200 mL	200 mL	200 mL	200 mL	200 mL	200 mL
+ 28	250 mL	250 mL	250 mL	250 mL	250 mL	250 mL	250 mL	250 mL	250 mL	250 mL	250 mL	250 mL
+ 35	200 mL	200 mL	200 mL	200 mL	200 mL	200 mL	200 mL	200 mL	200 mL	200 mL	200 mL	200 mL
+ 38	100 mL	100 mL	100 mL	100 mL	100 mL	100 mL	100 mL	100 mL	100 mL	100 mL	100 mL	100 mL
+ 42	200 mL	200 mL	200 mL	200 mL	200 mL	200 mL	200 mL	200 mL	200 mL	200 mL	200 mL	200 mL
+ 45	100 mL	100 mL	100 mL	100 mL	100 mL	100 mL	100 mL	100 mL	100 mL	100 mL	100 mL	100 mL
+ 49	200 mL	200 mL	200 mL	200 mL	200 mL	200 mL	200 mL	200 mL	200 mL	200 mL	200 mL	200 mL

+ 52	200 mL	200 mL	200 mL	200 mL	200 mL	200 mL	200 mL	200 mL	200 mL	200 mL	200 mL	200 mL
+ 56	400 mL	400 mL	400 mL	400 mL	400 mL	400 mL	400 mL	400 mL	400 mL	400 mL	400 mL	400 mL

Breeding conditions

The trolley was equipped with four square lighting panels with LEDs supplied by Becar.

Only the LEDs emitting Cool White light were activated in the lamps, with 50% of the maximum value emitted from sowing to germination after 6 days. From germination onwards, the emission was increased to 70% of the maximum value.

The emission values of the lighting system were set to emit a photosynthetically active photon flux of approximately $148 \mu\text{mol}\cdot\text{m}^{-2}\cdot\text{s}^{-1}$ (50% of the maximum value) and $206 \mu\text{mol}\cdot\text{m}^{-2}\cdot\text{s}^{-1}$ (70% of the maximum value). The photosynthetically active photon flux was determined by placing the probe on the back of a plastic tray resting on the cylinders in a central position, with a distance between the lower surface of the diffuser and the probe of approximately 57.5 cm.

By setting the light output to 70% of the maximum value and placing the sensor close to the diffusers, a photosynthetically active photon flux of $4460 \mu\text{mol}\cdot\text{m}^{-2}\cdot\text{s}^{-1}$ was recorded for lamp 1, $4460 \mu\text{mol}\cdot\text{m}^{-2}\cdot\text{s}^{-1}$ for lamp 2, $4482 \mu\text{mol}\cdot\text{m}^{-2}\cdot\text{s}^{-1}$ for lamp 3 and $4488 \mu\text{mol}\cdot\text{m}^{-2}\cdot\text{s}^{-1}$ for lamp 4.

The measurement was carried out using the LI-190/R (LI-COR) sensor and the LI-1500 (LI-COR) measurement processor (Figure 24).



Figure 24. Measurement of photosynthetically active photon flux.

The photoperiod was 14 hours of light and 10 hours of darkness per day, with the lamps switching on at 6 a.m. and switching off at 8 p.m.

Ventilation was directed from the bottom upwards and was active 24 hours a day.

The thermoperiod was that of the laboratory and is shown below (Table 19):

Table 19. Maximum and minimum temperatures recorded in the laboratory during the basil seed coating test with pectin and microbial biomass.

Time	Temperature (°C)	
	Minimum degree	Maximum degree
00	14	23
+ 03	18	22
+ 06	18	24

+ 10	17	22
+ 13	15	22
+ 17	15	21
+ 19	16	20
+ 21	20	24
+ 24	16	23
+ 26	17	22
+ 31	17	22
+ 35	17	23
+ 38	18	22
+ 40	17	22
+ 45	18	23
+ 52	19	24
+ 60	15	22

Phenotypic observations and biometric measurements

Throughout the cultivation period, observations were made on germination and plant condition, and at the end of the trial, various biometric parameters were measured.

The height of the plants and the number of nodes for each replicate were considered.

The height was determined on the tallest stem of the tallest plant in the group of plants present in the given cylinder, measured from the collar to the point of intersection of the floral axis, even straightening the stem along the metre.

The number of nodes was determined by counting the recognisable nodes on the main stem of the tallest plant in the group of plants in the given cylinder, starting from the first node above the cotyledons and ending at the last node before the floral scape.

To determine the biomass yield, 60 days after sowing, the fresh weights were determined, then the leaves, flower stalks and stems collected were left to dry in the air in the laboratory until they reached a constant weight.

The plants were cut at the collar and the leaves and flower stalks were separated from the stems.

For the survey, leaves that had fallen into the cylinders and were completely withered or dry biomass were not taken into account.

After 95 days, a constant weight was reached and the dry weight of leaves, stems and flower stalks was determined for all samples. The samples were then placed in paper bags and stored in a cool, dry place.

Measurement of Chlorophyll Content Index

Sixty days after sowing, the Chlorophyll Content Index (CCI) was measured using a SPAD-502 Plus meter (Konica Minolta).

The measurements were taken as if there were only one plant per cylinder, measuring four leaves per cylinder, two apical and two median, proceeding from the apical to the median leaves.

2.4 Evaluation of the potential of *Pseudomonas granadensis* CT364 to colonise plant tissues

An evaluation was made to assess the ability of the plant growth-promoting rhizobacterium *P. granadensis* CT364 to colonise the tissues of plants of significant agricultural interest, such as tomato and wheat.

Micro-Tom tomato was chosen as a model plant due to its global economic, agronomic and food importance.

The Cochise wheat (*Triticum aestivum* 'Cochise') was also selected as a model plant, it was not possible to assess the bacterium's ability to colonise the tissues due to problems with seed sterilisation.

The sterilisation procedures and their effect on wheat seeds are nevertheless reported.

The test data on tomato plants are reported in Annex II.

2.4.1 Tomato Micro-Tom tissues colonisation

Rationale

In order to assess the ability of *P. granadensis* CT364 to colonise plant tissues and improve the fitness of host plants, two theses were considered.

- Treatment with *P. granadensis* CT364 (PG).
- Treatment with magnesium sulfate (MS).

The experiment was divided into two phases: the first *in vitro* up to the seedling stage and the second *in vivo*, where the seedlings were transplanted into soil and grown in a growth chamber until advanced flowering. During the first phase, the presence of the bacterium in the root tissues was assessed using fluorescence. In the second phase, the presence of the bacterium in aerial tissues such as leaves, flowers and stems was evaluated through the bacterial re-isolation, while also assessing the fitness and phenological development of the plants throughout the growing cycle. At the end of the cycle, biometric measurements such as height, fresh and dry biomass weight were taken.

Preparation of Kanamycin stock samples

To prepare the stock samples useful for the bacterium breeding, 1 g of kanamycin monosulphate (kanamycin A), Melford Biolaboratories Ltd, has been added to 20 mL of MQ water.

Under the hood, the solution has been filtered through 22 µm cellulose acetate sterile filters (33 mm diameter) and used to fill 15 labelled Eppendorf tubes.

The tubes have been put in a plastic box and stored at - 20 °C.

***Pseudomonas granadensis* CT364-pSNW2 phiLOV1**

The used microorganism is a strain with constitutive GFP expression, developed by the team of Dr Thomas Howard at the School of Natural and Environmental Sciences at Newcastle University, via the genomic insertion of the suicide plasmid (gfp-pSNW2) downstream of *glmS*, a neutral intergenic region in *Pseudomonas* spp. (Torrescassana et al., 2025).

The strain contains a plasmid with the phiLOV gene sequence inserted for fluorescence and is resistant to kanamycin.

Preparation of Pseudomonas granadensis CT364 glycerol samples

The starting material consisted of a glycerol sample of the *Pseudomonas granadensis* CT364 – pSNW2 - phiLOV1 provided by Dr Thomas Howard and stored at –80°C.

To create new glycerol samples to use for testing, four Petri dishes filled with 50 mL of Tryptic Soy Agar (TSA) (40 g of TSA, Oxoid LTD/L of distilled water) and 50 µL of kanamycin were inoculated by streaking with a sterilised plastic loop that was slightly dipped into the glycerol tube. The plates were then incubated at 28°C for 24 hours.

After 24 hours, bacterial colonies were observed, including some isolated single colonies that were suitable for the inoculation of 10 mL of Luria – Bertani (LB) broth (20 g of LB broth, Melford/L of distilled water) with 10 µL of kanamycin.

In addition, it was verified that the raised bacterial colonies showed fluorescence by putting the Petri dishes under blue light.

After 24 h, the bacterium was grown in the LB broth, so 5 glycerol samples were prepared.

Briefly, 750 µL of LB broth have been mixed to 750 µL of glycerol 100% in each of the 5 sterile Eppendorf tubes. Then, the samples have been put in liquid nitrogen for 10 minutes, to be sure that the samples were completely frozen.

The labelled tubes have been put in a plastic box and stored at – 70 °C.

The procedure is made to be sure that *P. granadensis* CT364 – pSNW2 – phiLOV1 is the growing microorganism, since it is resistant to kanamycin and fluorescent.

Germoplasm

Tomato Micro - Tom (*Solanum lycopersicum* L. ‘Micro-Tom’) is a dwarf, determinate variety that can be grown in containers as small as 9 cm, as it presents a bushy habit, can reach a height of 25 cm and has become a well-recognised model organism in scientific research.

The starting material consisted of seeds.

Root colonisation test

Tomato seeds sterilisation and sowing

45 seeds of Tomato Micro Tom seeds have been sterilised by placing them in a Falcon tube with 3% sodium hypochlorite (NaClO) added with 2% Tween 20 (polysorbate 20, C₅₈H₁₁₄O₂₆) for 10 minutes and hand shaking.

The seeds have been washed 5 times with sterile distilled water.

Fifteen seeds have been placed in 3 rows of 5 in each of the 3 square Petri dishes, previously filled with ½ Murashige and Skoog (MS) (2.2 g of basal Sigma–Aldrich medium/L distilled water supplemented with 1% sucrose and 1% of agar, pH 5.7).

The dishes were sealed with micropore tape and stored horizontally at 22 °C for 1 day, covered to ensure the dark conditions required for germination.

After 1-day post-sowing, dishes were placed vertically, and after 7 days, they were exposed to light. The photoperiod consisted of 16 hours of light and 8 hours of darkness.

Visualisation of Tomato root colonisation by *P.granadensis* CT364

7-day-old Tomato Micro Tom seedlings have been transferred to fresh ½ MS medium supplemented with 3% sucrose in square Petri dishes.

An overnight synchronised *P. granadensis* CT364 culture was obtained by growing the bacterium for 15 hours in LB broth supplemented with kanamycin, incubated at 28°C with shaking at 110 rpm. To ensure the culture's synchronisation, a 1:10 dilution of the original culture was subsequently made using the same incubation conditions as the overnight culture.

Then, the synchronised culture was washed three times with 10 mM magnesium sulphate (MgSO₄), and the OD was adjusted to 0.5.

For each seedling (12 for both theseses), 50 µL of the bacterial suspension or magnesium sulphate was used to perform the treatments as described in the thesis.

Petri dishes have been incubated at 22 °C. The photoperiod consisted of 16 hours of light and 8 hours of darkness.

Throughout the entire growing cycle, the phytosanitary status was monitored, along with the growth and development of the shoots.

After 10 days, the presence of fluorescence in the tomato tissues was checked using white and blue light of a Safe Imager™ 2.0 Invitrogen lamp. Pictures were taken with a Nikon D3300 camera.

The test was considered complete 14 days after the treatments were administered.

Aerial tissues colonisation test

Fourteen days after the treatments, the sprouts were transplanted into Sinclair All Purpose Growing Medium to verify the bacterium's ability to colonise plant tissues during the entire crop cycle.

Reference time stamp

Below is the reference timestamp for the evaluation activity of *P. granadensis* CT364's ability to colonise the aerial tissues of Micro-Tom tomato (Table 20).

Table 20. Timetable of the experimental activity to evaluate the ability of *P. granadensis* CT364 to colonise Tomato Micro-Tom aerial tissues.

August 2025									
15	16	17	18	19	20	21	22	23	24
00	01	02	03	05	05	06	07	08	09
August – September 2025									
25	26	27	28	29	30	31	01	02	03
10	11	12	13	14	15	16	17	18	19
September 2025									
04	05	06	07	08	09	10	11	12	13
20	21	22	23	24	25	26	27	28	29
14	15	16	17	18	19	20	21	22	23
30	31	32	33	34	35	36	37	38	39
September – October 2025									
24	25	26	27	28	29	30	01	02	03
40	41	42	43	44	45	46	47	48	49

October 2025									
04	05	06	07	08	09	10	11	12	13
50	51	52	53	54	55	56	57	58	59
14	15	16	17	18	19	20	21	22	23
60	61	62	63	64	65	66	67	68	69
October – November 2025									
24	25	26	27	28	29	30	31	01	02
70	71	72	73	74	75	76	77	78	79
November 2025									
03	04	05	06	07	08	09	10	11	12
80	81	82	83	84	85	86	87	88	89

Plant cultivation

The photoperiod consisted of 16 hours of light and 8 hours of darkness with a constant temperature of 25°C.

28 days after transplanting, all the plants were treated with Miracle-Gro's "All Purpose Concentrated Plant Food" fertiliser.

Phenotypic observations and biometric measurements

Throughout the growing cycle, the phytosanitary status was monitored, along with the growth and development of the plants.

The cultivation was considered complete fifty-two days after transplantation, and the plants were harvested. At that moment, plant heights and fresh weights have been determined. After fifty-nine days dry weight has been determined.

Measurement of Chlorophyll fluorescence

28 days after transplanting, three plants were selected for each thesis to be subjected to chlorophyll fluorescence analysis using the Photon System Instruments spol. s r.o Closed FluorCam machine, a kinetic imaging fluorometer, to assess the Fv/Fm parameter.

The closed FluorCam system integrates a CCD camera with modules that control image acquisition and generate measuring light, actinic light, and saturating pulses. All components share a high-capacity power supply and are coordinated by a software-defined protocol transmitted via Ethernet, which also returns the acquired fluorescence data to the computer.

Chlorophyll fluorescence fluorimeters evaluate photosynthetic performance by exposing samples to controlled illumination: low-intensity measuring light captures basal fluorescence, actinic light stimulates photosynthesis, and saturating pulses provide maximal fluorescence needed to derive key parameters. The emitted fluorescence is recorded by the synchronized CCD camera and processed by dedicated software to obtain indicators such as F_0 , F_m , F_m' , Φ_{PSII} , and NPQ, providing quantitative insight into photosynthetic efficiency and stress.

The F_v/F_m (F_m = maximum fluorescence (after a saturated light pulse that closes all PSII reaction centres) and F_v = variable fluorescence ($F_m - F_0$, which is the minimum fluorescence)) measures the maximum quantum efficiency of PSII, i.e. the theoretical capacity with which absorbed light can be converted into chemical energy during photosynthesis, providing summary information on the “health status” of photosystem II (PSII).

Briefly, from each of the selected plants (PG1A, PG2B, PG3D, MS1D, MSA2C, MS3A) three leaf disc samples were taken from the terminal leaflet of a median leaf.

These discs were randomly placed in two Petri dishes filled with filter paper soaked in water.

With the lid on, the samples were left to adapt to the dark for 15 minutes. Once the lid was removed, the analysis was carried out.

The samples have been placed as reported (Figure 25):

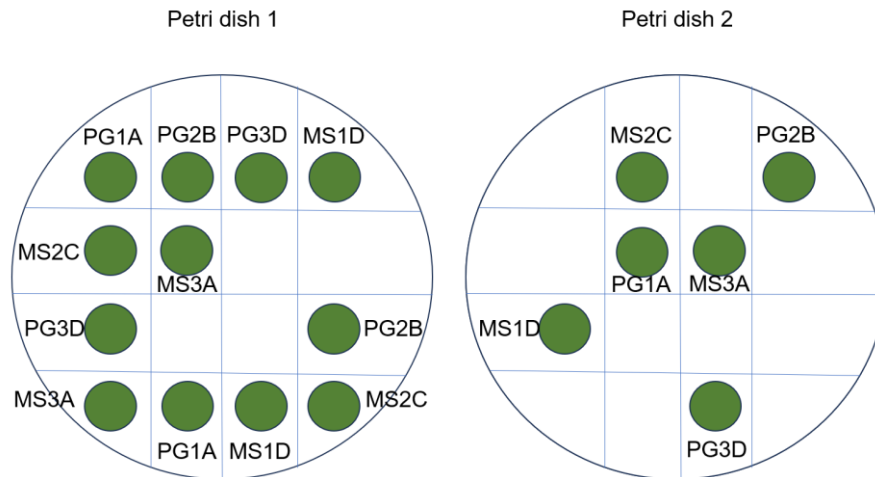


Figure 25. Arrangement of samples in Petri dishes for chlorophyll fluorescence analysis using Fluorcam equipment. PG: plant treated with *P. granadensis* CT364; MS: plants treated with magnesium sulfate.

The data were recorded by the FluorCam 7 software by PSI (Photon Systems Instruments). The software package is useful for controlling FluorCam imaging systems and analysing chlorophyll fluorescence.

The leaves from which the samples were taken were collected, weighed and frozen at -20°C . The same was done for the flowers of the selected plants.

Biometric measurements

Fifty-two days after transplantation, the heights and fresh weights of the leaves, stems, and flowers of each of the plants concerned were measured (PG1B, PG1C, PG1D, PG2A, PG2C, PG2D, PG3A, PG3B, PG3C, MS1A, MS1B, MS1C, MS2A, MS2B, MS2D, MS3B, MS3C and MS3D).

The height of plants PG1A, PG2B, PG3D, MS1D, MS2C and MS3A was also assessed, although these were not used to determine fresh and dry weights due to the samples required to determine chlorophyll fluorescence.

The leaves, stems and flowers of each plant were placed in an oven at 65°C for one week to assess their dry weight.

Re-isolation test

To assess the bacterium's ability to colonise the aerial tissues of Micro-Tom tomatoes, an *in vitro* re-isolation test was conducted 54 days after transplanting.

Specifically, the test focused on the six plants used to evaluate chlorophyll fluorescence, namely PG1A, PG2B, PG3D, MS1D, MS2C and MS3A.

Leaf, stem and flower samples were taken randomly from each plant, ensuring that they belonged to the basal, median and apical portions of the plant where possible.

Each sample was rinsed in running water for about 30 seconds and sterilised by immersion in 95% ethanol solutions for 5 seconds, 0.5% sodium hypochlorite for 1 minute, and 70% ethanol for 1 minute. Sterilisation was carried out under aseptic conditions.

The samples were left to dry in Petri dishes for approximately 10 minutes and then transferred to Petri dishes containing LB supplemented with kanamycin.

Three dishes were prepared for each plant, for a total of 9 leaf and stem samples for each and at least 3 flower samples.

The plates were sealed with micropore tape and incubated at 26°C.

Assessment of bacterial presence in root tissues at the end of the cultivation cycle

Sixty-one days after transplantation, the presence of *P. granadensis* CT346 in the roots of Micro-Tom tomatoes was re-evaluated.

Root tissue samples were taken from each of the 18 plants concerned: PG1B, PG1C, PG1D, PG2A, PG2C, PG2D, PG3A, PG3B, PG3C, MS1A, MS1B, MS1C, MS2A, MS2B, MS2D, MS3B, MS3C and MS3D.

Fluorescence was assessed using the blue light of a Safe Imager™ 2.0 Invitrogen lamp and photographs were taken with a Nikon D3300 camera.

2.4.2 Cochise wheat sterilisation procedures

Seed sterilisation represents a crucial step in reliably assessing the ability of beneficial microorganisms to colonise plant tissues. Seeds can, in fact, host a heterogeneous microflora on their surface — and in some cases even in deeper layers — composed of fungi, bacteria and environmental yeasts. The presence of these contaminants interferes with colonisation experiments because they can directly compete with the microorganism under study, alter seed physiology during germination, or mask the effects of the inoculated bacterium.

Using non-sterilised seeds would therefore make it impossible to distinguish between experimentally introduced microorganisms and pre-existing microflora, compromising the validity of the results.

Effective sterilisation, on the other hand, allows starting from plant material free of unwanted microbial load, ensuring that the observed colonisation is solely attributable to the tested beneficial microorganism and enabling accurate assessments of its ability to penetrate and settle in plant tissues.

Sterilisation with 3% sodium hypochlorite solution

The first attempt was carried out by immersing the seeds in a 3% sodium hypochlorite (NaClO) solution supplemented with Tween 20 for 10 minutes with manual agitation. The Tween 20 (20 mL/L solution) was added to allow greater contact between the seed surface and the sterilisation solution. The seeds were then rinsed five times with sterile distilled water for 30 seconds and placed in 6 square Petri dishes filled with 1/2 MS supplemented with 1% sucrose. Each dish contained 15 seeds, arranged in 3 rows of 5 positions, for a total of 90 seeds. The prepared dishes were sealed with micropore tape and stored in the dark at 4°C to break seed dormancy. After 2 days, they were moved to 25°C.

Three further attempts were carried out using a 3% sodium hypochlorite solution supplemented with Tween 20, considering different seed immersion times in the solution, changing the seed placement and also including immersion in 70% ethanol.

Specifically, in the first case (1), the seeds were immersed in the 3% sodium hypochlorite solution for 10 minutes and rinsed five times with sterile distilled water.

In the second case (2), the seeds were immersed in 3% sodium hypochlorite solution for 20 minutes and rinsed five times with sterile distilled water.

In the third case (3), the seeds were immersed in sodium hypochlorite solution for 10 minutes, rinsed five times with sterile distilled water, then immersed in a 70% ethanol (C₂H₆O). solution for 1 minute and rinsed again five times with sterile distilled water.

For each attempt, the seeds were agitated at 5000 rpm during immersion in sterilisation solutions and rinsed using a vortex. The seeds were then placed in round Petri dishes filled with sterilised Cytiva WhatmanTM filter paper (Ø 9 cm) for UV light exposure for 3 hours and 30 minutes. The blotting paper of each dish was moistened with 3 mL of sterile distilled

water to promote germination. Each attempt included 1 dish. Each plate hosted about 30 seeds.

Resuming the sterilisation procedures carried out in cases 2 and 3, two more procedures were performed (4 and 5), and the seeds were then placed on square Petri dishes filled with 1/2 MS supplemented with 1% sucrose. Each of the two dishes held 20 seeds arranged in 4 rows of 5 positions. The assembled dishes were kept in the dark at 4°C for 2 days and then at a constant 25°C.

All attempts were carried out under aseptic conditions.

Chlorine gas sterilisation

Seeds (dry and pre-soaked for 24 h in distilled water) were sterilised by exposure to chlorine (Cl₂) gas generated *in situ* by reacting 37% hydrochloric acid (HCl) with commercial sodium hypochlorite solution. The reagents were placed in a sealed glass chamber together with the seeds, and the seeds were exposed to the chlorine gas for 3 h.

After treatment, seeds were allowed to air out for 10 min inside the fume hood before further handling.

The seeds were then placed in square Petri dishes filled with 1/2 MS supplemented with 3% sucrose under a microbiological hood. Four plates were obtained (two for dry seeds and two for soaked seeds), and each plate held 20 seeds arranged in 4 rows of 5 positions. The seeds were then soaked with sterile distilled water; specifically, 1,5 mL/plate was used for dry seeds and 500 mL/plate for soaked seeds.

The plates prepared in this way were sealed with micropore tape and stored in the dark at 4°C for 2 days, and subsequently at 26°C.

2.5 Data analysis

The data obtained were analysed using the open-source integrated development environment (IDE) R Studio, designed to work with the R programming language.

This language is open source and specific to statistics and computational graphics.

In particular, the data were annotated and organised in Microsoft Excel and then analysed using one-way ANOVA in R Studio.

Pre-analyses tests such as the Shapiro-Wilk test and Levene test were also performed to determine the normality and homogeneity of the data, respectively, and thus their suitability for ANOVA testing.

Data that produced a $p < 0.05$ in ANOVA were considered statistically significant.

For statistically significant data, the Tukey test was also performed. This post-hoc test is useful for determining which group means are significantly different from each other.

The various graphs were produced in Microsoft Excel.

Some tables and graphs retain the comma-based decimal notation generated by the Italian version of Microsoft Excel. Throughout the text, however, decimal values follow the standard English point notation.

In cases where alternative analytical methods were employed, these are described in the respective section for each experiment.

3 Results

3.1. Microorganism selection

The *in vitro* screening of the antimicrobial activity of *Bacillus* spp. strains belonging to the ENEA microbial collection revealed that *Bacillus subtilis* ET-1 was the most effective biocontrol agent. This strain showed the highest percentage of mycelial growth inhibition against both *Botrytis cinerea* and *Penicillium digitatum* when compared with the other tested *Bacillus* isolates.

The inhibition percentages obtained against the selected phytopathogens are reported in Table 21.

Table 21. Percentage of mycelial growth inhibition (MGI%) exhibited by the tested biocontrol agents (BCAs) against *B. cinerea* and *P. digitatum* under *in vitro* conditions.

BCAs	Percentage of mycelial growth inhibition (MGI %)	
	<i>B. cinerea</i>	<i>P. digitatum</i>
<i>B. subtilis</i> ET-1	62	68
<i>Bacillus</i> spp.	55	59
<i>Bacillus licheniformis</i>	52	55

Microscopic observations further corroborated these findings, revealing marked morphological alterations in fungal hyphae exposed to *B. subtilis* ET-1. In particular, treated hyphae displayed evident crumpling and structural deformation, in contrast to the normal, intact hyphal morphology observed in the untreated control (Figure 26).

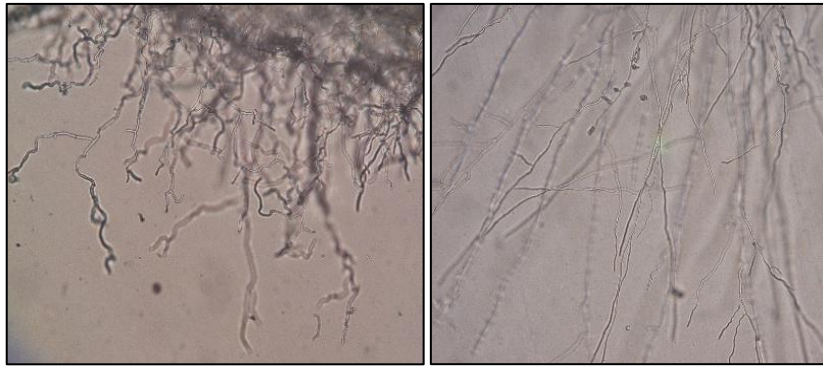


Figure 26. Effect of the antimicrobial activity of *B. subtilis* ET-1 on the growth of *P. digitatum* hyphae (left) compared to normal growth (right).

3.2 Agro-industrial waste selection for breeding the chosen microorganism

Among the 19 substrates initially tested at bench scale, substrate 14 was selected as the reference medium due to its superior ability to induce iturin A production, reaching a concentration of 400 mg/L. The formulation of substrate 14 consisted of a final volume of 150 mL, containing 0.3 g of casein-derived peptone, 0.3 g of yeast extract, 30 g of potato extract, 3 g of glucose, and 75 μ L of manganese chloride (MnCl_2).

To further optimise this formulation, agro-industrial waste-derived components were introduced and alternatives to MnCl_2 were evaluated.

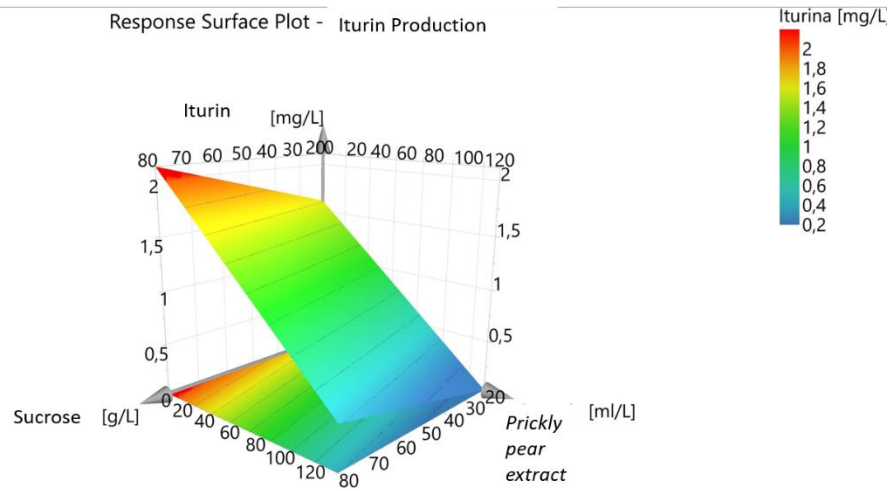
Although MnCl_2 is known to promote sporulation and secondary metabolite production in *Bacillus* spp., its toxicity and poor alignment with sustainability goals made it unsuitable for large-scale application. Consequently, 11 additional substrate formulations were developed and tested.

The substrates were screened based on their antimicrobial activity against *P. digitatum*, *P. italicum*, *B. cinerea*, and *M. laxa*.

On the basis of this screening, substrate 28 was identified as the most promising formulation. This medium had a final volume of 23 mL and contained 0.115 g of ammonium nitrate (NH_4NO_3), 20 mL of potato peel extract, 1.84 g of sucrose, 0.046 g of spent yeast, and 3 mL of prickly pear (*Opuntia ficus-indica* (L.) Mill., 1768) extract.

To determine the optimal concentrations of sucrose and prickly pear extract, an experimental design based on Response Surface Methodology (RSM) was implemented using a two-level full factorial design. The RSM analysis demonstrated that iturin A production was positively

correlated with sucrose concentration, up to an optimal value of 20 g/L, at which the maximum production of 2.45 g/L of iturin A was achieved. In contrast, the concentration of prickly pear extract showed no significant effect on iturin A production (Figures 27 and 28).



MODDE 13.0.2 - 01/02/2024 13:20:34 (UTC+1)

Figure 27. Response Surface Methodology (RSM) based on a two-level full factorial design showing that iturin A production increases with sucrose concentration up to 20 g/L, while prickly pear extract does not significantly influence production

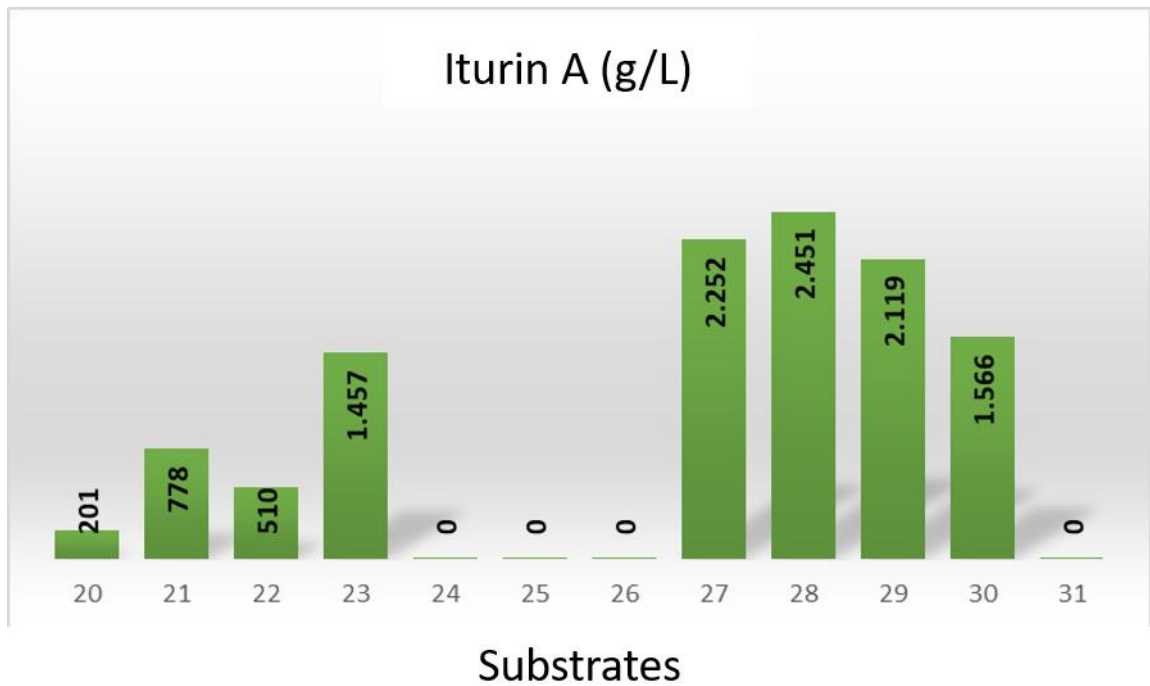


Figure 28. Amount of iturin A (g/L) produced by *B. subtilis* ET-1 when grown on different substrate formulations.

Kinetic analysis further revealed that maximum lipopeptide production occurred 96 h after inoculation, coinciding with the onset of sporulation. This observation supports the close association between secondary metabolite biosynthesis and the sporulation phase in *B. subtilis* (Figure 29).

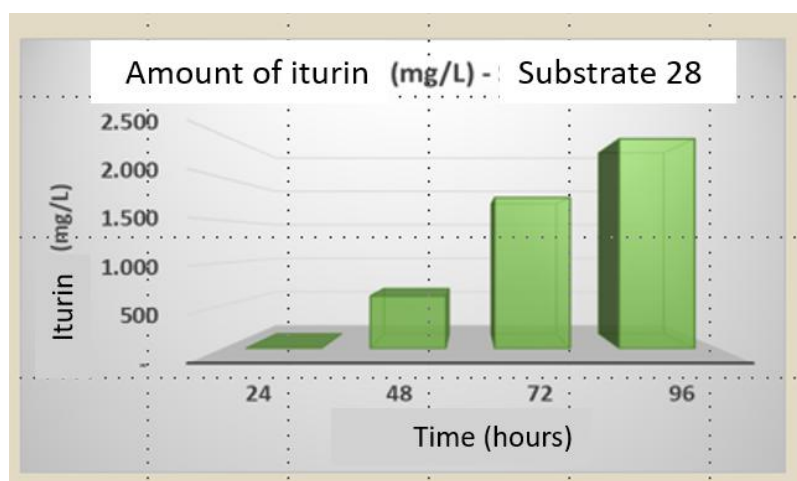


Figure 29. Time-course of iturin A production (mg/L) by *B. subtilis* ET-1 grown on substrate 28 at 24, 48, 72, and 96 h post-inoculation.

3.3 Antimicrobial activity evaluation during the scaling-up and optimisation process

3.3.1 *In vitro* test

Antimicrobial efficacy of the substrate 14

To verify the suitability of **substrate 14**, both the growth performance of the selected microorganism and the biocontrol activity of its cell-free supernatant (CFS) against *Penicillium digitatum* were evaluated.

In particular, microbial growth was assessed by quantifying colony-forming units (CFUs), while antifungal activity was determined by measuring the inhibition of *P. digitatum* conidia germination.

The effects of the different growth substrates on *B. subtilis* ET-1 biomass production and on the inhibition of *P. digitatum* conidia germination are reported in Table 22 and Figure 30.

Table 22. Effect of substrate composition on colony-forming units (CFUs mL⁻¹) of *B. subtilis* ET-1 at the steady growth phase and on the inhibition of *P. digitatum* conidia germination, expressed as the highest serial dilution of the cell-free supernatant causing ≥95% inhibition.

Progressive substrate number	CFUs mL ⁻¹ (steady growth phase)	Highest dilution with ≥95% inhibition
1	5.7 × 10 ⁸	1:32
2	5.2 × 10 ⁷	1:4
3	1.9 × 10 ⁸	1:32
4	1.2 × 10 ⁷	1:1
5	5.0 × 10 ⁷	1:1
6	6.6 × 10 ⁸	1:1
7	2.3 × 10 ⁷	1:1
8	1.9 × 10 ⁷	1:1
9	1.9 × 10 ⁷	1:1
10	5.0 × 10 ⁸	1:1
11	3.3 × 10 ⁸	1:2
12	2.8 × 10 ⁷	1:1
13	6.5 × 10 ⁸	1:16
14	9.0 × 10⁸	1:128
15	3.6 × 10 ⁸	1:32
16	5.0 × 10 ⁸	1:32
17	6.9 × 10 ⁷	1:4

Substrate 14 resulted in the highest bacterial biomass production and showed the strongest antifungal activity, maintaining more than 95% inhibition of *P. digitatum* conidia germination up to a 1:128 dilution of the CFS.

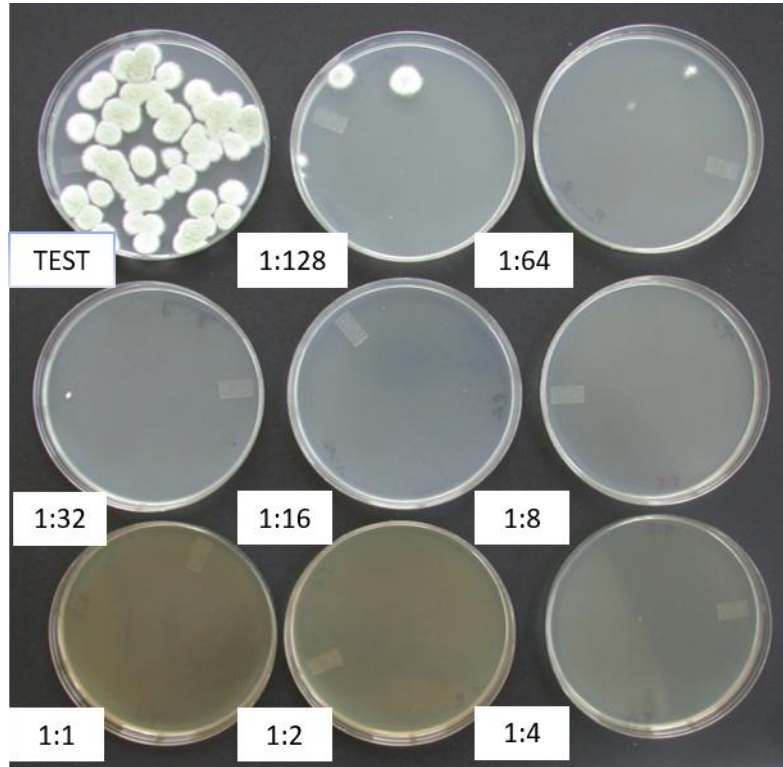


Figure 30. Effect of increasing dilutions of the cell-free supernatant obtained from *B. subtilis* ET-1 grown in substrate 14 on the growth of *P. digitatum* colonies.

Further experiments were conducted using substrate 28 to evaluate the antifungal potential of the corresponding cell-free supernatant. The results showed that the CFS obtained from ET-1 grown in substrate 28 was able to inhibit more than 95% of *P. digitatum* conidia germination even at a 1:512 dilution, indicating a markedly higher antifungal efficacy compared to the other tested substrates (Figure 31).

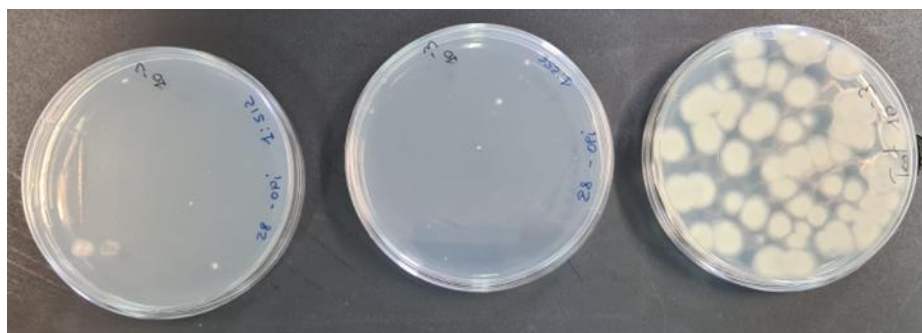


Figure 31. Figure 31. Inhibitory effect on *P. digitatum* conidia germination observed in serial dilutions of the cell-free supernatant obtained from *B. subtilis* ET-1 grown in substrate 28.

3.3.2 In vivo test

Biological preparations containing iturin A against P. xanthii on melon plants

To further assess the suitability of substrate 14, the antimicrobial activity of both the cell-free supernatant (CFS) and a crude lipopeptide extract containing 100 ppm of iturin A produced by *Bacillus subtilis* ET-1 was evaluated through an *in vivo* assay on melon plants (*Cucumis melo* L.) artificially infected with *Podosphaera xanthii*.

Both biological treatments significantly reduced powdery mildew severity compared with the chemical fungicide fenbuconazole, used as a positive control. The results of the field experiment are reported in Table 23

Table 23. Control efficacy of powdery mildew in field experiments on melon plants treated with cell-free supernatant and crude lipopeptide extract (100 ppm iturin A) produced by *B. subtilis* ET-1. Values followed by different letters are significantly different according to statistical analysis ($p \leq 0.05$).

Treatment	Disease severity (%) (15 days after first symptoms)	Control efficacy (%)
Cell-free supernatant 25% (100 ppm iturin A)	7.2 a	88.5 a
Crude lipopeptide extract (100 ppm iturin A)	8.9 a	85.8 a
Fenbuconazole (chemical control)	9.6 a	84.7 a
Water (negative control)	63.0 b	—

Dried cell-free supernatant against *P. digitatum* on clementine fruits

The antifungal efficacy of liquid and stabilised (dried) CFS obtained from substrate 28 was evaluated against *P. digitatum* on clementine fruits. Both formulations provided excellent disease control, and no significant differences were observed between the liquid and dried CFS treatments (Table 24 and Figure 32).

Table 24. Percentage of wounds infected by *P. digitatum* on clementine fruits following treatment with liquid CFS, stabilised CFS, chemical fungicide, and water.

Thesis	Wounds with symptoms (%)
Liquid CFS	20 b*
Stabilized CFS	18 b
Chemical	0 c
Water	95 a

* Values are statistically different at $P \geq 0.05$ (Duncan test)

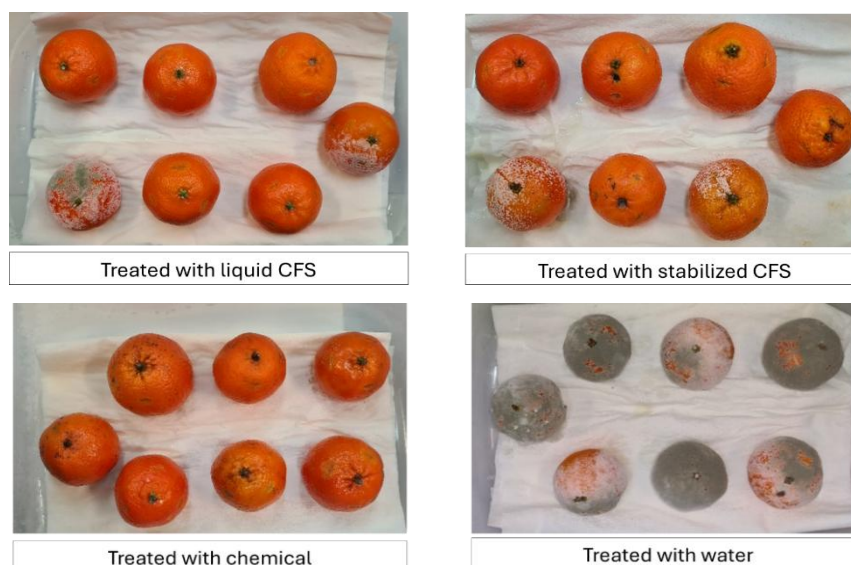


Figure 32. Clementine fruits infected with *P. digitatum* and treated with liquid CFS, stabilised CFS, imazalil (chemical control), and water (negative control).

The stabilisation process based on drying technology did not negatively affect the antifungal activity of the secondary metabolites present in the CFS, indicating that the bioactive compounds retained their efficacy after processing.

3.4 Microbial biomass production for plant biostimulation

The microbial biomass obtained through submerged fermentation followed by spray-drying resulted in a fine white powder (Figure 33), indicating successful dehydration and preservation of the bacterial material.



Figure 33. Microbial biomass containing spores of *B. subtilis* ET-1 obtained through fermentation and spray-drying processes.

The dry biomass yield reached $25 \text{ g}\cdot\text{L}^{-1}$ of centrifuged culture broth, reflecting a high conversion efficiency of the fermentation process into a stable solid product.

Viability assays performed after spray-drying revealed that the formulated biomass retained a high level of biological activity, with a final concentration of $7.2 \times 10^8 \text{ CFU}\cdot\text{g}^{-1}$. This result confirms the robustness of *B. subtilis* ET-1 spores and their ability to withstand thermal and mechanical stresses associated with industrial-scale drying processes.

The combination of high biomass yield and substantial post-processing viability highlights the suitability of spray-dried *B. subtilis* ET-1 biomass as a stable and effective bio-based formulation for plant biostimulation applications.

3.5 Biostimulant test on Basil

3.5.1 Phenotypic observations

Ten days after transplanting, the roots of all seedlings treated with biomass became visible, as well as those of two seedlings treated with ammonium sulfate (treatments 1 and 2) and one seedling treated with water (treatment 3).

After 13 days, the roots of the other three seedlings treated with water (treatments 1, 2, 4) became visible.

After 17 days, the roots of the other two seedlings treated with ammonium sulfate (treatments 3 and 4) became visible.

After 17 days, the roots of all plants treated with microbial biomass and water, as well as treatments 1, 2, 4 of the plants treated with ammonium sulfate, had reached the bottom of the cylinders.

In general, plants treated with microbial biomass show greater branching of the root systems (Figure 34).

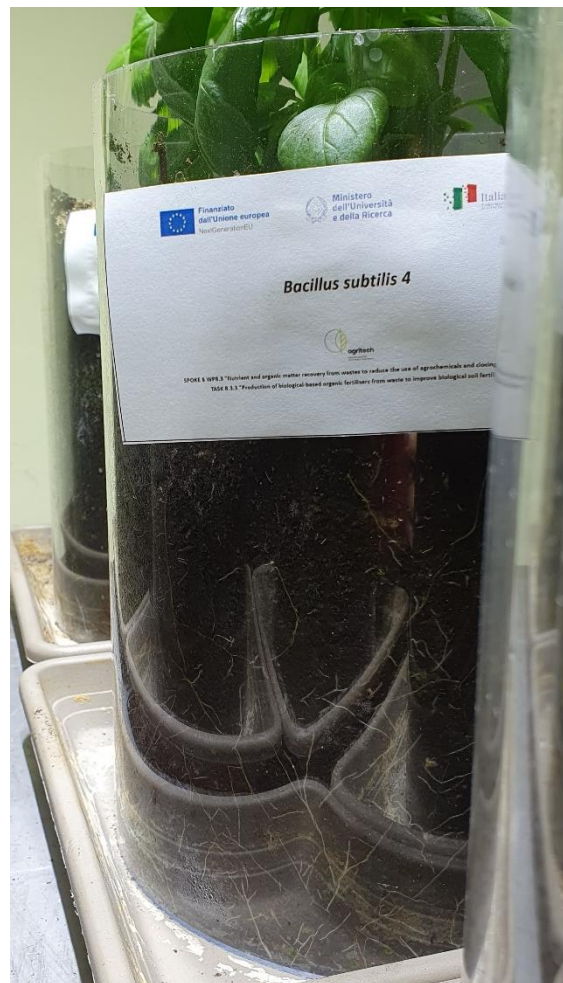


Figure 34. Details of basil roots treated with microbial biomass.

After 37 days, the plant corresponding to thesis B2 produced a floral stem primordium (Figure 35).



Figure 35. Details of the early stage of floral bud development on the B2 thesis basil.

After 41 days, the emergence of floral shoots was also observed in the plants of trials B4 and S2 (Figure 36).



Figure 36. Details of early floral bud development on the B4 and S2 basil specimens.

After 44 days, floral shoots emerged from the plants in trials C1, C3, and B3 (Figure 37).



Figure 37. Figure 37. Details of the early floral bud on Basil of the C1, C3 and B3 theses.

After 48 days, the plants of treatments C2 and C4 had produced flower stalks, while the plants of treatments B1, S1, S3 and S4 had not yet produced flower stalks (Figure 38).



Figure 38. Detailed comparison between C4 and S1 theses 48 days after transplantation.

After 48 days, anthesis began on the apical floral bud of plant B2 (Figure 39).



Figure 39. Details of the anthesis on Basil from the B2 thesis

After 51 days, flowering was also observed in the S2 plant and elongation of the flower stalk was observed in the plants of trials B3, B4, C1, C3. Flower stalk primordia were shown by the plants of trials B1 and S4. The plants of trials S1 and S3 did not produce a flower stalk.

3.5.2 Biometric measurements

As shown in the graph below (Figure 40), there is a statistically significant difference ($p < 0.05$) in plant height, with higher values recorded for plants treated with microbial biomass.

In particular, the Tuckey test shows that plants treated with microbial biomass and water show similar and better results than plants treated with ammonium sulphate.

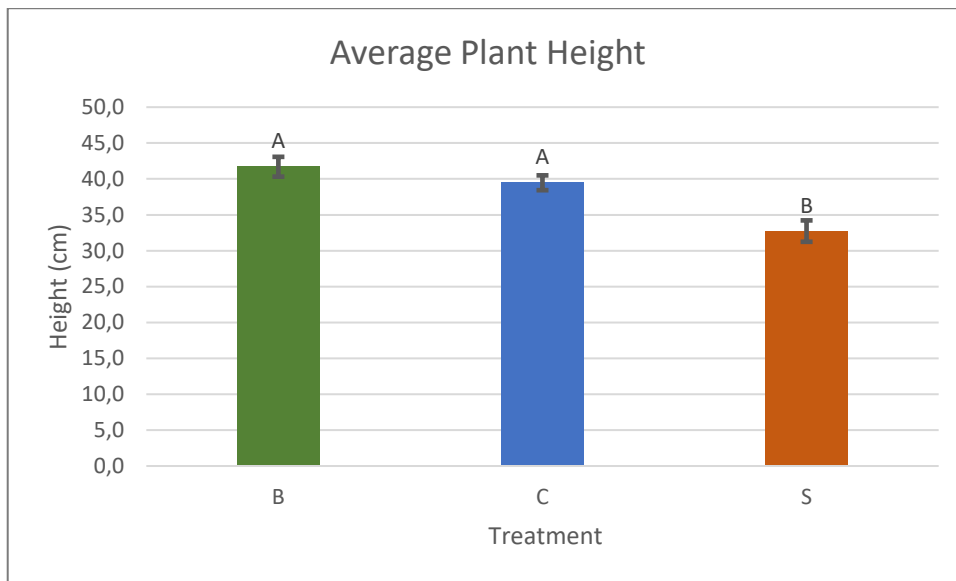


Figure 40. Graph showing the average height of plants treated with microbial biomass (B), spring water (C) and ammonium sulphate (S). The values were rounded to one decimal place to simplify presentation, in accordance with the instrument's precision.

The height of the plants was correlated with the number of nodes: plants with 13 nodes (treatment C) reached greater heights than those with 11 nodes (treatment S). In cases where the number of nodes was constant (12 nodes), differences in height were attributable to variations in internode length.

As shown in the graph below, plants treated with microbial biomass have higher total fresh weights than plants treated with spring water and plants treated with ammonium sulphate (Figure 41). However, there is no statistically significant difference between the three treatments.

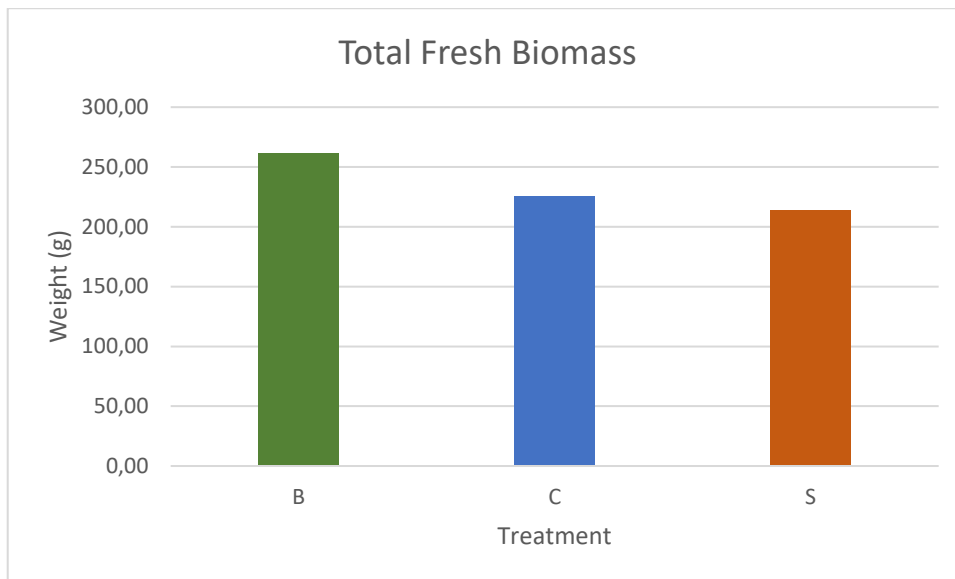


Figure 41. Graph showing the total fresh biomass (leaves, flowers and stems) of plants treated with microbial biomass (B), spring water (C) and ammonium sulphate (S). The values were rounded to two decimal places to simplify presentation, in accordance with the instrument's precision.

The same trend observed for fresh biomass was also seen in dry biomass. In particular, particularly high values were recorded for plants treated with microbial biomass (Figure 42).

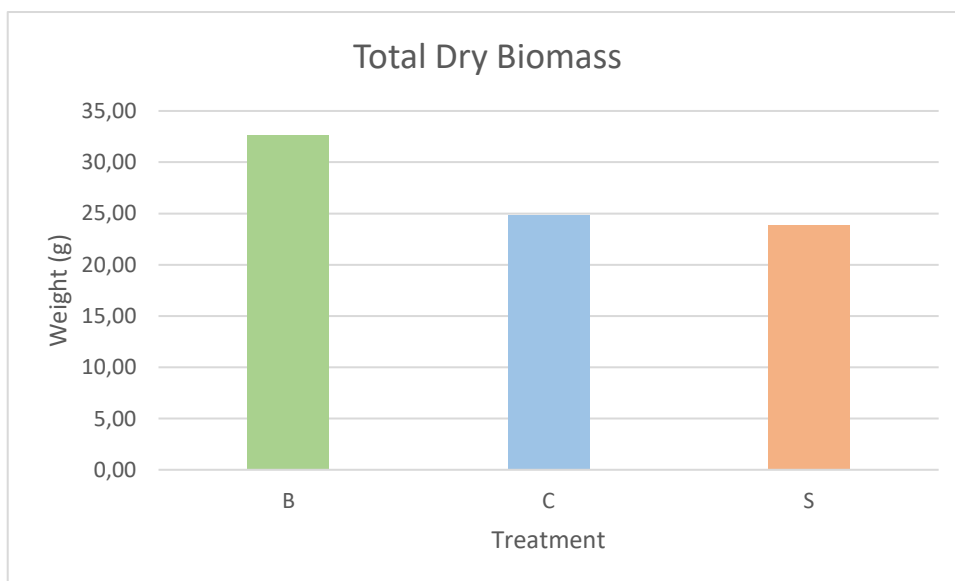


Figure 42. Graph showing the total dry biomass (leaves, flowers and stems) of plants treated with microbial biomass (B), spring water (C) and ammonium sulphate (S). The values were rounded to two decimal places to simplify presentation, in accordance with the instrument's precision.

3.5.3 Measurement of Chlorophyll Content Index

The data obtained from SPAD-502 Plus meter (Konica Minolta) measurements on apical and median leaves are shown below (Table 25 and Figure 43).

Table 25 shows data relating to the chlorophyll content index (CCI) recorded for the apical (F1-F2) and median (F3-F4) leaves of basil plants treated with microbial biomass (B), spring water (C) and ammonium sulphate (S).

Treatment	Chlorophyll content index (CCI)			
	F1	F2	F3	F4
B1	32,5	43,4	29,8	71,6
B2	37,3	36,7	39,7	33,2
B3	46,3	39,3	31,5	36,1
B4	45,5	44	40,4	37,2
C1	43,2	32,8	58,7	52,3
C2	42,1	38,2	37,3	40,3
C3	48,2	39,3	40,8	36,4
C4	38,8	41,2	40,9	43,2
S1	35,5	41,2	32,8	38,6
S2	45,2	42,1	37,9	37,8
S3	32,2	30,5	48,2	48,8
S4	35,8	37	36,1	38,2

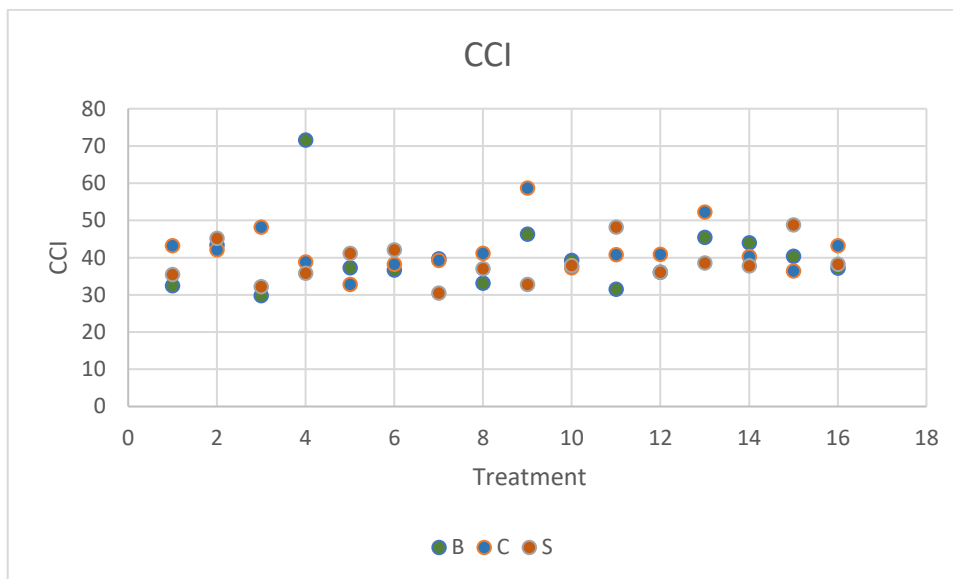


Figure 43. Graph showing the Chlorophyll Content Index (CCI) of plants treated with microbial biomass (B), spring water (C) and ammonium sulphate (S).

As can be seen especially from the scatter plot, the sensitivity error of the instrument exceeds the expected biological variability in the samples; therefore, the differences between treatments may not have been accurately detected.

This was further verified by using the SPAD to take new and more numerous measurements on basil.

In particular, 10 measurements were taken, 5 on the front of the leaf blade and 5 on the back. The measurements were taken on 3 basil plants, with 2 apical leaves and 2 median leaves for each plant. Data are shown below (Table 26).

Table 26 shows data relating to the chlorophyll content index (CCI) recorded on the front and back of leaf blades for the apical (F1A-F3A) and median (F2M-F4M) leaves of basil plants (P1, P2, P3).

Sample	Chlorophyll content index (CCI)									
	Front of the leaf blade measurements					Back of the leaf blade measurements				
	1	2	3	4	5	1	2	3	4	5
P1F1A	39,1	38,6	10,4	37,1	38	39,1	40,2	38,1	41,6	36,3
P1F2M	40,6	41,2	40,4	39,1	32,9	37,6	41,8	41,5	38,5	39
P1F3A	46,3	44,5	37,5	76,9	42,1	44,4	40,9	48	43	25,6
P1F4M	39,2	34	37,8	37,1	38	35	35,4	37,4	37,6	32,6
P2F1A	38,1	33,2	39,3	37	35,5	81,6	42,8	40,4	36,8	41,7
P2F2M	66,2	65,7	60,2	39,5	65,2	34,6	32,8	40,3	56,2	34
P2F3A	39,3	41,1	41,8	74,8	81,2	38,4	40,4	37	38,5	39,3
P2F4M	30	30,2	33,5	33,6	32,3	32,5	29,4	24,8	32,9	26,7
P3F1A	49,9	45,3	49,9	44,3	42,8	42	41	47,1	51,6	49,1
P3F2M	34,9	31,8	37	39,7	38,4	31	31,6	32,6	31,2	36,7
P3F3A	45,8	33,4	35,5	31,7	36,6	37,1	39	41,7	44,7	48,1
P3F4M	31,1	19,9	18,7	19,7	20,7	33,3	33,9	32,8	32,8	32,7

The data obtained show a normal distribution (Figure 44), but there are still values that deviate from the mean.

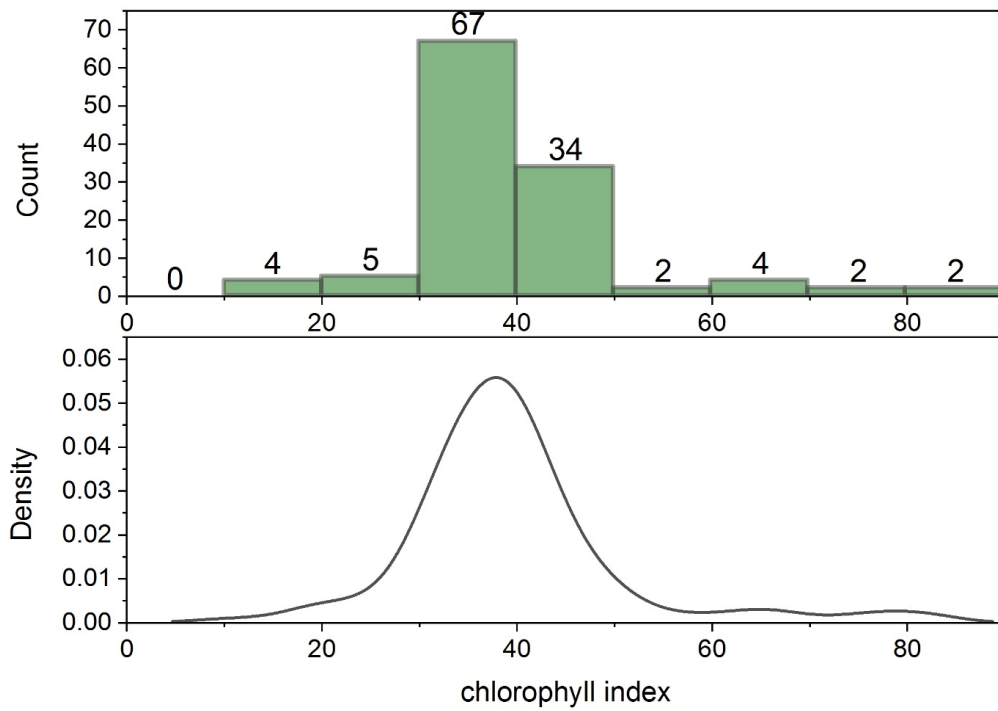


Figure 44. Graph relating to the normal distribution of chlorophyll content indices obtained on Basil plants. It is noticeable that a large number of measurements are required to achieve a normal distribution, although even in this case, there are values that deviate significantly from the mean.

As can be seen from the graph below (Figure 45), in fact, across the 10 measurements carried out for apical and median leaves, values often fall outside the trend.

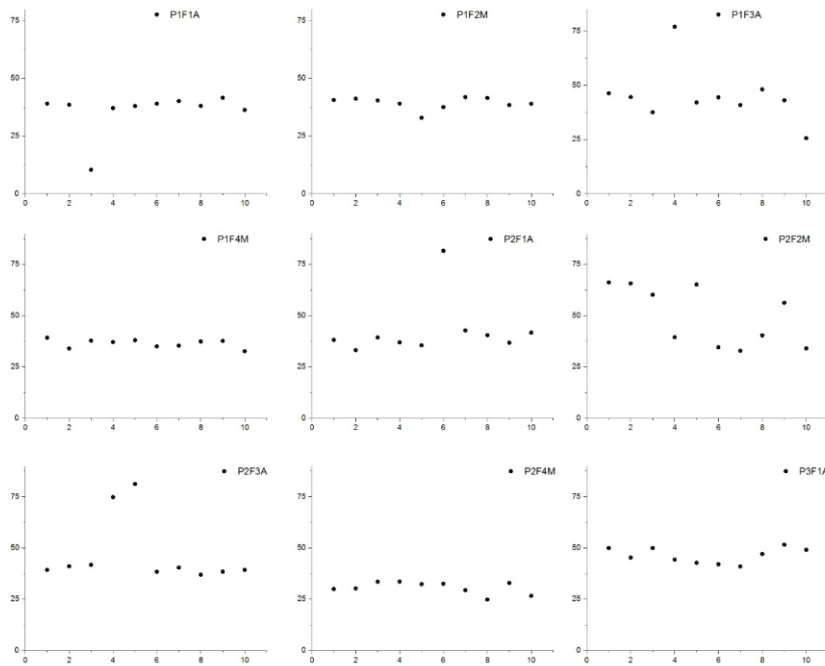


Figure 45. Graph showing the 10 SPAD measurements taken on the 3 plants (P1-P2-P3) on apical leaves (1A-3A) and median leaves (2M-4M).

This indicates that when only a few measurements can be taken, the SPAD does not necessarily provide accurate data. Therefore, the lack of statistical significance may not be due to the microbial biomass treatment not having positive effects on plant fitness, but rather to the inaccuracy of the instrument.

3.6 Evaluation of the biostimulant activity of microbial biomass through coating of Basil seeds

3.6.1 Germination percentage

Germination began 6 days after sowing.

The data relating to the number of seeds germinated and the germination percentages 13 days after sowing are reported below (Table 27):

Table 27. Number of germinated seeds and germination percentages obtained 13 days after sowing for seeds coated with microbial biomass (B), coated with pectin (C) and uncoated (N).

Thesis	+ 13 days post - sowing		
	No. Germinated seeds/No. Total seeds	Germination percentage (%)	Average germination percentage (%)
B1	6/20	30	28.75
B2	4/20	20	
B3	6/20	30	
B4	7/20	35	
C1	13/20	65	62.25
C2	12/20	60	
C3	14/20	70	
C4	14/20	70	
N1	14/20	70	80.00
N2	17/20	85	
N3	16/20	80	
N4	17/20	85	

Germination was still ongoing 19 days after sowing. Data are reported below (Table 28).

Table 28. Number of germinated seeds and germination percentages obtained 19 days after sowing for seeds coated with microbial biomass (B), coated with pectin (C) and uncoated (N).

Thesis	+ 19 days post-sowing		
	No. Germinated seeds/No. Total seeds	Germination percentage (%)	Average germination percentage (%)
B1	6/20	30	32.50
B2	7/20	35	
B3	6/20	30	
B4	7/20	35	
C1	16/20	80	80.00

C2	13/20	65	
C3	17/20	85	
C4	18/20	90	
N1	14/20	70	
N2	18/20	90	83.75
N3	18/20	90	
N4	17/20	85	

Nineteen days after sowing, seeds coated only with pectin showed a germination rate similar to that recorded for uncoated seeds.

Seeds that were either uncoated or coated only with pectin had a higher germination rate than seeds coated with a combination of pectin and biomass.

3.6.2 Phenotypic observations

Nineteen days after sowing, germination was still ongoing, and the emergence of true leaves had also begun in the earliest seedlings (Figure 46).



Figure 46. Details of the emergence of the first true leaves 19 days after sowing.

After 31 days from sowing, the number of seedlings was standardised to 4 in each cylinder (Figure 47).

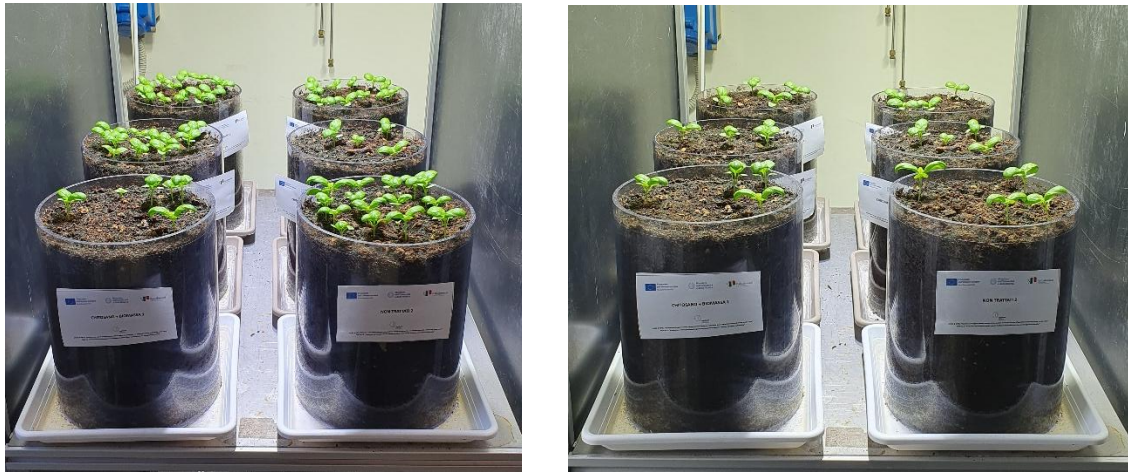


Figure 47. Side A before (on the left) and after (on the right) standardising the number of seedlings to 4 per cylinder.

Some of the sprouts detected during the germination percentage determination phase were aborted. After 35 days from sowing, the seedlings were in the stage of developing the fifth and sixth true leaves (Figure 48).



Figure 48. Details of the emergence of the fifth and sixth true leaves on Basil Prospera F1 35 days after sowing.

Sixty days after sowing, the plants were in the flowering stalk emission stage (Figure 49).



Figure 49. Detail of the floral scape emission on Basilico Prospera F1 60 days after sowing.

After 60 days from sowing, no differences in root branching were observed between the 3 groups (Figure 50).

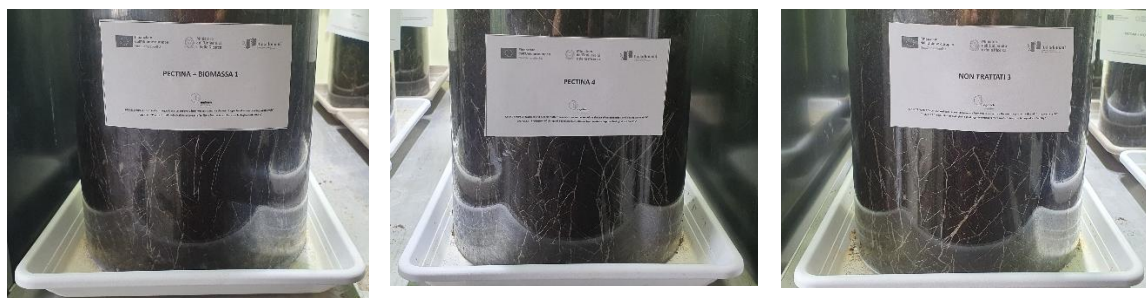


Figure 50. Details of the root branching on Basilico Prospera F1 60 days after sowing.

3.6.3 Biometric measurements

As can be seen from the graph below, plants derived from seeds coated with microbial biomass (B) have intermediate heights between uncoated seeds (N), which show the highest values, and seeds coated only with pectin (C). (Figure 51)

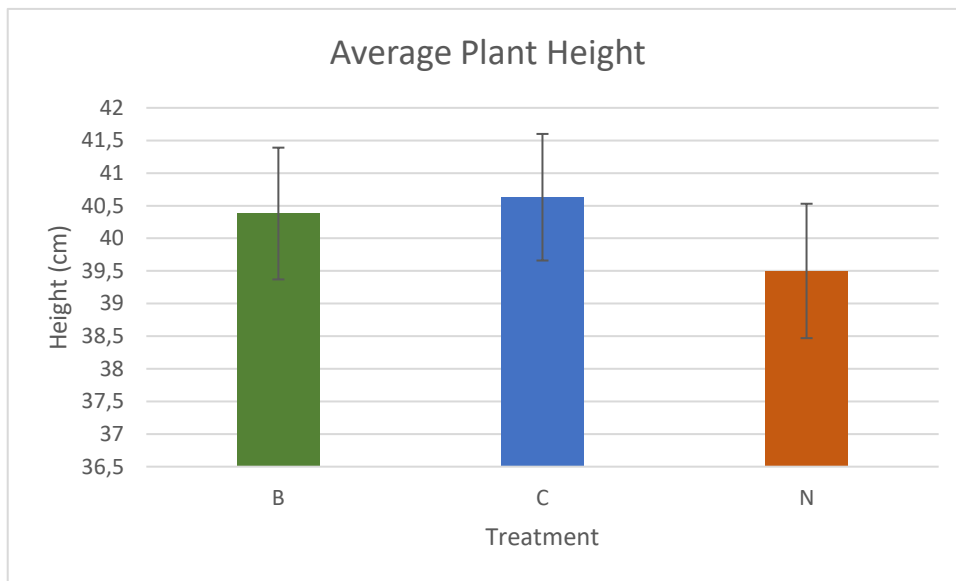


Figure 51. Graph showing the height differences between plants grown from seeds coated with microbial biomass and pectin (B), pectin only (C), and uncoated (N). The Y-axis does not start at zero to improve the readability of the differences between treatments. The values were rounded to one decimal place to simplify presentation, in accordance with the instrument's precision.

All plants had 5 nodes at the time of harvest; therefore, the differences in height are attributable to variations in internode length.

In terms of total fresh biomass, the highest values were recorded for plants grown from seeds coated only with pectin (C). Plants from treatment B produced the lowest results (Figure 52).

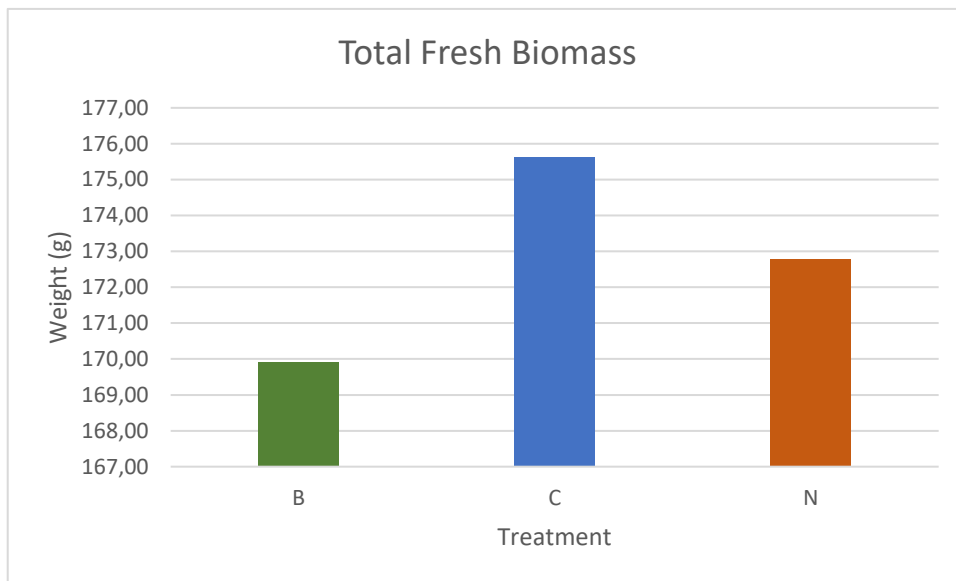


Figure 52. Graph showing the differences in fresh biomass between plants grown from seeds coated with microbial biomass and pectin (B), with pectin only (C) and uncoated (N). The Y-axis does not start at zero to improve the readability of the differences between treatments. The values were rounded to two decimal places to simplify presentation, in accordance with the instrument's precision.

From the determination of the dry biomass, it was observed that even in this case, the plants from treatment C showed the highest values, but the trend between the plants from treatment B and treatment N is reversed, so the lowest values are recorded for the plants derived from untreated seeds (Figure 53).

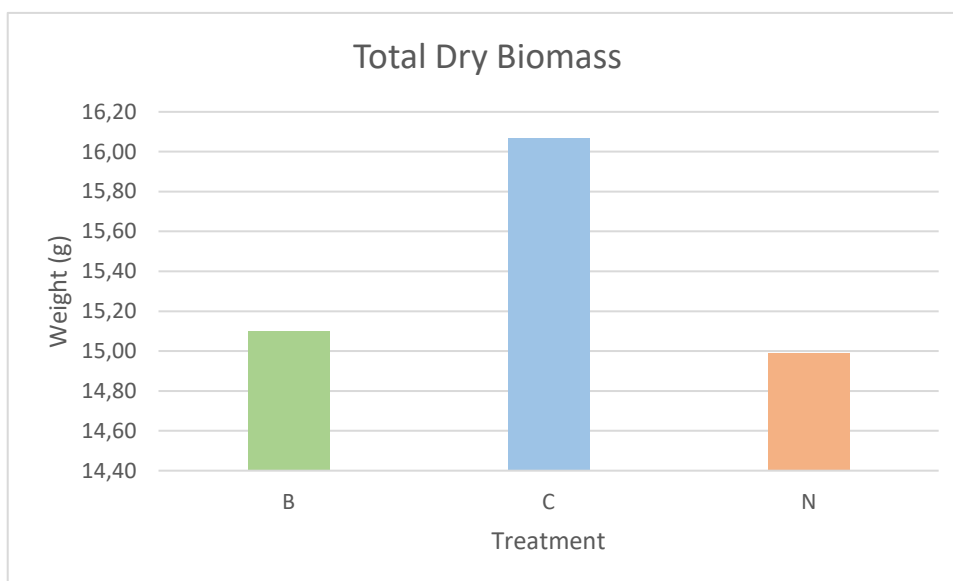


Figure 53. Graph showing the differences in dry biomass between plants grown from seeds coated with microbial biomass and pectin (B), with pectin only (C) and uncoated (N). The Y-axis does not start at zero to improve the readability of the differences between treatments. The values were rounded to two decimal places to simplify presentation, in accordance with the instrument's precision.

3.6.4 Measurement of Chlorophyll Content Index

Chlorophyll content indices obtained 60 days after sowing are reported below (Table 29):

Table 29 shows data relating to the chlorophyll content index (CCI) recorded for the apical (F1-F2) and median (F3-F4) leaves of basil plants derived from seeds coated with biomass and pectin (B), with pectin only (C) and uncoated (N).

Treatment	Chlorophyll content index (CCI)			
	F1	F2	F3	F4
B1	33,4	33,3	63,5	33,5
B2	37,7	32,2	31,5	34,3
B3	31,7	32,1	65,6	30,6
B4	35,7	32,1	31,6	33,7
C1	36	36,1	29,7	33,2
C2	31,7	26,8	61,1	35,2
C3	32,1	39,7	63,5	29,2
C4	28,2	30,9	29,9	26,8
N1	36,1	34,2	29,9	28,6
N2	34,9	34,1	47,9	27,9
N3	44	36	27,4	33,3
N4	34,6	31,6	65,2	29,3

Also in this case, the CCI values detected with SPAD are unreliable for the reasons previously reported in the relevant results of the 'Biostimulant test on Basil' paragraph (Figure 54).

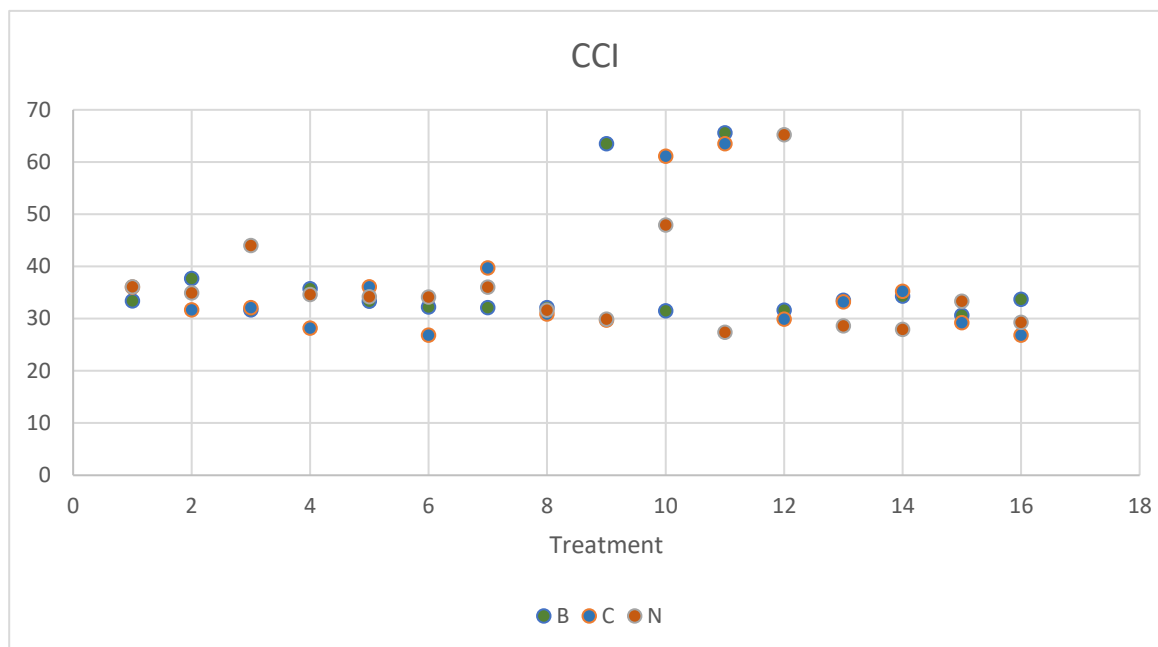


Figure 54. Graph showing the Chlorophyll Content Index (CCI) of plants derived from seeds coated with microbial biomass and pectin (B), with pectin only (C) and uncoated (N).

3.7 Evaluation of the potential of *Pseudomonas granadensis* CT364 to colonise Tomato tissues

3.7.1 Visualisation of Tomato root colonisation by *P.granadensis* CT364

During the *in vitro* cultivation of Micro-Tom tomato seedlings, it was observed that their phytosanitary status was good and their phenotypic development matched expectations, although after about ten days of treatment, the seedlings exhibited symptoms of stress due to confinement in the plate.

However, the sprouts treated with *P. granadensis* CT364 appeared more vigorous, with more expanded leaves and greater root branching than the sprouts treated only with magnesium sulphate. In addition, the roots of the sprouts treated with the bacterium showed growth in the direction of the inoculum (Figures 55 and 56).

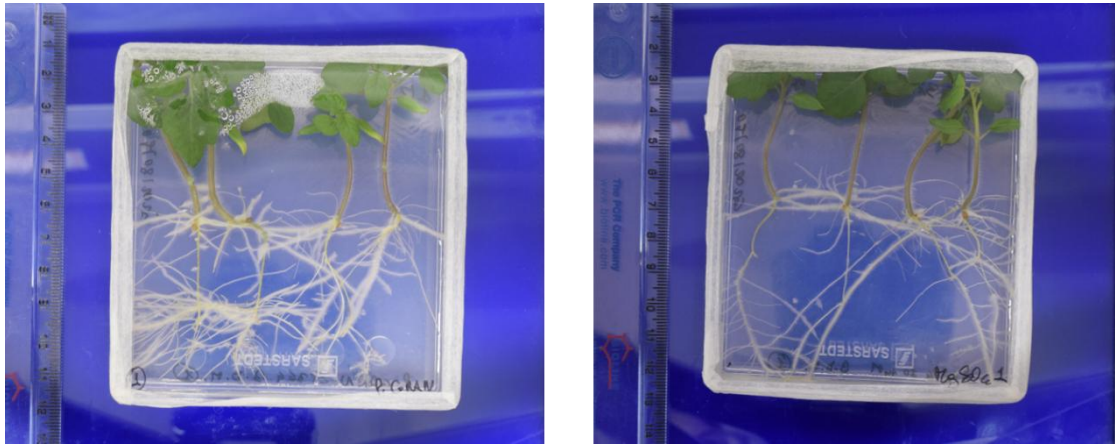


Figure 55. Differences in root development and growth between Micro-Tom tomato seedlings treated with *P. granadensis* CT364 (left) and magnesium sulphate (right). Plants treated with the bacterium have greater root branching and root architecture development in the direction of the bacterial inoculum



Figure 56. Differences in root development and growth between Micro-Tom tomato seedlings treated with *P. granadensis* CT364 (left) and magnesium sulphate (right). Plants treated with the bacterium have more expanded leaves.

Just 10 days after treatment, fluorescence was evident in the roots of the shoots treated with the bacterium.

Fourteen days after treatment, there was greater colonisation of the root tissues by the bacterium compared to the first day of fluorescence testing (Figure 57).

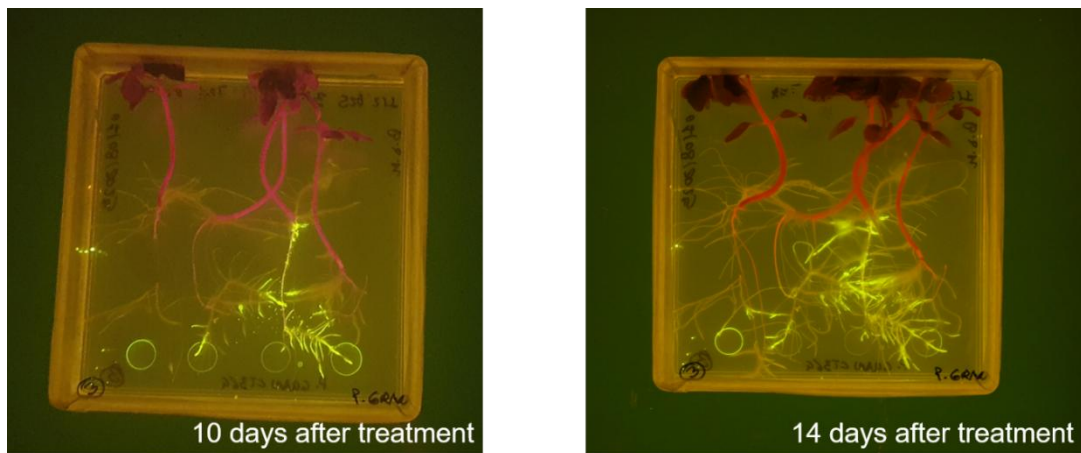


Figure 57. Differences in the colonisation of Micro-Tom tomato root tissues by *P. granadensis* CT364 after 10 (left) and 14 days (right) from treatment.

3.7.2 Visualisation of Tomato aerial tissues colonisation by *P.granadensis* CT364

Phenotypic observations and biometric measurements

Three days after replanting the shoots into soil, it was observed that the shoots treated with the bacterium had coped better with the transplant shock, appearing more vigorous and with more expansive leaves than the shoots treated with magnesium sulphate alone (Figure 58).

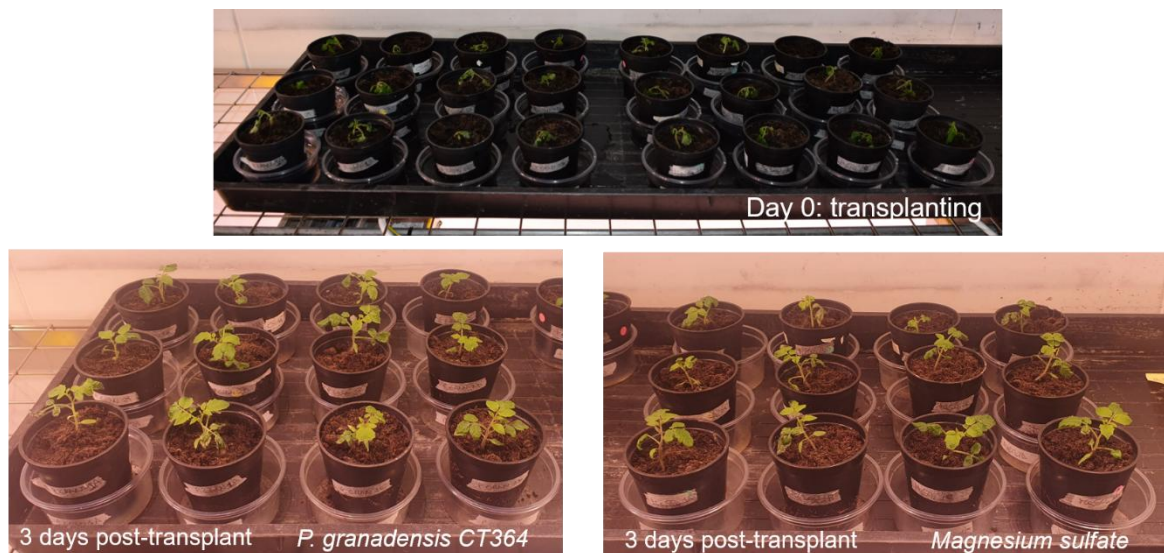


Figure 58. Three days after replanting the shoots into soil, it was observed that the shoots treated with the bacterium had coped better with the transplant shock, appearing more vigorous and with more expansive leaves than the control shoots.

Nineteen days after transplanting, floral buds began to appear. The first plants were some of those from the ‘magnesium sulphate’ thesis (for instance, plant MS1C).

During anthesis, the leaf blades of both types of plants show burns and necrosis of the margins, probably due to excessive light exposure and the presence of water droplets (from guttation or watering) on the leaf tissues (Figure 59).



Figure 59. Details of burns and necrosis affecting the leaf blades of Micro-Tom tomatoes during anthesis.

Measurement of Chlorophyll fluorescence

The analysis of chlorophyll fluorescence yielded the following Fv/Fm values (Table 30):

Table 30 of average Fv/Fm values obtained for plants treated with *P. granadensis* CT364 (PG1A, PG2B, PG3D) and for control plants treated only with magnesium sulphate (MS1D, MS2C, MS3A).

Thesis	Average Fv/Fm Value	Standard Error (±)
PG1A	0.765	0.006
PG2B	0.750	0.003
PG3D	0.780	0.002
MS1D	0.730	0.004
MS2C	0.760	0.003

MS3A	0.780	0.007
------	-------	-------

Biometric measurements

Plants treated with the bacterial suspension are, on average taller than plants treated with ammonium sulphate alone (Figure 60).

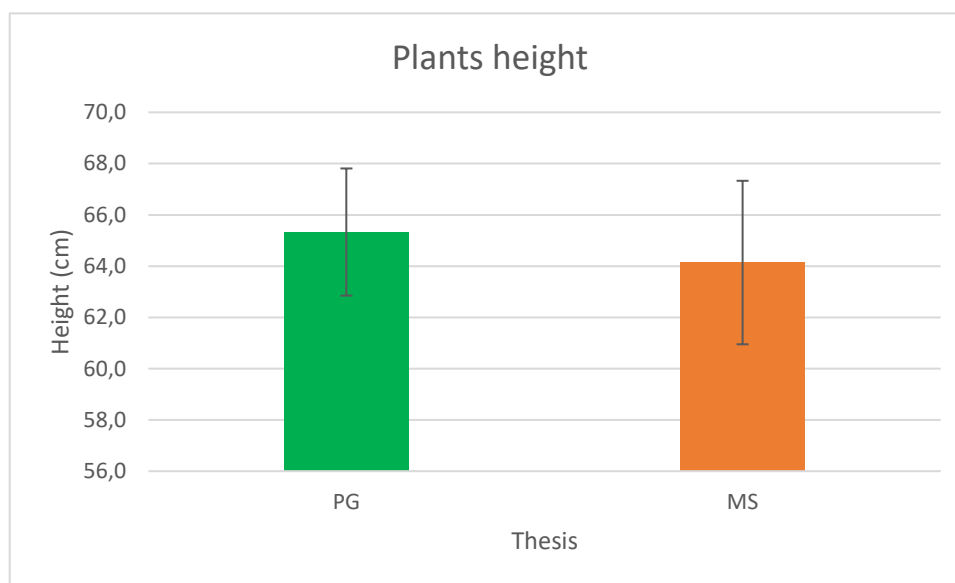


Figure 60. Comparison between the average heights of plants treated with *P. granadensis* CT364 (PG) and the control plants (MS). The Y-axis does not start at zero to improve the readability of the differences between treatments. The values were rounded to one decimal place to simplify presentation, in accordance with the instrument's precision.

Plants treated with *P. granadensis* CT364 showed consistently higher values in both fresh and dry biomass, as illustrated in the graphs below (Figures 61 and 62).

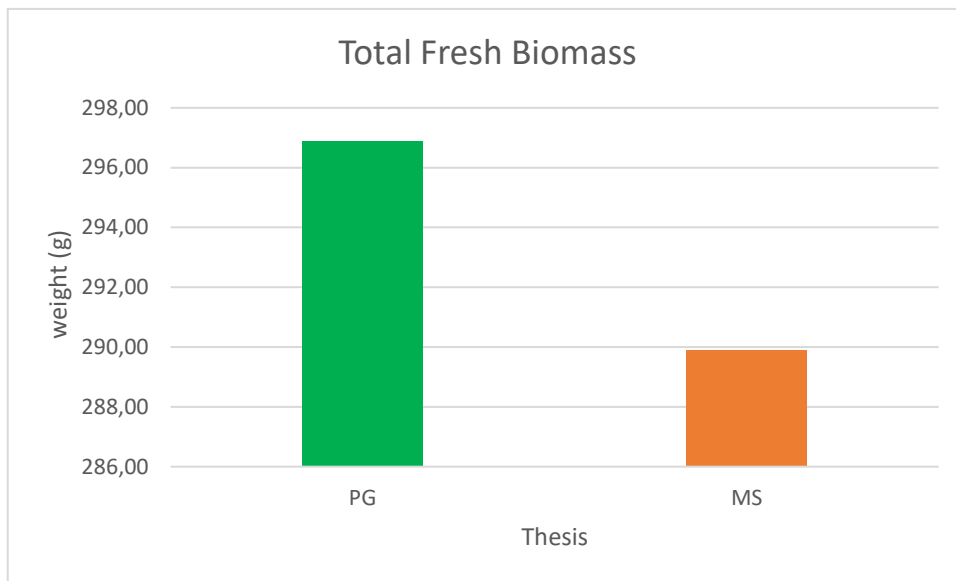


Figure 61. Comparison between the fresh biomass (stems, leaves and flowers) of plants treated with *P. granadensis* CT364 (PG) and control plants (MS). The Y-axis does not start at zero to improve the readability of the differences between treatments. The values were rounded to two decimal places to simplify presentation, in accordance with the instrument's precision.

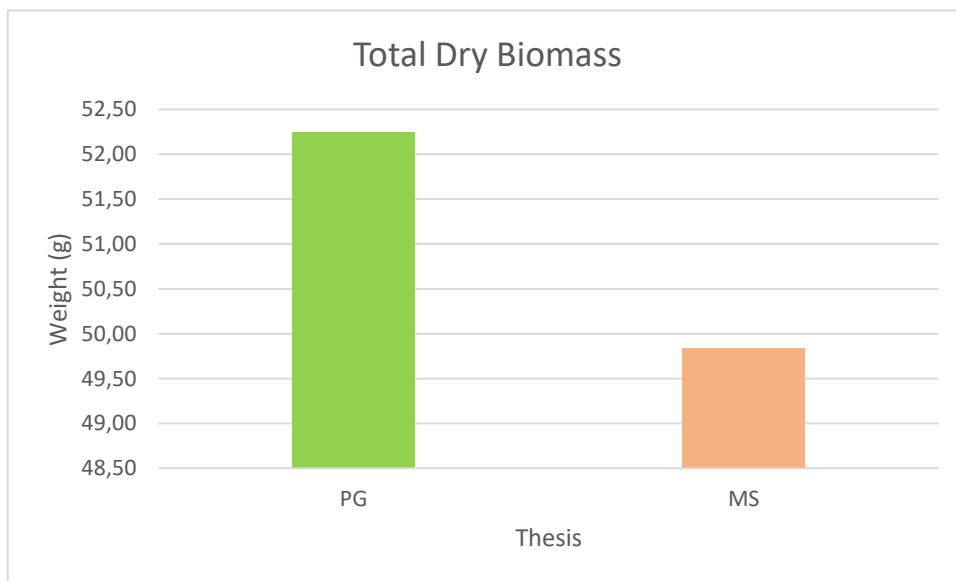


Figure 62. Comparison between the fresh biomass (stems, leaves and flowers) of plants treated with *P. granadensis* CT364 (PG) and control plants (MS). The Y-axis does not start at zero to improve the readability of the differences between treatments. The values were rounded to two decimal places to simplify presentation, in accordance with the instrument's precision.

The biometric data show a normal distribution and homogeneous variance, but the ANOVA test does not show statistical significance.

Re-isolation of *P. granadensis* CT364 from aerial tissues of Micro-To tomato

Five days after the start of the test, two drums of thesis PG1A3 showed bacterial colonies and fluorescence indicative of colonisation of these tissues by *P. granadensis* CT364 (Figure 63).

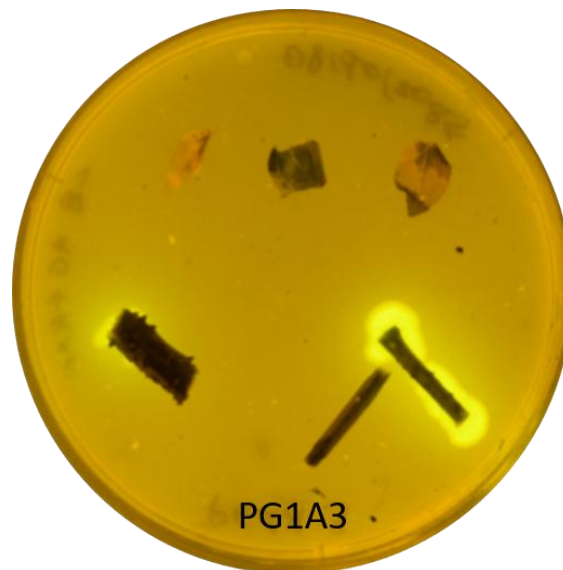


Figure 63. Details of the bacterial outgrowth and fluorescence expressed by *P. granadensis* CT364 in the stems of the PG13A plant.

Twelve days after the start of the test, one drum of thesis PG2B3 also showed fluorescence (Figure 64).



Figure 64. Details of the fluorescence expressed by *P. granadensis* CT364 in a stem of the PG2B3 plant.

3.7.3 Cochise wheat sterilisation procedures

The following Table 31 briefly lists the attempts to sterilise Cochise wheat seeds and the results obtained. These results are discussed in more detail in the respective paragraphs.

Table 31. Summary of sterilisation procedures carried out on Cochise wheat seeds and respective results.

Sterilisation procedure		Washing time with sterile distilled water	Seeds placement	Cultivation settings	Results
1	Dipping in 3% NaClO and Tween 20 for 10 minutes	5 times	Squared Petri dishes filled with 1/2 MS with 1% sucrose	In the dark at 4°C for 2 days to break dormancy, and then kept at 25°C for 3 days	Contamination but high germination
2	Dipping in 3% NaClO and Tween 20 for 10 minutes	5 times	Petri dishes filled with filter paper sterilised by UV light for 3 hours and 30 minutes and wetted with 3 mL of sterilised distilled water	In the dark at 4°C for 2 days to break dormancy, and then kept at 25°C for 4 days	Contamination but high germination

3	Dipping in 3% NaClO and Tween 20 for 20 minutes	5 times	Petri dishes filled with filter paper sterilised by UV light for 3 hours and 30 minutes and wetted with 3 mL of sterilised distilled water	In the dark at 4°C for 2 days to break dormancy, and then kept at 25°C for 4 days	Contamination but high germination
4.	Dipping in 3% NaClO and Tween 20 for 10 minutes, followed by 70% ethanol for 1 minute	5 times	Petri dishes filled with filter paper sterilised by UV light for 3 hours and 30 minutes and wetted with 3 mL of sterilised distilled water	In the dark at 4°C for 2 days to break dormancy, and then kept at 25°C for 4 days*	Contamination but high germination
5	Dipping in 3% NaClO and Tween 20 for 20 minutes	5 times	Squared Petri dishes filled with 1/2 MS with 1% sucrose	* Then 25-18 °C arranging the plates vertically	Contamination but high germination
6	Dipping in 3% NaClO and Tween 20 for 10 minutes, followed by 70% ethanol for 1 minute	5 times in both cases	Squared Petri dishes filled with 1/2 MS with 1% sucrose	* Then 25-18 °C arranging the plates vertically	Contamination but high germination
7	Exposure to chlorine gas for 3h on seeds left to soak in distilled water for 24 hours	-	Squared Petri dishes filled with 1/2 MS with 3% sucrose	In the dark at 4°C for 2 days to break dormancy, and then kept at 26°C	Contamination (higher than dry seeds) but low germination
8	Exposure to chlorine gas on dry seeds for 3 h	-	Squared Petri dishes filled with 1/2 MS with 3% sucrose	In the dark at 4°C for 2 days to break dormancy, and then kept at 26°C	Contamination but low germination (higher than wet seeds)

Sterilisation with 3% sodium hypochlorite solution

Regarding the first attempt at sterilisation with 3% sodium hypochlorite and placement of the seeds on 1/2 MS, Germination occurred 24 hours after the plates were set at a constant 25°C in the dark.

After 6 days post-sterilisation, 89 out of 90 total seeds germinated, but all showed fungal contamination, as can be seen from the following photo (Figure 65).



Figure 65. Details of the germination and contamination of Cochise wheat seeds sterilised with 3% sodium hypochlorite and placed in square Petri dishes filled with 1/2 MS supplemented with 1% sucrose.

In the case of attempts 2, 3 and 4, germination occurred 4 days after sowing; however, contamination was also observed. Specifically, in plates 1-2 (attempts 2-3), mould was present (Figure 66). In plate 3 (attempt 4), rot was observed, and germination appeared less vigorous compared to the other two plates.



Figure 66. Details of the germination (at the top), the fungal contamination (at the bottom left) and the rot (at the bottom right) of Cochise wheat seeds sterilised with 3% sodium hypochlorite and placed in Petri dishes filled with Whatman filter paper wetted with sterile distilled water.

Even in attempts 5 and 6, the sterilisation procedure did not cause problems from a germination standpoint (18/20 seeds germinated in attempt 5 and 16/20 in attempt 6, 3 days post sowing), but fungal contamination still occurred, affecting all the seeds (Figure 67).

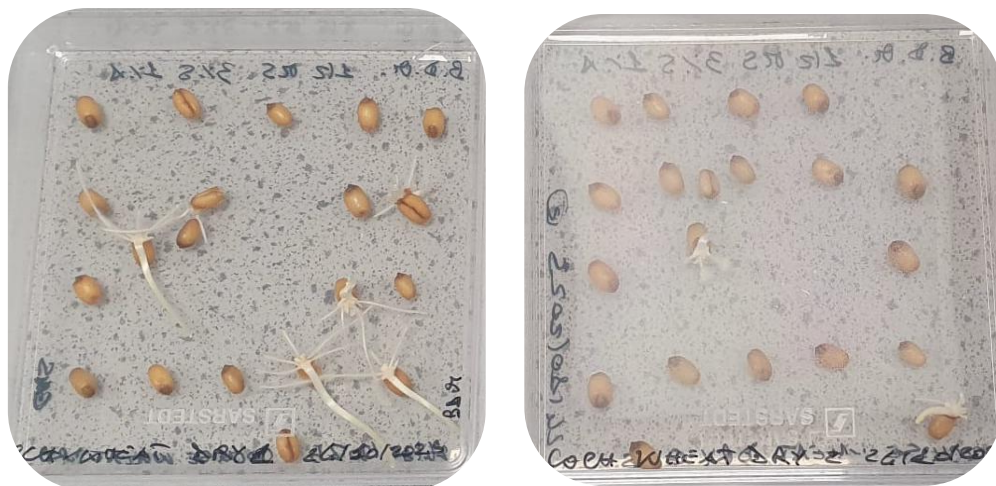


Figure 67. Details of the germination and contamination of Cochise wheat seeds sterilised with 3% sodium hypochlorite (left) and 3% sodium hypochlorite + 70% ethanol. and placed in square Petri dishes filled with 1/2 MS supplemented with 1% sucrose.

Chlorine gas sterilisation

Exposure to chlorine gas for 3 hours and 30 minutes significantly impaired germination; in particular, 7 days after sowing, 8 out of 40 seeds had germinated in trial 7, while 1 out of 40 seeds had germinated in trial 8 (Figure 68).

No soaking



24h soaking in distilled water

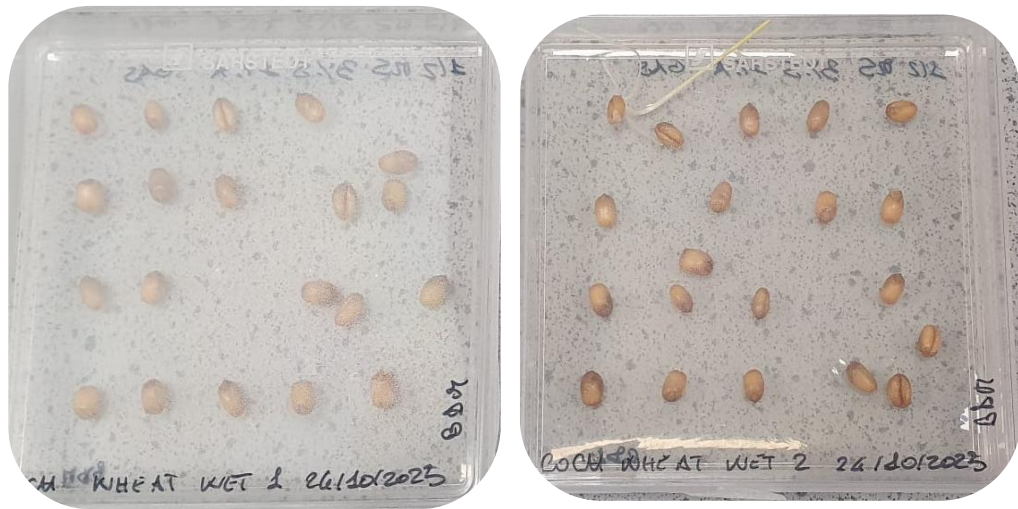
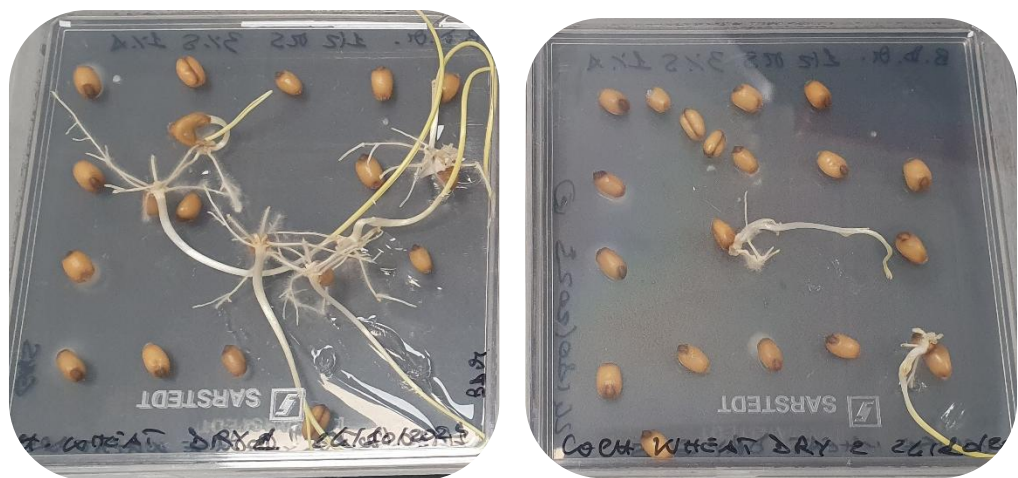


Figure 68. Details of the germination of Cochise wheat seeds exposed to chlorine gas for 3 hours and 30 minutes and placed in square Petri dishes filled with 1/2 MS supplemented with 3% sucrose.

After 17 days from sowing, contamination occurred in 10 out of 40 seeds in attempt 7 and in 21 out of 40 seeds in attempt 8 (Figure 69).

No soaking



24h soaking in distilled water



Figure 69. Details of the germination and contamination of Cochise wheat seeds 17 days after sowing, following exposure to chlorine gas for 3 hours and 30 minutes and subsequent incubation in square Petri dishes containing 1/2 MS medium supplemented with 3% sucrose.

4 Discussion

4.1. Production of iturin A-based biological preparations with antimicrobial activity

The results obtained in this study confirm the strong potential of *Bacillus subtilis* ET-1 as a multifunctional biocontrol agent and biostimulant, highlighting its ability to produce high levels of bioactive lipopeptides and to exert consistent antimicrobial activity under diverse experimental conditions. The integration of strain selection, substrate optimisation, and biological validation provides a comprehensive framework for the development of sustainable microbial-based agricultural inputs.

4.1.1 Selection of *Bacillus subtilis* ET-1 as an effective biocontrol agent

The initial *in vitro* screening demonstrated that *B. subtilis* ET-1 exhibited the highest inhibition of mycelial growth against both *Botrytis cinerea* and *Penicillium digitatum* when compared with other *Bacillus* isolates. Such antagonistic activity aligns with previous reports indicating that *B. subtilis* strains producing iturins, fengycins and surfactins can exert broad-spectrum antifungal effects against multiple phytopathogens through direct antibiosis and disruption of fungal membranes. These cyclic lipopeptides have been widely described as key components of biocontrol mechanisms in *Bacillus* spp. (e.g., *i.e.*, iturin, fengycin, surfactin) (Lastochkina et al., 2019). Studies have similarly identified these lipopeptides in *B. subtilis* strains with antifungal activity, supporting the mode of action observed in our experiments (e.g., inhibition of conidial germination and hyphal deformation) (Harish et al., 2023).

4.1.2 Influence of substrate composition on growth and antifungal activity

The evaluation of growth substrates revealed a strong correlation between substrate composition, bacterial biomass production, and antimicrobial efficacy of the resulting cell-free supernatants. Substrate 14 supported the highest biomass and antifungal activity, suggesting that nutrient balance and carbon source availability are critical determinants of secondary metabolite synthesis. Previous work on *Bacillus* fermentation endorses the concept that carbon source and growth conditions influence LP production, with impacts on the types and quantities of surfactins, iturins, and fengycins produced by different strains under varying media compositions (e.g., sucrose-based formulations influencing lipopeptide profiles) (Singh et al., 2014b).

4.1.3 Optimisation through agro-industrial waste and Response Surface Methodology

The introduction of agro-industrial waste as alternative substrate components successfully aligned metabolite production with sustainability objectives. Substrate 28, formulated with waste-derived ingredients, maintained strong antifungal activity while eliminating the use of manganese chloride, a compound incompatible with environmentally oriented production strategies. The application of Response Surface Methodology further demonstrated that sucrose concentration was the main factor influencing iturin A production, with maximum yields achieved at 20 g/L. The observation that peak lipopeptide production coincided with sporulation at 96 h post-inoculation corroborates previous reports describing lipopeptide biosynthesis as a stationary-phase-associated process in *B. subtilis* (Ambrico and Trupo, 2017; Chen et al., 2009).

4.1.4 Biological validation *in vivo* and post-harvest systems

The *in vivo* assays conducted on melon plants infected with *Podosphaera xanthii* demonstrated that both the cell-free supernatant and crude iturin A extracts achieved disease control levels comparable to, or higher than, the chemical fungicide fenbuconazole. These results confirm the translational potential of *Bacillus*-derived lipopeptides and are consistent with previous studies reporting effective suppression of powdery mildew in cucurbits using *Bacillus* culture filtrates (Romero et al., 2007; Chowdhury et al., 2015).

Post-harvest trials further showed that drying and stabilisation processes did not reduce the antifungal activity of the cell-free supernatant against *P. digitatum*, addressing a major bottleneck in microbial product formulation. The preservation of bioactivity after processing represents a significant advantage for the development of shelf-stable biological products.

4.2 Microbial biomass production and biostimulant activity

Beyond metabolite production, this study demonstrated the feasibility of producing a stable and highly viable microbial biomass of *B. subtilis* ET-1 through fermentation and spray-drying. The high spore viability obtained after processing provides a solid basis for agronomic application and supports the dual use of this microorganism as both a biocontrol agent and a plant biostimulant.

In line with the regulatory framework defined by Regulation (EU) 2019/1009 (European Parliament and Council of the European Union, 2019), the application of *Bacillus subtilis* ET-1 microbial biomass via fertigation was selected to specifically target plant biostimulant functions rather than plant protection activity. Commercial products containing *B. subtilis* currently authorised for use on basil are predominantly registered as plant protection products and applied via foliar spraying, where their mode of action is mainly based on direct antagonism against foliar pathogens through antibiosis and competition. Such products are therefore designed to exert a pesticidal effect, rather than to enhance plant nutritional efficiency or physiological performance.

By contrast, fertigation enables direct delivery of microbial biomass to the rhizosphere, favouring root colonisation and functional interaction with the plant–soil system. This application strategy is consistent with the regulatory definition of plant biostimulants, which are required to stimulate plant nutrition processes independently of the product’s nutrient content and without exerting direct pesticidal effects. For basil, a fast-growing leafy crop with high nutrient demand and sensitivity to abiotic stress, rhizosphere-mediated effects such as improved nutrient use efficiency, root system development and stress mitigation are particularly relevant.

Soil application of microbial biomass resulted in enhanced root system development, earlier root emergence, and increased plant height compared with mineral fertilisation.

Since the number of nodes reflects the rate of leaf emergence, while internode length depends on cell elongation, the treatments appear to have influenced both processes, resulting in morphological differences among the groups.

Although differences in fresh and dry biomass were not always statistically significant, plants treated with microbial biomass consistently performed at least as well as, and often better than, controls. Importantly, the absence of statistical significance does not imply the absence of biological relevance, particularly in complex biological systems characterised by intrinsic variability and limited experimental replication (Amrhein et al., 2019; Wasserstein et al., 2019). The observed trends are coherent with known PGPR-mediated mechanisms, including improved nutrient use efficiency, modulation of phytohormone balance, and stimulation of root architecture (Vessey, 2003; Rouphael and Colla, 2020).

A key outcome of this work is that no phytotoxic effects or growth penalties were observed in plants treated with microbial biomass, despite the presence of biologically active metabolites. This result is particularly relevant in the context of plant biostimulants, which—according to Regulation (EU) 2019/1009 (European Parliament and Council of the European Union, 2019)—must enhance plant performance without exerting direct fertilising or pesticidal effects. The demonstrated agronomic safety therefore supports the classification of *B. subtilis* ET-1 biomass as a biostimulant-compatible bioinput (du Jardin, 2015; Rouphael and Colla, 2020).

4.2.1 Limitations associated with seed coating application

In contrast to soil application, seed coating of basil (*Ocimum basilicum* L.) with *Bacillus subtilis* ET-1 microbial biomass resulted in reduced germination percentages. Although this outcome is undesirable from an applicative perspective, it should be interpreted as an informative result rather than a failure. In formulation-dependent technologies such as seed coating, particularly in small-seeded species like basil, suboptimal early responses can provide valuable insights into the interaction between seed physiology, coating composition, and microbial load (Halmer, 2008; Rocha et al., 2019).

In the present study, the absence of phytotoxic effects, growth inhibition, or developmental abnormalities in soil- and fertigation-based applications strongly suggests that the observed reduction in basil seed germination was not attributable to intrinsic microbial toxicity. Instead, formulation-related factors are more likely responsible. Osmotic stress associated with concentrated microbial coatings may have impaired water uptake during imbibition, a critical phase for germination in small and fast-germinating seeds such as basil (Taylor et al., 1998). Additionally, excessive coating thickness may have interfered with gas exchange and seed respiration, while the uncontrolled release of microbial metabolites at the seed surface may have transiently affected hormonal signalling pathways involved in germination regulation (Halmer, 2008; Rocha et al., 2019).

Importantly, plants derived from coated seeds that successfully emerged exhibited normal development at later growth stages, indicating that the early germination delay did not translate into long-term growth penalties. This observation is particularly relevant in the context of plant biostimulants, which—according to Regulation (EU) 2019/1009 (European

Parliament and Council of the European Union, 2019)—are defined as products that stimulate plant nutritional processes independently of their nutrient content, to improve nutrient use efficiency, stress tolerance, or crop quality, without causing adverse effects on plant health. The absence of negative effects on basil growth and development therefore, supports the biostimulant compatibility of *B. subtilis* ET-1 biomass, while highlighting that seed coating requires further formulation optimisation to ensure full alignment between early seed performance and biostimulant functionality.

Overall, these results emphasise that, for basil, soil or fertigation-based application of microbial biomass currently represents a more reliable delivery strategy than seed coating. Nevertheless, the information gained from the coating assays provides a valuable foundation for future optimisation of binders, coating thickness, and microbial load, which are widely recognised as critical parameters for the successful development of seed-applied PGPR-based biostimulants (Bashan et al., 2014; Malusá and Vassilev, 2014).

4.2.2 Nutritional Assessment as a Limiting Factor in Biostimulant Evaluation

Although the biostimulant activity of *Bacillus subtilis* ET-1 on basil plants was evaluated through biometric and phenological parameters following both fertigation and seed coating applications, a more comprehensive assessment would have benefited from the inclusion of mineral nutrient analyses in plant tissues. Quantification of macro- and micronutrient content would have provided direct evidence of how bacterial inoculation influenced nutrient uptake and assimilation compared with non-inoculated controls.

Several studies have demonstrated that PGPR-mediated biostimulant effects are often closely linked to enhanced nutrient acquisition, including phosphorus solubilisation, improved nitrogen use efficiency, and increased availability of micronutrients such as iron and zinc (Vessey, 2003; Calvo et al., 2014; Rouphael and Colla, 2020). In aromatic plants such as basil, changes in nutrient status can significantly affect biomass accumulation, physiological performance, and secondary metabolite production, making nutrient profiling particularly relevant for interpreting growth responses (Zheljazkov et al., 2008; Nguyen et al., 2010).

In the present study, although plant samples were collected and preserved, it was not possible to perform elemental analyses within the experimental timeframe. As a result, the interpretation of biostimulant effects relies primarily on morphological and developmental

indicators. Nevertheless, the observed trends in plant growth and the absence of negative effects support a positive interaction between *B. subtilis* ET-1 and basil plants.

Future investigations should integrate nutrient analysis of plant tissues with physiological and molecular parameters to better elucidate the mechanisms underlying the biostimulant action of *B. subtilis* ET-1 and to discriminate between direct nutritional effects and indirect growth stimulation mediated by microbial activity

4.3 Concluding remarks

Overall, this study demonstrates that *Bacillus subtilis* ET-1, cultivated on optimised agro-industrial waste-based substrates, produces high levels of bioactive lipopeptides and exhibits strong biocontrol and biostimulant activity without negative effects on plant health. The integration of metabolite production and microbial biomass application represents a promising strategy for the development of multifunctional, sustainable bioinputs, contributing to reduced reliance on chemical fertilisers and plant protection products. Future work should focus on formulation optimisation, large-scale field validation, and deeper mechanistic understanding of plant–microbe–metabolite interactions.

4.4 Colonisation ability and plant interaction of *Pseudomonas granadensis* CT364

The results obtained in this study demonstrate that *Pseudomonas granadensis* CT364 can efficiently colonise tomato tissues and positively interact with the host plant, supporting its classification as a plant-associated beneficial bacterium with potential plant growth-promoting activity.

4.4.1 Root colonisation and early plant–microbe interactions

The *in vitro* assays on Micro-Tom tomato seedlings provided clear evidence of effective root colonisation by *P. granadensis* CT364. Fluorescence signals detected as early as 10 days after inoculation, and their intensification at 14 days, indicate progressive bacterial establishment within root tissues. Root-oriented growth toward the inoculation point, together with increased root branching and altered root architecture, suggests the presence of chemotactic responses and active plant–microbe signalling.

Such responses are commonly reported for beneficial *Pseudomonas* spp., which are known to produce phytohormones (e.g. indole-3-acetic acid), siderophores, and volatile compounds capable of modulating root development and promoting lateral root formation (Lugtenberg

and Kamilova, 2009; Vacheron et al., 2013). The observed enhancement of root branching is therefore consistent with well-established PGPR-mediated mechanisms and supports the hypothesis that CT364 actively interacts with the tomato root system rather than passively adhering to the rhizoplane.

4.4.2 Colonisation of aerial tissues and endophytic behaviour

Beyond root colonisation, the re-isolation of *P. granadensis* CT364 from stem tissues and the detection of fluorescence in aerial organs provide strong evidence of systemic colonisation and endophytic behaviour. The ability of *Pseudomonas* spp. to move from roots to aerial tissues through vascular systems has been previously documented and is considered a key trait for long-term plant association and systemic effects on plant physiology (Compant et al., 2005; Hardoim et al., 2015).

The recovery of fluorescent bacterial colonies from internal stem tissues further confirms that CT364 is capable of surviving and proliferating within the plant without inducing visible disease symptoms. This asymptomatic colonisation is a hallmark of beneficial endophytes and distinguishes PGPR from opportunistic or pathogenic bacteria (Santoyo et al., 2016).

4.4.3 Effects on plant performance and stress tolerance

Following transplantation into soil, plants treated with *P. granadensis* CT364 displayed improved vigour and better tolerance to transplant shock compared with control plants treated with magnesium sulphate alone. Enhanced leaf expansion and overall plant appearance during the early post-transplant phase suggest that bacterial inoculation contributed to mitigating abiotic stress associated with transplantation, a phenomenon widely reported for PGPR-inoculated plants (Yang et al., 2009).

Chlorophyll fluorescence measurements (Fv/Fm) indicated that all plants remained within physiologically acceptable ranges, although bacterium-treated plants showed a tendency toward slightly higher values. Since Fv/Fm is a sensitive indicator of photosystem II efficiency and plant stress status, these results suggest that *P. granadensis* CT364 did not negatively affect photosynthetic performance and may have contributed to maintaining photosynthetic efficiency under suboptimal conditions (Maxwell and Johnson, 2000).

4.4.5 Biometric measurements and interpretation of statistical outcomes

Biometric analyses revealed consistently higher plant height, fresh biomass, and dry biomass in bacterium-treated plants compared with controls. However, despite normal data distribution and homogeneous variance, these differences were not statistically significant according to ANOVA. Importantly, the lack of statistical significance should not be interpreted as evidence of biological irrelevance.

As emphasised in recent discussions on statistical inference in biological research, absence of statistical significance does not equate to absence of an effect, particularly in systems characterised by high biological variability and limited sample size (Amrhein et al., 2019; Wasserstein et al., 2019). In the present study, the consistent direction of the observed effects across multiple parameters strongly suggests a biologically meaningful trend, coherent with known PGPR-mediated growth promotion mechanisms such as enhanced nutrient acquisition, hormonal modulation, and stress alleviation (Vessey, 2003; Backer et al., 2018).

4.4.6 Phytosanitary observations and environmental stress factors

Leaf margin necrosis and burns observed during anthesis affected both treated and control plants, indicating that these symptoms were unrelated to bacterial inoculation. Instead, excessive light exposure and the presence of water droplets on leaf surfaces are well-known causes of localised photodamage and tissue necrosis, particularly under greenhouse conditions (Taiz et al., 2015). The absence of differential symptoms between treatments further supports the conclusion that *P. granadensis* CT364 did not exert phytotoxic effects.

4.4.7 Methodological constraints: seed sterilisation challenges

The difficulties encountered during Cochise wheat seed sterilisation highlight a common methodological challenge in plant–microbe interaction studies. Despite multiple sterilisation strategies, including sodium hypochlorite, ethanol, and chlorine gas treatments, complete elimination of microbial contamination was not achieved without severely compromising seed germination.

Such trade-offs are frequently reported in cereal crops, whose seed-associated microbiota can be particularly resistant to surface sterilisation (Bulgarelli et al., 2013). Chlorine gas treatments, while effective against contaminants, are known to reduce seed viability when exposure conditions are not carefully optimised (Lindsey et al., 2017). These results

underline the importance of balancing sterility and seed viability and suggest that alternative experimental systems or milder sterilisation protocols may be required for future studies.

4.4.8 Concluding remarks

Overall, this study demonstrates that *Pseudomonas granadensis* CT364 is capable of efficient root and systemic colonisation of tomato plants, promotes favourable trends in plant growth and stress tolerance, and does not induce phytotoxic effects. Despite the absence of statistically significant differences in some biometric parameters, the consistency of the observed biological responses supports the role of CT364 as a promising plant-associated bacterium. Future work should focus on larger-scale experiments, refined inoculation strategies, and mechanistic analyses to further elucidate the functional traits underlying plant–*Pseudomonas* interactions under agronomically relevant conditions.

4.5 Complementary microbial strategies for sustainable crop management

The results obtained with *Bacillus subtilis* ET-1 and *Pseudomonas granadensis* CT364 highlight two complementary microbial strategies for sustainable crop management. While *B. subtilis* ET-1 combines the production of bioactive secondary metabolites with the application of a stable and viable microbial biomass, *P. granadensis* CT364 primarily exerts its beneficial effects through efficient root colonisation, systemic movement within plant tissues, and modulation of plant physiological responses.

Spore-forming *Bacillus* spp. are particularly suited for formulation and large-scale application due to their robustness, long shelf life, and capacity to deliver both immediate (metabolite-mediated) and long-term (microbial-mediated) effects in the rhizosphere (Nicholson et al., 2000; Ongena and Jacques, 2008). In contrast, non-spore-forming *Pseudomonas* spp. rely on rapid colonisation, metabolic versatility, and intimate interactions with plant hosts to promote growth and stress tolerance (Lugtenberg and Kamilova, 2009; Vacheron et al., 2013).

The coexistence of these two functional paradigms reflects the increasing interest in diversified microbial consortia and multifunctional bioinputs, where different microbial traits contribute synergistically to plant health, nutrient acquisition, and resilience against biotic and abiotic stresses (Backer et al., 2018; Berg et al., 2020). In this context, the present study supports the notion that no single microbial strategy is universally optimal, and that

the selection of microbial inoculants should be tailored to specific agronomic objectives and application scenarios.

4.6 Technology readiness and application potential of the investigated microbial systems

From a technology readiness perspective, the two microbial systems investigated in this study differ in their degree of proximity to practical application. The production of *B. subtilis* ET-1 biomass through fermentation and spray-drying, coupled with demonstrated antimicrobial and biostimulant activity, places this system at an intermediate-to-advanced technology readiness level. Similar *Bacillus*-based products are already commercially available as biofertilisers and biocontrol agents, supporting the feasibility of scale-up and field deployment (Malusá et al., 2016; Calvo et al., 2014).

In contrast, *P. granadensis* CT364 should be considered at an earlier developmental stage, primarily focused on proof-of-concept demonstrations of colonisation ability, plant compatibility, and biological trends in growth promotion. While promising, further work is required to optimise formulation, delivery methods, and consistency of performance under field conditions, which are known bottlenecks for non-spore-forming PGPR (Herrmann and Lesueur, 2013; Bashan et al., 2014).

Distinguishing between these levels of maturity is essential to contextualise the results and to guide future research efforts. While *B. subtilis* ET-1 is closer to translational application, *P. granadensis* CT364 represents a valuable candidate for further mechanistic and formulation studies aimed at expanding the portfolio of effective plant-associated bacteria.

Conclusions

This thesis investigated the potential of microbial-based strategies as sustainable alternatives to conventional agrochemical inputs, focusing on the selection, optimisation, and biological validation of beneficial bacterial strains for plant protection and biostimulation. In particular, the work addressed the production of bioactive metabolites and microbial biomass from *Bacillus subtilis* ET-1 and the evaluation of colonisation and plant growth-promoting traits of *Pseudomonas granadensis* CT364.

The results obtained confirmed that *B. subtilis* ET-1 is a highly effective producer of antimicrobial lipopeptides, especially iturin A, with strong antagonistic activity against economically relevant phytopathogens such as *Botrytis cinerea*, *Penicillium digitatum*, *Penicillium italicum* and *Monilia laxa*. Through substrate optimisation and the incorporation of agro-industrial waste streams, it was possible to significantly enhance lipopeptide production while aligning the fermentation process with principles of environmental sustainability. The use of Response Surface Methodology further allowed the identification of key nutritional factors influencing iturin A biosynthesis, highlighting sucrose concentration as a major driver of metabolite yield.

Biological validation assays demonstrated that both cell-free supernatants and crude lipopeptide extracts derived from *B. subtilis* ET-1 were effective in controlling plant diseases under in vivo and post-harvest conditions, in some cases achieving levels of protection comparable to or exceeding those of chemical fungicides. Importantly, stabilisation through drying technologies did not compromise antifungal activity, supporting the feasibility of developing shelf-stable microbial formulations suitable for practical agricultural use.

The production of a viable and stable microbial biomass containing *B. subtilis* ET-1 spores further expanded the applicability of the system. Soil application of the biomass resulted in improved root development, enhanced plant height, and overall agronomic performance comparable or superior to mineral fertilisation. Although some biometric parameters did not reach statistical significance, the observed biological trends were consistent with known PGPR-mediated mechanisms and, critically, no phytotoxic or growth-inhibitory effects were detected. This confirms the agronomic safety of the biomass and supports its classification as a plant biostimulant according to current EU regulatory definitions.

In contrast, seed coating with microbial biomass revealed formulation-related limitations, including reduced germination percentages. These effects were not attributable to microbial toxicity but were instead likely linked to osmotic stress, physical interference with seed imbibition, or uncontrolled release of bioactive metabolites. The absence of long-term negative impacts on plant development indicates that these constraints can be addressed through targeted optimisation of coating materials, biomass concentration, and release kinetics.

Finally, the evaluation of *Pseudomonas granadensis* CT364 demonstrated its strong capacity to colonise tomato root and aerial tissues and to promote plant vigour, particularly during early developmental stages and following transplant stress. The successful re-isolation of the bacterium from internal tissues confirmed its endophytic behaviour, reinforcing its potential role as a plant growth-promoting bacterium capable of establishing stable and beneficial associations with the host plant.

Overall, this work highlights the versatility and promise of microbial-based bioinputs that integrate biocontrol, biostimulation, and environmental sustainability. The combined use of optimised microbial biomass and metabolite-rich formulations represents a viable pathway toward reducing dependence on synthetic agrochemicals while maintaining plant health and productivity. Future research should focus on large-scale field validation, formulation refinement, and mechanistic studies to further support the transition of these biological solutions from experimental systems to practical agricultural applications.

Collectively, these findings contribute to the development of next-generation microbial bioinputs and support the broader transition toward more resilient and environmentally sustainable agricultural systems.

Acknowledgements

At the conclusion of this PhD journey, I would like to express my deepest gratitude to all those who made this work possible, providing me with scientific, technical, and human support.

A special thank you goes to my supervisors, Prof. Giuseppe Martelli, Ing. Antonio Molino, and Dr. Roberto Balducci. Thank you for guiding me with patience and expertise, for the trust you placed in my abilities, and for the invaluable lessons that I will carry with me throughout my professional future.

I would also like to sincerely thank the PhD Coordinator, Prof. Patrizia Falabella, for her constant availability and impeccable management of the academic program, which allowed me to conduct my research in a stimulating and well-organised environment.

Heartfelt thanks go to the entire research group at ENEA Trisaia: Alfredo Ambrico, Mario Trupo, Enzo Larocca, Alessandra Magarelli, Maria Martino, Anna Spagnoletta, and Stefania Moliterni. A special thank you to Dr. Tiziana Marino for her invaluable support of the research activities. I also extend my gratitude to the group at ENEA Portici, particularly to Luigi d'Aquino and Emilia Gambale, for their valuable scientific collaboration.

I would also like to thank Prof. Paola Montoro and my colleague Francesca Monzillo for the opportunity to participate in other research lines; these collaborations represented a significant opportunity for growth, deeply enriching me from a professional perspective.

My heartfelt thanks go to my supervisors at Newcastle University, Prof. Angharad Gatehouse and Dr. Martin Edwards. I am deeply grateful for the warm welcome I received in their laboratories and for being included in an international environment of scientific excellence. This experience gave me the invaluable opportunity to carry out part of my PhD research within their teams, enriching both my professional and personal growth.

A very special thought goes to my international colleagues, now dear friends: Veronika, Fabiana, Mansura, Danish, Anqi, Thamer, Malak, Solafa, and Habibah. Thank you for making my time in England an unforgettable and unique experience, turning every day into an opportunity for intercultural and personal exchange. However, despite the open-mindedness I have gained, there are some principles I simply cannot compromise on: espresso remains the one and only true coffee, pasta must never be broken, and—most

importantly—it is never to be topped with ketchup. On this, I am afraid, I will not change my mind!

I want to warmly thank my housemates, Cream, Anju, and Ken, for making me feel at home from the very first moment. Your closeness was precious and helped bridge the distance from my homeland, making my stay a happy chapter of my life, brightened by the presence of the big dog Teddy, whose warm welcome always cheered my English days.

Thanks to my friends Armando, Giulietta, Giulia “Diflo”, Adriana, and Giammarco, who stayed by my side through both the best and worst moments, believing in me even when I struggled to believe in myself. Thank you to Zia Lucia and Zio Roberto, family by choice and a precious presence in my life.

A thank you filled with affection goes to Nonno Andrea, an iconic and legendary pillar of our family; I will always carry your words with me, especially those spoken before I departed for England. A sweet thought goes to Nonna Carla: as I always say, you left us far too soon, but I know you are always with me. I hope you are proud of who I am and what I do, as I am inspired every day by your teachings.

A heartfelt thank-you to zio Gigi, zio Saverio, zietta Olimpia, and the “little bishop” Andrea Giovanni: each of you, in your own unmistakable way, made this journey lighter, louder, funnier, and profoundly mine. Your presence — a mix of wisdom, laughter, and unexpected blessings — has been a precious support I will always carry with me.

Finally, the most heartfelt thank you goes to my family: my mother Lucia, my father Luigi, and my brother Antonio. You are my safe harbour, the place I will always want to return to and that I always carry in my heart. Thank you to my parents for always supporting—and putting up with—me. I am well aware of the sacrifices you made so that Antonio and I never lacked anything, and those you made to allow me to study and advance in my career. I know the strength you showed even when things were far from easy: to you, most of all, goes my sincerest gratitude and admiration. If I am the woman I am today, I owe it above all to your example and your integrity.

Bibliography

- AGRITECH National Research Centre, 2022. *AGRITECH – National Research Centre for Agricultural Technologies*. Available at: <https://agritechcenter.it/> (accessed 5 January 2026).
- Adesemoye, A.O., Torbert, H.A., Kloepper, J.W., 2009. Plant growth-promoting rhizobacteria allow reduced application rates of chemical fertilizers. *Microbial Ecology* 58, 921–929. <https://doi.org/10.1007/s00248-009-9531-y>.
- Ahmad, I., Ahmad, M., Hussain, A., Jamil, M., 2021. Integrated use of phosphate-solubilizing *Bacillus subtilis* strain IA6 and zinc-solubilizing *Bacillus* sp. strain IA16: a promising approach for improving cotton growth. *Folia Microbiologica* 66(1), 115–125. <https://doi.org/10.1007/s12223-020-00818-3>.
- Ahmed, W., Wang, Y., Ji, W., Liu, S., Zhou, S., Pan, J., Li, Z., Wang, F., Wang, X., 2025. Unravelling the mechanism of the endophytic bacterial strain *Pseudomonas oryzihabitans* GDW1 in enhancing tomato plant growth. *International Journal of Molecular Sciences* 26(5), 1922. <https://doi.org/10.3390/ijms26051922>.
- Al-Dhabi, N.A., Esmail, G.A., Valan Arasu, M., 2020. Enhanced production of antimicrobial metabolites by *Streptomyces* sp. and their biological activities. *International Journal of Environmental Research and Public Health* 17, 8446. <https://doi.org/10.3390/ijerph17228446>.
- Alghanmi, L., Alzahrani, H.S., Alharbi, N.S., Alghamdi, S.A., Alzahrani, A.M., Alghamdi, A.A., 2024. Genome sequence of the desert endophyte *Pseudomonas granadensis* R4-79 reveals potential for plant growth promotion and disease suppression. *Research Square* (preprint). <https://doi.org/10.21203/rs.3.rs-6620576/v1>.
- Almanaa, T.N., Vijayaraghavan, P., Alharbi, N.S., Kadaikunnan, S., Khaled, J.M., Alyahya, S.A., 2020. Production and characterization of biosurfactants from *Bacillus* species and their antimicrobial activity. *Journal of King Saud University – Science* 32, 1555–1561. <https://doi.org/10.1016/j.jksus.2019.11.012>.

- Aloo, B.N., Makumba, B.A., Mbega, E.R., Makonde, H.M., 2025. Microbial inoculants for sustainable agriculture: mechanisms and future prospects. *Frontiers in Sustainable Food Systems* 9, 1298743. <https://doi.org/10.3389/fsufs.2025.1298743>.
- Ambrico, A., Trupo, M., 2017. Fermentation strategies for lipopeptide production by *Bacillus* species. *Applied Microbiology and Biotechnology* 101, 1–15. <https://doi.org/10.1007/s00253-017-8354-2>.
- Ambrico, A., Trupo, M., Magarelli, R.A., 2019. Optimization of lipopeptide production by *Bacillus* spp. *Current Microbiology* 76, 1487–1494. <https://doi.org/10.1007/s00284-019-01762-7>
- Amrhein, V., Greenland, S., McShane, B., 2019. Scientists rise up against statistical significance. *Nature* 567, 305–307. <https://doi.org/10.1038/d41586-019-00857-9>.
- Anwar, M.R., Liu, D.L., Macadam, I., Kelly, G., 2013. Adapting agriculture to climate change: a review. *Theoretical and Applied Climatology* 113, 225–245. <https://doi.org/10.1007/s00704-012-0793-5>.
- Arasu, M.V., Al-Dhabi, N.A., 2024. Improved production of extremophilic protease using low-cost substrate by *Bacillus subtilis* ZB isolated from extreme environment for tannery effluent treatment. *Biomass Conversion and Biorefinery* 14, 22605–22615. <https://doi.org/10.1007/s13399-023-04190-0>.
- Arnaouteli, S., Bamford, N.C., Stanley-Wall, N.R., Kovács, Á.T., 2021. *Bacillus subtilis* biofilm formation and social interactions. *Nature Reviews Microbiology* 19, 600–614. <https://doi.org/10.1038/s41579-021-00564-7>.
- Backer, R., Rokem, J.S., Ilangumaran, G., et al., 2018. Plant growth-promoting rhizobacteria: mechanisms and applications. *Frontiers in Plant Science* 9, 1473. <https://doi.org/10.3389/fpls.2018.01473>.
- Bajpai, A., Johri, B.N., 2019. Endophytic pseudomonads and their metabolites. In: *Endophytes and Secondary Metabolites*. Springer, Cham, pp. 33–59. https://doi.org/10.1007/978-3-319-76900-4_2.

- Barra-Bucarei, L., González, M.G., Iglesias, A.F., Aguayo, G.S., Peñalosa, M.G., Vera, P.V., 2020. Antagonistic activity of endophytic fungi against plant pathogens. *Insects* 11, 1–15. <https://doi.org/10.3390/insects11010001>.
- Bashan, Y., de Bashan, L.E., Prabhu, S.R., Hernandez, J.P., 2014. Advances in plant growth-promoting bacterial inoculant technology: formulations and practical perspectives. *Plant and Soil* 378, 1–33. <https://doi.org/10.1007/s11104-013-1956-x>.
- Bektas, I., Kusek, M., 2021. Biological control of plant pathogens using beneficial bacteria. *Biocontrol Science and Technology* 31, 190–205. <https://doi.org/10.1080/09583157.2020.1863971>.
- Beltran-Gracia, E., Macedo-Raygoza, G., Villafaña-Rojas, J., et al., 2017. Production of lipopeptides by fermentation processes. In: *Fermentation Processes*. InTechOpen. <https://doi.org/10.5772/intechopen.69005>.
- Berg, G., Rybakova, D., Fischer, D., et al., 2020. Microbiome definition revisited: old concepts and new challenges. *Microbiome* 8, 103. <https://doi.org/10.1186/s40168-020-00875-0>.
- Biniarz, P., Henkel, M., Hausmann, R., Łukaszewicz, M., 2020. Biosurfactants in biological control and plant growth promotion. *Frontiers in Bioengineering and Biotechnology* 8, 556. <https://doi.org/10.3389/fbioe.2020.00556>
- BioRender.com, 2026. *BioRender – Scientific Illustration Software*. Available at: <https://www.biorender.com> (accessed 5 January 2026).
- Blake, C., Christensen, M.N., Kovács, Á.T., 2021. Molecular aspects of plant growth promotion and protection by *Bacillus subtilis*. *Molecular Plant–Microbe Interactions* 34, 15–25. <https://doi.org/10.1094/MPMI-05-20-0123-CR>.
- Bouassida, M., Mnif, I., Ghribi, D., 2023a. Lipopeptide biosynthesis and biocontrol potential of *Bacillus* spp. *Bioprocess and Biosystems Engineering* 46, 555–563. <https://doi.org/10.1007/s00449-022-02846-1>.
- Bouassida, M., Mnif, I., Hammami, I., Triki, M.A., Ghribi, D., 2023b. Antifungal activity of *Bacillus*-derived lipopeptides. *Food Science and Biotechnology* 32, 1595–1609. <https://doi.org/10.1007/s10068-023-01190-2>.

- Bouchard-Rochette, M., Machrafi, Y., Cossus, L., Nguyen, T.T.A., Antoun, H., Droit, A., Tweddell, R.J., 2022. Biocontrol activity of bacterial endophytes against soil-borne pathogens. *Biological Control* 170, 104925. <https://doi.org/10.1016/j.biocontrol.2022.104925>.
- Bulgarelli, D., Schlaeppi, K., Spaepen, S., van Themaat, E.V.L., Schulze-Lefert, P., 2013. Structure and functions of the bacterial microbiota of plants. *Annual Review of Plant Biology* 64, 807–838. <https://doi.org/10.1146/annurev-arplant-050312-120106>.
- Burpee, L.L., 1990. The influence of abiotic factors on biological control of soilborne plant pathogenic fungi. *Canadian Journal of Plant Pathology* 12(3), 308–317. <https://doi.org/10.1080/07060669009501005>.
- Calvo, P., Nelson, L., Kloepper, J.W., 2014. Agricultural uses of plant biostimulants. *Plant and Soil* 383, 3–41. <https://doi.org/10.1007/s11104-014-2131-8>
- Carson, R., 1962. *Silent Spring*. Houghton Mifflin, Boston.
- Cea-Torrescassana, E., López-Pérez, M., Rodríguez-Díaz, M., Sánchez-Porro, C., Ventosa, A., Pujalte, M.J., 2024. Genomic and functional analyses reveal *Pseudomonas granadensis* CT364 is a plant growth-promoting endophyte. *BMC Microbiology* 25(1), 15. <https://doi.org/10.1186/s12866-024-03125-7>.
- Chakraborty, M., Mahmud, N.U., Gupta, D.R., Tareq, F.S., Shin, H.J., Islam, T., 2020. Role of microbial secondary metabolites in plant disease control. *Frontiers in Microbiology* 11, 1309. <https://doi.org/10.3389/fmicb.2020.01309>.
- Chen, X.H., Koumoutsis, A., Scholz, R., Borriss, R., 2009. More than anticipated: production of antibiotics and other secondary metabolites by *Bacillus amyloliquefaciens* FZB42. *Journal of Molecular Microbiology and Biotechnology* 16(1–2), 14–24. <https://doi.org/10.1159/000142891>.
- Cho, W.I., Chung, M.S., 2020. *Bacillus* spores: properties and inactivation processing technologies. *Food Science and Biotechnology* 29, 1–10. <https://doi.org/10.1007/s10068-020-00751-9>.

- Chowdhury, S.P., Hartmann, A., Gao, X., Borriss, R., 2015. Biocontrol mechanism by root-associated *Bacillus amyloliquefaciens* FZB42 – a review. *Frontiers in Microbiology* 6, 780. <https://doi.org/10.3389/fmicb.2015.00780>.
- Ciurko, D., Czyżnikowska, Ż., Kancelista, A., Łaba, W., Janek, T., 2022. Sustainable production of biosurfactant from agro-industrial oil wastes by *Bacillus subtilis* and its potential application as antioxidant and ACE inhibitor. *International Journal of Molecular Sciences* 23(18), 10824. <https://doi.org/10.3390/ijms231810824>.
- Compant, S., Clément, C., Sessitsch, A., 2010. Plant growth-promoting bacteria in the rhizosphere, root colonization and endophytic lifestyles. *Soil Biology and Biochemistry* 42, 669–678. <https://doi.org/10.1016/j.soilbio.2009.11.024>.
- Compant, S., Reiter, B., Sessitsch, A., Nowak, J., Clément, C., Barka, E.A., 2005. Endophytic colonization of *Vitis vinifera* L. by *Burkholderia phytofirmans* strain PsJN. *Applied and Environmental Microbiology* 71(8), 4602–4612. <https://doi.org/10.1128/AEM.71.8.4602-4612.2005>.
- Crouzet, J., Arguelles-Arias, A., Dhondt-Cordelier, S., et al., 2020. Biosurfactants in plant protection against diseases: rhamnolipids and lipopeptides case study. *Frontiers in Bioengineering and Biotechnology* 8, 101. <https://doi.org/10.3389/fbioe.2020.00101>
- Das, A.J., Kumar, R., 2018. Utilization of agro-industrial waste for biosurfactant production under submerged fermentation and its application in oil recovery from sand matrix. *Bioresource Technology* 260, 233–240. <https://doi.org/10.1016/j.biortech.2018.03.093>.
- DeClerck, F.A.J., Koziell, I., Benton, T., Garibaldi, L.A., Kremen, C., Maron, M., Del Rio, C.R., Sidhu, A., Wirths, J., Clark, M., Dickens, C., Carmona, N.E., Fremier, A.K., Jones, S.K., Khoury, C.K., Lal, R., Obersteiner, M., Remans, R., Rusch, A., Schulte, L.A., Simmonds, J., Stringer, L.C., Weber, C., Winowiecki, L., 2023. A whole Earth approach to nature-positive food: biodiversity and agriculture. In: *Science and Innovations for Food Systems Transformation*. Springer International Publishing, pp. 469–496.
- Dimkić, I., Janakiev, T., Petrović, M., Degrassi, G., Fira, D., 2022. Plant-associated *Bacillus* and *Pseudomonas* antimicrobial activities in plant disease suppression via biological control mechanisms – a review. *Physiological and Molecular Plant Pathology* 117, 101754. <https://doi.org/10.1016/j.pmpp.2021.101754>.

- Directive 2009/128/EC, n.d. *Establishing a framework for Community action to achieve the sustainable use of pesticides*. Available at: <https://eur-lex.europa.eu/legal-content/EN/ALL/?uri=celex:32009L0128> (accessed 2 January 2024).
- Domínguez Rivera, Á., Martínez Urbina, M.Á., López y López, V.E., 2019. Advances on research in the use of agro-industrial waste in biosurfactant production. *World Journal of Microbiology and Biotechnology* 35, 155. <https://doi.org/10.1007/s11274-019-2729-3>.
- du Jardin, P., 2015. Plant biostimulants: definition, concept, main categories and regulation. *Scientia Horticulturae* 196, 3–14. <https://doi.org/10.1016/j.scienta.2015.09.021>.
- Duque-Acevedo, M., Belmonte-Ureña, L.J., Cortés-García, F.J., Camacho-Ferre, F., 2020. Agricultural waste: review of the evolution, approaches and perspectives on alternative uses. *Global Ecology and Conservation* 22, e00902. <https://doi.org/10.1016/j.gecco.2020.e00902>.
- Earl, A.M., Losick, R., Kolter, R., 2008. Ecology and genomics of *Bacillus subtilis*. *Trends in Microbiology* 16(6), 269–275. <https://doi.org/10.1016/j.tim.2008.03.004>.
- Ehteshamul Haque, S., Sultana, V., Ara, J., Athar, M., 2007. Cultivar response against root-infecting fungi and efficacy of *Pseudomonas aeruginosa* in controlling soybean root rot. *Plant Biosystems* 141(1), 51–55. <https://doi.org/10.1080/11263500601153843>.
- Elnahal, A.S.M., El-Saadony, M.T., Saad, A.M., Desoky, E.S.M., El-Tahan, A.M., Rady, M.M., AbuQamar, S.F., El-Tarabily, K.A., 2022. The use of microbial inoculants for biological control, plant growth promotion, and sustainable agriculture: a review. *European Journal of Plant Pathology* 164, 1–28. <https://doi.org/10.1007/s10658-022-02539-1>.
- Elsevier, n.d. *Scopus Preview*. Available at: <https://www.scopus.com> (accessed 5 January 2026).
- English, A., 2019. *The State of Food and Agriculture 2019: Moving Forward on Food Loss and Waste Reduction*. Food and Agriculture Organization of the United Nations.
- Errington, J., van der Aa, L.T., 2020. Editorial overview: microbiology. *Microbiology (United Kingdom)* 166, 425–427. <https://doi.org/10.1099/mic.0.000955>.

- EU Pesticides Database, n.d. Available at: <https://ec.europa.eu/food/plant/pesticides/eu-pesticides-database/start/screen/active-substances> (accessed 2 January 2024).
- European Commission, 2026. *EU Pesticides Database*. Available at: https://food.ec.europa.eu/plants/pesticides/eu-pesticides-database_en (accessed 5 January 2026).
- European Commission, 2019. *The European Green Deal*. COM(2019) 640 final. Available at: <https://eur-lex.europa.eu/legal-content/EN/TXT/?uri=CELEX:52019DC0640>.
- European Commission, 2009. Regulation (EC) No 1107/2009 of the European Parliament and of the Council of 21 October 2009 concerning the placing of plant protection products on the market. *Official Journal of the European Union* L 309, 1–50.
- European Parliament & Council of the European Union, 2019. Regulation (EU) 2019/1009 of the European Parliament and of the Council of 5 June 2019 laying down rules on the making available on the market of EU fertilising products. *Official Journal of the European Union* L 170, 1–114.
- FAO, 2019. *The State of Food and Agriculture 2019: Moving forward on food loss and waste reduction*. FAO, Rome. <https://doi.org/10.4060/CA6030EN>.
- FAO, 2021. *The State of the World's Land and Water Resources for Food and Agriculture – Systems at Breaking Point (SOLAW 2021)*. FAO, Rome.
- FAO, 2025. *The State of the World's Land and Water Resources for Food and Agriculture 2025*. FAO, Rome.
- Fira, D., Dimkić, I., Berić, T., Lozo, J., Stanković, S., 2018. Biological control of plant pathogens by *Bacillus* species. *Journal of Biotechnology* 285, 44–55. <https://doi.org/10.1016/j.jbiotec.2018.08.009>
- Francl, L.J., 2001. The disease triangle: a plant pathological paradigm revisited. *The Plant Health Instructor* 10. <https://doi.org/10.1094/PHI-T-2001-0517-01>.
- Franco-Sierra, N.D., Posada, L.F., Santa-María, G., Romero-Tabarez, M., Villegas-Escobar, V., Álvarez, J.C., 2020. Genomic and functional characterization of endophytic bacteria.

- Functional & Integrative Genomics* 20, 575–589. <https://doi.org/10.1007/s10142-020-00741-0>.
- Gowtham, H.G., Murali, M., Singh, S.B., Lakshmeesha, T.R., Murthy, K.N., Amruthesh, K.N., 2018. Induction of drought tolerance in tomato (*Solanum lycopersicum* L.) by *Bacillus subtilis* Rhizo SF 48 through physiological and biochemical mechanisms. *Journal of Plant Growth Regulation* 37, 1258–1270. <https://doi.org/10.1007/s00344-018-9834-3>.
- Guan, Y., Bak, F., Hennessy, R.C., Horn Herms, C., Elberg, C.L., Dresbøll, D.B., Winding, A., Sapkota, R., Nicolaisen, M.H., 2024. The potential of *Pseudomonas fluorescens* SBW25 to produce viscosin enhances wheat root colonization and shapes root-associated microbial communities in a plant genotype-dependent manner in soil systems. *mSphere*
- Gullino, M.L., Tinivella, F., Garibaldi, A., Kemmitt, G.M., Bacci, L., Sheppard, B., 2009. Mancozeb: past, present, and future. *Plant Disease* 94(9), 1076–1087. <https://doi.org/10.1094/PDIS-94-9-1076>.
- Gupta, R., Kumari, A., Sharma, S., Alzahrani, O.M., Noureldeen, A., Darwish, H., 2022. Identification, characterization and optimization of phosphate-solubilizing rhizobacteria (PSRB) from rice rhizosphere. *Saudi Journal of Biological Sciences* 29(1), 35–42. <https://doi.org/10.1016/j.sjbs.2021.08.064>.
- Gupta, R., Noureldeen, A., Darwish, H., 2021. Rhizosphere-mediated growth enhancement using phosphate-solubilizing rhizobacteria and their tricalcium phosphate solubilization activity under pot culture assays in rice (*Oryza sativa*). *Saudi Journal of Biological Sciences* 28(7), 3692–3700. <https://doi.org/10.1016/j.sjbs.2021.03.018>.
- Hadj Saadoun, J., Bertani, G., Levante, A., Vezzosi, F., Ricci, A., Bernini, V., Lazzi, C., 2021. Fermentation of agri-food waste: a promising route for the production of aroma compounds. *Foods* 10, 707. <https://doi.org/10.3390/foods10040707>.
- Halmer, P., 2008. Seed technology and seed enhancement. *Acta Horticulturae* 771, 17–26. <https://doi.org/10.17660/ActaHortic.2008.771.1>.
- Hardoim, P.R., van Overbeek, L.S., Berg, G., et al., 2015. The hidden world within plants: ecological and evolutionary considerations for defining functioning of microbial

- endophytes. *Microbiology and Molecular Biology Reviews* 79(3), 293–320. <https://doi.org/10.1128/MMBR.00050-14>.
- Harish, B.N., Nagesha, S.N., Ramesh, B.N., et al., 2023a. Molecular characterization and antifungal activity of lipopeptides produced from *Bacillus subtilis* against the plant fungal pathogen *Alternaria alternata*. *BMC Microbiology* 23, 179. <https://doi.org/10.1186/s12866-023-02917-3>.
- Harish, B.N., Nagesha, S.N., Ramesh, B.N., Shyamamma, S., Nagaraj, M.S., Girish, H.C., Pradeep, C., Shiva Kumar, K.S., Tharun Kumar, K.S., Pavan, S.N., Kavan Kumar, V., 2023b. Molecular characterization and antifungal activity of lipopeptides produced from *Bacillus subtilis* against the plant fungal pathogen *Alternaria alternata*. *BMC Microbiology* 23, 179. <https://doi.org/10.1186/s12866-023-02922-w..>
- Harman, G.E., Howell, C.R., Viterbo, A., Chet, I., Lorito, M., 2004. *Trichoderma* species: opportunistic, avirulent plant symbionts. *Nature Reviews Microbiology* 2, 43–56. <https://doi.org/10.1038/nrmicro797>.
- Hashem, A., Tabassum, B., Fathi Abd_Allah, E., 2019. *Bacillus subtilis*: a plant-growth-promoting rhizobacterium that also impacts biotic stress. *Saudi Journal of Biological Sciences* 26(6), 1291–1297. <https://doi.org/10.1016/j.sjbs.2019.05.004>.
- Hassan, M.A., Bakhiet, E.K., Hussein, H.R., Ali, S.G., 2019. Heavy metal tolerance and biosorption potential of *Bacillus* spp. *International Journal of Environmental Science and Technology* 16, 3497–3512. <https://doi.org/10.1007/s13762-018-1861-1>.
- Herrmann, L., Lesueur, D., 2013. Challenges of formulation and quality of biofertilizers for successful inoculation. *Applied Microbiology and Biotechnology* 97, 8859–8873. <https://doi.org/10.1007/s00253-013-5228-8>.
- Hussain, M., Mehboob, N., Naveed, M., Shehzadi, K., Yasir, T.A., 2020. Optimizing boron seed coating level and boron-tolerant bacteria for improving yield and biofortification of chickpea. *Journal of Soil Science and Plant Nutrition* 20(4), 2471–2478. <https://doi.org/10.1007/s42729-020-00303-2>.

- Idris, E.E., Iglesias, D.J., Talon, M., Borriss, R., 2007. Tryptophan-dependent production of indole-3-acetic acid by *Bacillus amyloliquefaciens* FZB42. *Applied and Environmental Microbiology* 73, 6353–6360. <https://doi.org/10.1128/AEM.01006-07>.
- Iqbal, S., Begum, F., Rabaan, A.A., Aljeldah, M., Al Shammari, B.R., Alawfi, A., Alshengeti, A., Sulaiman, T., Khan, A., 2023. *Molecules* 28, 927. <https://doi.org/10.3390/molecules28030927>.
- Jabborova, D., Enakiev, Y., Sulaymanov, K., Kadirova, D., Ali, A., Annapurna, K., 2021. *Plant Science Today* 8, 66–71. <https://doi.org/10.14719/pst.2021.8.1.1032>.
- Jia, Y., Niu, H., Zhao, P., Li, X., Yan, F., Wang, C., Qiu, Z., 2023. *Applied Microbiology and Biotechnology* 107, 6071–6083. <https://doi.org/10.1007/s00253-023-12698-4>.
- Jiang, M., Pang, X., Liu, H., Lin, F., Lu, F., Bie, X., Lu, Z., Lu, Y., 2021. *Molecules* 26, 6002. <https://doi.org/10.3390/molecules26196002>.
- Jiang, X., Cui, Z., Wang, L., Xu, H., Zhang, Y., 2020. *LWT – Food Science and Technology* 131, 109744. <https://doi.org/10.1016/j.lwt.2020.109744>.
- Jimoh, A.A., Senbadejo, T.Y., Adeleke, R., Lin, J., 2021. Development and genetic engineering of hyper-producing microbial strains for improved synthesis of biosurfactants. *Molecular Biotechnology* 63, 1033–1050. <https://doi.org/10.1007/s12033-021-00359-4>.
- Ju, W., Liu, L., Fang, L., Cui, Y., Duan, C., Wu, H., 2019. Impact of co-inoculation with plant growth-promoting rhizobacteria and *Rhizobium* on biochemical responses of the alfalfa–soil system in copper-contaminated soil. *Ecotoxicology and Environmental Safety* 167, 218–226. <https://doi.org/10.1016/j.ecoenv.2018.09.111>.
- Junges, E., Toebe, M., Santos, R.F.D., Finger, G., Muniz, M.F.B., 2013. Effect of priming and seed coating when associated with *Bacillus subtilis* in maize seeds. *Revista Ciência Agronômica* 44, 520–526. <https://doi.org/10.1590/S1806-66902013000300020>.
- Kaspar, F., Neubauer, P., Gimpel, M., 2019. Bioactive secondary metabolites from *Bacillus subtilis*: a comprehensive review. *Journal of Natural Products* 82, 2038–2053. <https://doi.org/10.1021/acs.jnatprod.9b00110>.

- Khan, M., Salman, M., Jan, S.A., et al., 2021. Biological control of fungal phytopathogens: a comprehensive review based on *Bacillus* species. *MOJ Biology and Medicine* 6(2), 90–92. <https://doi.org/10.15406/mojbm.2021.06.00137>.
- Khare, T., Anand, U., Dey, A., Assaraf, Y.G., Chen, Z.S., Liu, Z., Kumar, V., 2021. Exploring phytochemicals for combating antibiotic resistance in microbial pathogens. *Frontiers in Pharmacology* 12, 720726. <https://doi.org/10.3389/fphar.2021.720726>.
- Kourmentza, K., Gromada, X., Michael, N., Degraeve, C., Vanier, G., Ravallec, R., Coutte, F., Karatzas, K.A., Jauregi, P., 2021. *Frontiers in Microbiology* 11, 610. <https://doi.org/10.3389/fmicb.2020.610>.
- Kumar, A., Rabha, J., Jha, D.K., 2021. *Biocatalysis and Agricultural Biotechnology* 36, 102132. <https://doi.org/10.1016/j.bcab.2021.102132>.
- Lastochkina, O., Seifikalhor, M., Aliniaiefard, S., Baymiev, A., Pusenkova, L., Garipova, S., Kulabuhova, D., Maksimov, I., 2019. *Bacillus* spp.: efficient biotic strategy to control postharvest diseases of fruits and vegetables. *Plants* 8(4), 97. <https://doi.org/10.3390/plants8040097>.
- Leal, C., Richet, N., Guise, J.F., Gramaje, D., Armengol, J., Fontaine, F., Trotel-Aziz, P., 2021. *Frontiers in Microbiology* 12, 642. <https://doi.org/10.3389/fmicb.2021.642>.
- Leconte, A., Tournant, L., Muchembled, J., Paucellier, J., Héquet, A., Deracinois, B., Deweer, C., Krier, F., Deleu, M., Oste, S., Jacques, P., Coutte, F., 2022. *Microorganisms* 10, 210. <https://doi.org/10.3390/microorganisms10020210>.
- Li, W., Wang, T., 2021. *International Journal of Food Microbiology* 338, 109016. <https://doi.org/10.1016/j.ijfoodmicro.2020.109016>.
- Li, Y., Héloir, M.C., Zhang, X., Geissler, M., Trouvelot, S., Jacquens, L., Henkel, M., Su, X., Fang, X., Wang, Q., Adrian, M., 2019. *Molecular Plant Pathology* 20, 1037–1050. <https://doi.org/10.1111/mpp.12816>.
- Lindsey, L.E., Maul, J.E., Davis, A.S., 2017. Evaluation of chlorine gas for surface sterilization of seeds. *Plant Disease* 101(7), 1231–1237. <https://doi.org/10.1094/PDIS-10-16-1424-RE>.

- López-Caballero, M.E., Rodríguez-Díaz, M., Sánchez-Porro, C., Roselló-Mora, R., Ventosa, A., 2009. *Pseudomonas granadensis* sp. nov., isolated from cultivated soil. *International Journal of Systematic and Evolutionary Microbiology* 59(12), 3148–3152. <https://doi.org/10.1099/ijs.0.010702-0>.
- Lugtenberg, B., Kamilova, F., 2009. Plant-growth-promoting rhizobacteria. *Annual Review of Microbiology* 63, 541–556. <https://doi.org/10.1146/annurev.micro.62.081307.162918>
- Maan, H., Gilhar, O., Porat, Z., Kolodkin-Gal, I., 2021. *Frontiers in Cellular and Infection Microbiology* 11, 639. <https://doi.org/10.3389/fcimb.2021.639>.
- Malik, J., Moosa, A., Zulfiqar, F., Aslam, M.N., Albalawi, M.A., Almowallad, S., Mahmood, T., Alasmari, A., Yong, J.W.H., 2024. Biocontrol potential of lipopeptides produced by the novel *Bacillus altitudinis* strain TM22A against postharvest *Alternaria* rot of tomato. *LWT – Food Science and Technology* 192, 115541. <https://doi.org/10.1016/j.lwt.2023.115541>.
- Malusá, E., Sas Paszt, L., Ciesielska, J., 2016. Technologies for beneficial microorganism inocula used as biofertilizers. *The Scientific World Journal* 2016, 4912064. <https://doi.org/10.1155/2016/4912064>.
- Malusá, E., Vassilev, N., 2014. A contribution to set a legal framework for biofertilizers. *Applied Microbiology and Biotechnology* 98, 6599–6607. <https://doi.org/10.1007/s00253-014-5828-y>.
- Maxwell, K., Johnson, G.N., 2000. Chlorophyll fluorescence — a practical guide. *Journal of Experimental Botany* 51(345), 659–668. <https://doi.org/10.1093/jexbot/51.345.659>.
- Meena, K.R., Sharma, A., Kumar, R., Kanwar, S.S., 2020. *Journal of King Saud University – Science* 32, 337–348. <https://doi.org/10.1016/j.jksus.2019.11.005>.
- Mehmood, S., Muneer, M.A., Tahir, M., Javed, M.T., Mahmood, T., Afridi, M.S., Pakar, N.P., Abbasi, H.A., Munis, M.F.H., Chaudhary, H.J., 2021. *Physiology and Molecular Biology of Plants* 27, 2101–2114. <https://doi.org/10.1007/s12298-021-01063-4>.
- Ministry of Agriculture, Food Sovereignty and Forestry, 2026. *National Agricultural Information System – Organic Database*. Available at: <https://www.sian.it> (accessed 5 January 2026).

- Mishra, J., Singh, R., Arora, N.K., 2021. Plant growth-promoting microorganisms: diversity and applications. *Environmental Sustainability* 4, 333–347. <https://doi.org/10.1007/s42398-021-00190-5>.
- Mnif, I., Rajhi, H., Bouallegue, A., Trabelsi, N., Ghribi, D., 2022. *Journal of Polymers and the Environment* 30, 2378–2391. <https://doi.org/10.1007/s10924-021-02290-3>.
- Mok, W.K., Tan, Y.X., Lee, J., Kim, J., Chen, W.N., 2019. *AMB Express* 9, 1–12. <https://doi.org/10.1186/s13568-019-0760-1>.
- Montero-Calasanz, M.C., Santamaría, C., Albareda, M., Daza, A., Duan, J., Glick, B.R., Camacho, M., 2013. *Spanish Journal of Agricultural Research* 11, 146–154. <https://doi.org/10.5424/sjar/20131111-3294>.
- Murolo, S., Concas, J., Romanazzi, G., 2019. *Biological Control* 132, 102–109. <https://doi.org/10.1016/j.biocontrol.2019.02.012>.
- Nam, J.H., Thibodeau, A., Qian, Y.L., Qian, M.C., Park, S.H., 2023. *AMB Express* 13, 1–12. <https://doi.org/10.1186/s13568-023-01591-4>.
- Nicholson, W.L., Munakata, N., Horneck, G., Melosh, H.J., Setlow, P., 2000. Resistance of *Bacillus* endospores to extreme terrestrial and extraterrestrial environments. *Microbiology and Molecular Biology Reviews* 64, 548–572. <https://doi.org/10.1128/MMBR.64.3.548-572.2000>
- Nguyen, P.M., Kwee, E.M., Niemeyer, E.D., 2010. Potassium rate alters the antioxidant capacity and phenolic concentration of basil (*Ocimum basilicum* L.) leaves. *Food Chemistry* 123, 1235–1241. <https://doi.org/10.1016/j.foodchem.2010.05.097>.
- Nordgaard, M., Blake, C., Maróti, G., Hu, G., Wang, Y., Strube, M.L., Kovács, Á.T., 2022. *iScience* 25, 104–112. <https://doi.org/10.1016/j.isci.2022.104112>.
- Nurfarahin, A.H., Mohamed, M.S., Phang, L.Y., 2018. Culture medium development for microbial-derived surfactants production — an overview. *Molecules* 23, 1049. <https://doi.org/10.3390/molecules23051049>.

- Ongena, M., Jacques, P., 2008. *Bacillus* lipopeptides: versatile weapons for plant disease biocontrol. *Trends in Microbiology* 16, 115–125. <https://doi.org/10.1016/j.tim.2007.12.009>.
- Palermo, J.S., Palermo, T.B., Cappellari, L.d.R., Balcke, G.U., Tissier, A., Giordano, W., Banchio, E., 2025. Influence of plant growth-promoting rhizobacteria (PGPR) inoculation on phenolic content and key biosynthesis-related processes in *Ocimum basilicum* under *Spodoptera frugiperda* herbivory. *Plants* 14(6), 857. <https://doi.org/10.3390/plants14060857>.
- Palleroni, N.J., 2015. The genus *Pseudomonas*. In: *eLS*. Wiley. <https://doi.org/10.1002/9781118960608.gbm01210>.
- Paravar, A., Piri, R., Balouchi, H., Ma, Y., 2023. Microbial seed coating: an attractive tool for sustainable agriculture. *Biotechnology Reports* 37, e00781. <https://doi.org/10.1016/j.btre.2022.e00781>.
- Pascual, J., et al., 2015. *Pseudomonas granadensis* sp. nov., a new bacterial species isolated from the Tejada, Almirajara and Alhama Natural Park, Granada, Spain. *International Journal of Systematic and Evolutionary Microbiology* 65(2), 625–632. <https://doi.org/10.1099/ijs.0.070151-0>.
- Peña-Jurado, E., Pérez-Vega, S., Zavala-Díaz de la Serna, F.J., Pérez-Reyes, I., Gutiérrez-Méndez, N., Vazquez-Castillo, J., Salmerón, I., 2019. *Biochemical Engineering Journal* 151, 107–115. <https://doi.org/10.1016/j.bej.2019.107315>.
- Pilz, M., Cavelius, P., Qoura, F., Awad, D., Brück, T., 2023. Lipopeptides development in cosmetics and pharmaceutical applications: a comprehensive review. *Biotechnology Advances* 61, 108–120. <https://doi.org/10.1016/j.biotechadv.2022.108120>.
- Powers, M.J., Sanabria-Valentín, E., Bowers, A.A., Shank, E.A., 2015. *Journal of Bacteriology* 197, 2129–2138. <https://doi.org/10.1128/JB.00150-15>.
- Pranav, P.S., Sivakumar, R., Suvekbala, V., et al., 2024. Genome-wide identification of root colonization fitness genes in plant growth-promoting *Pseudomonas asiatica* employing transposon-insertion sequencing. *Annals of Microbiology* 74, 40. <https://doi.org/10.1186/s13213-024-01784-5>.

- PubChem, n.d. *PubChem Compound Database*. Available at: <https://pubchem.ncbi.nlm.nih.gov/> (accessed 5 January 2026).
- Qiu, F., Liu, W., Chen, L., Wang, Y., Ma, Y., Lyu, Q., Zheng, Y., 2021. *Bacillus subtilis* biofertilizer application reduces chemical fertilization and improves fruit quality in fertigated Tarocco blood orange groves. *Scientia Horticulturae* 281, 110004. <https://doi.org/10.1016/j.scienta.2021.110004>.
- Radhakrishnan, R., Hashem, A., Abd_Allah, E.F., 2017. *Bacillus*: a biological tool for crop improvement through biomolecular changes. *Plant Growth Regulation* 82, 123–138. <https://doi.org/10.1007/s10725-017-0266-4>.
- Rahimi, S., Modin, O., Roshanzamir, F., Neissi, A., Saheb Alam, S., Seelbinder, B., Pandit, S., Shi, L., Mijakovic, I., 2020. *Chemical Engineering Journal* 397, 125506. <https://doi.org/10.1016/j.cej.2020.125506>.
- Rathika, R., Janaki, V., Shanthi, K., Kamala-Kannan, S., 2019. *International Journal of Environmental Science and Technology* 16, 5725–5734. <https://doi.org/10.1007/s13762-018-1867-8>.
- Rocha, I., Ma, Y., Souza-Alonso, P., Vosátka, M., Freitas, H., Oliveira, R.S., 2019. Seed coating: a tool for delivering beneficial microbes to agricultural crops. *Frontiers in Plant Science* 10, 1357. <https://doi.org/10.3389/fpls.2019.01357>.
- Romero, D., de Vicente, A., Rakotoaly, R.H., et al., 2007. The iturin and fengycin families of lipopeptides are key factors in antagonism of *Bacillus subtilis* toward plant pathogenic fungi. *Molecular Plant–Microbe Interactions* 20(4), 430–440. <https://doi.org/10.1094/MPMI-20-4-0430>.
- Roncalli Amici, R., 2001. The history of Italian parasitology. *Veterinary Parasitology* 98(1–3), 3–30. [https://doi.org/10.1016/S0304-4017\(01\)00420-](https://doi.org/10.1016/S0304-4017(01)00420-).
- Rouphael, Y., Colla, G., 2020. Biostimulants in agriculture. *Frontiers in Plant Science* 11, 40. <https://doi.org/10.3389/fpls.2020.00040>.
- Ruiz-Muñoz, B., Rodríguez-García, M., Heredia-Ponce, Z., Tienda, S., Villar-Moreno, R., Arrebola, E., de Vicente, A., Cazorla, F.M., Gutiérrez-Barranquero, J.A., 2025. A putative novel type of tight adherence (tad)-like gene cluster of *Pseudomonas*

- chlororaphis* PCL1606 exhibits a crucial role in avocado roots colonization, fostering its biological control activity. *Plant and Soil* 513, 551–567. <https://doi.org/10.1007/s11104-024-07200-w>.
- Sadik, M.W., Zohair, M.M., El-Beih, A.A., Hamed, E.R., Sedik, M.Z., 2021. *Jordan Journal of Biological Sciences* 14, 157–161.
- Samaras, A., Kamou, N., Tzelepis, G., Karamanoli, K., Menkissoglu-Spiroudi, U., Karaoglanidis, G.S., 2022. *Plants* 11, 611. <https://doi.org/10.3390/plants11050611>.
- Samaras, A., Nikolaidis, M., Antequera-Gómez, M.L., Cámara-Almirón, J., Romero, D., Moschakis, T., Skandalis, N., 2019. Whole genome sequencing and root colonization studies reveal *Bacillus subtilis* 713 as a potential biocontrol agent against *Botrytis cinerea*. *Frontiers in Microbiology* 10, 1–14. <https://doi.org/10.3389/fmicb.2019.00481>.
- Samaras, A., Roumeliotis, E., Ntasiou, P., Karaoglanidis, G., 2021. *Plants* 10, 1210. <https://doi.org/10.3390/plants10061210>.
- Santos-Lima, D., de Castro Spadari, C., de Morais Barroso, V., Carvalho, J.C.S., de Almeida, L.C., Alcalde, F.S.C., Ferreira, M.J.P., Sannomiya, M., Ishida, K., 2023. *Applied Microbiology and Biotechnology* 107, 6103–6120. <https://doi.org/10.1007/s00253-023-12709-5>.
- Santoyo, G., Moreno-Hagelsieb, G., del Carmen Orozco-Mosqueda, M., Glick, B.R., 2016. Plant growth-promoting bacterial endophytes. *Microbiological Research* 183, 92–99. <https://doi.org/10.1016/j.micres.2015.11.008>.
- Santoyo, G., Urtis-Flores, C.A., Loeza-Lara, P.D., Orozco-Mosqueda, M.C., Glick, B.R., 2021. Rhizosphere colonization determinants by plant growth-promoting rhizobacteria (PGPR). *Biology* 10(6), 475. <https://doi.org/10.3390/biology10060475>.
- Seddon, N., Smith, A., Smith, P., Key, I., Chausson, A., Girardin, C., House, J., Srivastava, S., Turner, B., 2021. *Global Change Biology* 27, 1518–1546. <https://doi.org/10.1111/gcb.15559>.
- Sharma, R., Singh, J., Verma, N., 2020. *Biocatalysis and Agricultural Biotechnology* 25, 101600. <https://doi.org/10.1016/j.bcab.2020.101600>.

- Shahzad, S.M., Khalid, A., Arshad, M., et al., 2017. Integrated use of plant growth-promoting rhizobacteria and reduced nitrogen fertilization improves growth, yield and nitrogen use efficiency of canola (*Brassica napus* L.). *Soil Science and Plant Nutrition* 63, 460–468. <https://doi.org/10.1080/00380768.2017.1362485>.
- Sidorova, T.M., Asaturova, A.M., Homyak, A.I., Zhevnova, N.A., Shternshis, M.V., Tomashevich, N.S., 2020. *Saudi Journal of Biological Sciences* 27, 1879–1885. <https://doi.org/10.1016/j.sjbs.2020.05.004>.
- Singh, A., Jain, A., Sarma, B.K., Upadhyay, R.S., Singh, H.B., 2014a. Rhizosphere-competent microbial consortium mediates rapid changes in phenolic profiles in chickpea during *Sclerotium rolfsii* infection. *Microbiological Research* 169(5–6), 353–360. <https://doi.org/10.1016/j.micres.2013.09.008>.
- Singh, D., Pujari, A., 2022. Microbial biomass-based fertilizers: prospects and limitations. *Journal of Soil Science and Plant Nutrition* 22, 1801–1816. <https://doi.org/10.1007/s42729-022-00909-4>.
- Singh, A.K., Rautela, R., Cameotra, S.S., 2014b. Substrate-dependent *in vitro* antifungal activity of *Bacillus* sp. strain AR2. *Microbial Cell Factories* 13, 67. <https://doi.org/10.1186/1475-2859-13-67>.
- Singh, S., Sequeira, R.A., Kumar, P., Ghadge, V.A., Vaghela, P., Mohanty, A.K., Ghosh, A., Prasad, K., Shinde, P.B., 2022. *ACS Omega* 7, 46646–46652. <https://doi.org/10.1021/acsomega.2c06018>.
- Sistema Informativo Agricolo Nazionale (SIAN) – Banca Dati Bio, n.d. Available at: <https://www.sian.it> (accessed 2 January 2024).
- Song, P., Zhao, B., Sun, X., Li, L., Wang, Z., Ma, C., Zhang, J., 2023. Effects of *Bacillus subtilis* HS5B5 on maize seed germination and seedling growth under NaCl stress conditions. *Agronomy* 13(7), 1874. <https://doi.org/10.3390/agronomy13071874>.
- Stamenković, S., Beškoski, V., Karabegović, I., Lazić, M., Nikolić, N., 2018. Microbial fertilizers: a comprehensive review of current findings and future perspectives. *Spanish Journal of Agricultural Research* 16(1), e03R01. <https://doi.org/10.5424/sjar/2018161-12117>.

- Su, Y., Liu, C., Fang, H., Zhang, D., 2020. *Bacillus subtilis*: a universal cell factory for industry, agriculture, biomaterials and medicine. *Microbial Cell Factories* 19, 173. <https://doi.org/10.1186/s12934-020-01442-7>.
- Sundaram, T., Govindarajan, R.K., Vinayagam, S., Krishnan, V., Nagarajan, S., Gnanasekaran, G.R., Baek, K.-H., Rajamani Sekar, S.K., 2024. Advancements in biosurfactant production using agro-industrial waste for industrial and environmental applications. *Frontiers in Microbiology* 15, 1357302. <https://doi.org/10.3389/fmicb.2024.1357302>.
- Taiz, L., Zeiger, E., Møller, I.M., Murphy, A., 2015. *Plant Physiology and Development*. 6th ed. Sinauer Associates, Sunderland, MA.
- Tall, S., Meyling, N.V., 2018. *Microbial Ecology* 76, 1002–1008. <https://doi.org/10.1007/s00248-018-1180-5>.
- Taylor, A.G., et al., 1998. Seed enhancements. *Horticultural Reviews* 20, 301–346.
- Teymouri, M., Akhtari, J., Karkhane, M., Marzban, A., 2016. Assessment of phosphate solubilization activity of rhizobacteria in mangrove forest. *Biocatalysis and Agricultural Biotechnology* 5, 168–172. <https://doi.org/10.1016/j.bcab.2015.12.010>.
- Tienda, S., Vida, C., Villar-Moreno, R., de Vicente, A., Cazorla, F.M., 2024. Development of a *Pseudomonas*-based biocontrol consortium with effective root colonization and extended beneficial side effects for plants under high-temperature stress. *Microbiological Research* 292, 127761. <https://doi.org/10.1016/j.micres.2024.127761>.
- Tran, C., Cock, I.E., Chen, X., Feng, Y., 2022. Antimicrobial *Bacillus*: metabolites and their mode of action. *Antibiotics* 11, 1034. <https://doi.org/10.3390/antibiotics11081034>.
- Trupo, M., Magarelli, R.A., Martino, M., Larocca, V., Giorgianni, A., Ambrico, A., 2023. Crude lipopeptides from culture of *Bacillus subtilis* strain ET-1 against *Podospaera xanthii* on *Cucumis melo*. *Journal of Natural Pesticide Research* 4, 100032. <https://doi.org/10.1016/j.napere.2023.100032>.
- Tu, L., He, Y., Shan, C., Wu, Z., 2016. Preparation of microencapsulated *Bacillus subtilis* SL13 seed coating agents and their effects on cotton seedling growth. *BioMed Research International* 2016, 3251357. <https://doi.org/10.1155/2016/3251357>.

- Umar, A., Zafar, A., Wali, H., Siddique, M.P., Qazi, M.A., Naeem, A.H., Malik, Z.A., Ahmed, S., 2021. *AMB Express* 11, 1–12. <https://doi.org/10.1186/s13568-021-01233-3>.
- Ünlü, E., Yilmaz, S., Yetişir, H., et al., 2024. Characterization of multi-trait plant growth-promoting rhizobacteria isolated from alfalfa rhizosphere and evaluation of their efficacy on tomato and watermelon growth. *Discover Agriculture* 2, 117. <https://doi.org/10.1007/s44279-024-00125-z>.
- Vacante, V., 2011. *Bulletin of Insectology* 64, 93–99.
- Vacheron, J., Desbrosses, G., Bouffaud, M.L., et al., 2013. Plant growth-promoting rhizobacteria and root system functioning. *Frontiers in Plant Science* 4, 356. <https://doi.org/10.3389/fpls.2013.00356>.
- van Veen, J.A., van Overbeek, L.S., van Elsas, J.D., 1997. Fate and activity of microorganisms introduced into soil. *Microbiology and Molecular Biology Reviews* 61, 121–135.
- Vassaux, A., Rannou, M., Peers, S., Daboudet, T., Jacques, P., Coutte, F., 2021. *Frontiers in Bioengineering and Biotechnology* 9, 1–12. <https://doi.org/10.3389/fbioe.2021.635>.
- Venkataraman, S., Rajendran, D.S., Kumar, P.S., Vo, D.V.N., Vaidyanathan, V.K., 2022. Extraction, purification and applications of biosurfactants based on microbial-derived glycolipids and lipopeptides: a review. *Environmental Chemistry Letters* 20, 2383–2408. <https://doi.org/10.1007/s10311-021-01379-0>.
- Vessey, J.K., 2003. Plant growth-promoting rhizobacteria as biofertilizers. *Plant and Soil* 255, 571–586. <https://doi.org/10.1023/A:1026037216893>.
- Wang, Y., Liang, J., Zhang, C., Wang, L., Gao, W., Jiang, J., 2020. *Frontiers in Microbiology* 11, 593. <https://doi.org/10.3389/fmicb.2020.00593>.
- Wang, Y., Pei, Y., Wang, X., Dai, X., Zhu, M., 2024. Antimicrobial metabolites produced by plant growth-promoting rhizobacteria (PGPR): *Bacillus* and *Pseudomonas*. *Advanced Agrochem* 3, 07.007. <https://doi.org/10.1016/j.aac.2024.07.007>.
- Wang, Y., Zhang, C., Liang, J., Wu, L., Gao, W., Jiang, J., 2020. Iturin A extracted from *Bacillus subtilis* WL-2 affects *Phytophthora infestans* via cell structure disruption,

- oxidative stress and energy supply dysfunction. *Frontiers in Microbiology* 11, 536083. <https://doi.org/10.3389/fmicb.2020.536083>.
- Wasserstein, R.L., Schirm, A.L., Lazar, N.A., 2019. Moving to a world beyond “ $p < 0.05$ ”. *The American Statistician* 73(sup1), 1–19. <https://doi.org/10.1080/00031305.2019.1583913>.
- Wei, Q.Y., Li, Y.Y., Xu, C., Wu, Y.X., Zhang, Y.R., Liu, H., 2020. Endophytic colonization by *Beauveria bassiana* increases the resistance of tomatoes against *Bemisia tabaci*. *Arthropod-Plant Interactions* 14, 289–300. <https://doi.org/10.1007/s11829-020-09746-9>.
- Willenbacher, J., Yeremchuk, W., Mohr, T., Syltatk, C., Hausmann, R., 2015. *AMB Express* 5, 1–12. <https://doi.org/10.1186/s13568-015-0104-5>.
- Woo, O.G., Kim, H., Kim, J.S., Keum, H.L., Lee, K.C., Sul, W.J., Lee, J.H., 2020. *Bacillus subtilis* strain GOT9 confers enhanced tolerance to drought and salt stresses in *Arabidopsis thaliana* and *Brassica campestris*. *Plant Physiology and Biochemistry* 148, 359–367. <https://doi.org/10.1016/j.plaphy.2020.01.030>.
- Wu, H., Gu, Q., Xie, Y., Lou, Z., Xue, P., Fang, L., Yu, C., Jia, D., Huang, G., Zhu, B., Schneider, A., Blom, J., Lasch, P., Borriss, R., Gao, X., 2019. *Environmental Microbiology* 21, 3505–3526. <https://doi.org/10.1111/1462-2920.14795>.
- Xiong, Z.R., Cobo, M., Whittal, R.M., Snyder, A.B., Worobo, R.W., 2022. *PLoS ONE* 17, e0271234. <https://doi.org/10.1371/journal.pone.0271234>.
- Xu, W., Yang, Q., Xie, X., Goodwin, P.H., Deng, X., Zhang, J., Sun, R., Wang, Q., Xia, M., Wu, C., Yang, L., 2022a. *Biology* 11, 1–15. <https://doi.org/10.3390/biology11060879>.
- Xu, W., Yang, Q., Yang, F., Xie, X., Goodwin, P.H., Deng, X., Tian, B., Yang, L., 2022b. *Frontiers in Microbiology* 13, 1–12. <https://doi.org/10.3389/fmicb.2022.873>.
- Yáñez-Mendizábal, V., Falconí, C.E., Kanaley, K., 2023. *Biological Control* 185, 105–112. <https://doi.org/10.1016/j.biocontrol.2023.105112>.
- Yang, P., Condrich, A., Scranton, S., Hebner, C., Lu, L., Ali, M.A., 2024. Utilizing plant growth-promoting rhizobacteria (PGPR) to advance sustainable agriculture. *Bacteria* 3(4), 434–451. <https://doi.org/10.3390/bacteria3040030>.

- Yang, J., Kloepper, J.W., Ryu, C.M., 2009. Rhizosphere bacteria help plants tolerate abiotic stress. *Trends in Plant Science* 14(1), 1–4. <https://doi.org/10.1016/j.tplants.2008.10.004>.
- Yang, L., Qian, X., Zhao, Z., Wang, Y., Ding, G., Xing, X., 2024. Mechanisms of rhizosphere plant–microbe interactions: molecular insights into microbial colonization. *Frontiers in Plant Science* 15, 1491495. <https://doi.org/10.3389/fpls.2024.1491495>.
- Yaseen, Y., Gancel, F., Béchet, M., Drider, D., Jacques, P., 2017. *Archives of Microbiology* 199, 1371–1382. <https://doi.org/10.1007/s00203-017-1400-3>.
- Yi, Y.J., Yin, Y.N., Yang, Y.A., Liang, Y.Q., Shan, Y.T., Zhang, C.F., Zhang, Y.R., Liang, Z.P., 2022. *Phytopathology* 112, 2476–2485. <https://doi.org/10.1094/PHYTO-03-22-0089-R>.
- Yu, Z., Tang, J., Khare, T., Kumar, V., 2020. *Fitoterapia* 140, 104433. <https://doi.org/10.1016/j.fitote.2019.104433>.
- Zhang, D., Qiang, R., Zhou, Z., Pan, Y., Yu, S., Yuan, W., Cheng, J., Wang, J., Zhao, D., Zhu, J., Yang, Z., 2022. Biocontrol and action mechanism of *Bacillus subtilis* lipopeptides' fengycins against *Alternaria solani* in potato as assessed by a transcriptome analysis. *Frontiers in Microbiology* 13, 861113. <https://doi.org/10.3389/fmicb.2022.861113>.
- Zhang, X., Al-Dossary, A., Hussain, M., Setlow, P., Li, J., 2020. *Applied and Environmental Microbiology* 86, e01234–20. <https://doi.org/10.1128/AEM.01234-20>.
- Zhao, H., Shao, D., Jiang, C., Shi, J., Li, Q., Huang, Q., Rajoka, M.S.R., Yang, H., Jin, M., 2017. Biological activity of lipopeptides from *Bacillus*. *Applied Microbiology and Biotechnology* 101, 5951–5960. <https://doi.org/10.1007/s00253-017-8396-5>.
- Zheljazkov, V.D., Cantrell, C.L., Tekwani, B., Khan, S.I., 2008. Content, composition and bioactivity of essential oils of three basil genotypes as a function of harvesting. *Journal of Agricultural and Food Chemistry* 56, 380–385. <https://doi.org/10.1021/jf072447y>.
- Zouari, R., Ellouze-Chaabouni, S., Ghribi-Aydi, D., 2014. *Achievements in the Life Sciences* 8, 162–169. <https://doi.org/10.1016/j.als.2014.05.003>.

Annex A

Scientific publications

The appendix gathers the scientific contributions produced during the three-year PhD programme, including both the posters and abstracts directly related to the doctoral project and the publications arising from collateral activities that enriched the training and research experience.

Scientific papers

- Monzillo, F., **Della Mura, B.**, Matarazzo, C., Crescenzi, M.A., Piacente, S., d'Aquino, L., Cozzolino, R. and Montoro, P., 2025. Evolution of secondary metabolites in *Eruca sativa* from the microgreen to the reproductive stage: An integrative multi-platform metabolomics approach. *Foods*, 14(23), 4148. <https://doi.org/10.3390/foods14234148>.
- Verardi, A., Sangiorgio, P., **Della Mura, B.**, Moliterni, S., Spagnoletta, A., Dimatteo, S., Bassi, D., Cortimiglia, C., Rebuzzi, R., Palazzo, S. and Errico, S., 2025. *Tenebrio molitor* frass: A cutting-edge biofertilizer for sustainable agriculture and advanced adsorbent precursor for environmental remediation. *Agronomy*, 15(3), 758. <https://doi.org/10.3390/agronomy15030758>.
- d'Aquino, L., Cozzolino, R., Malorni, L., Bodhuin, T., Gambale, E., Sighicelli, M., **Della Mura, B.**, Matarazzo, C., Piacente, S. and Montoro, P., 2024. Light flux density and photoperiod affect growth and secondary metabolism in fully expanded basil plants. *Foods*, 13(14), 2273. <https://doi.org/10.3390/foods13142273>.

Conference contributions

- Monzillo, F., **Della Mura, B.**, Crescenzi, M.A., Piacente, S., d'Aquino, L. and Montoro, P., 2025. *Metabolic profile variation at different growth stages in Eruca sativa leaves cultivated in a closed system: Metabolomics by UHPLC–Q-Exactive–MS/MS analysis*. Poster presented at: 73rd International Congress and Annual Meeting of the Society for Medicinal Plant and Natural Product Research (GA), jointly with the Italian Society of Phytochemistry (SIF), 31 August–3 September 2025, Naples.
- Monzillo, F., **Della Mura, B.**, Crescenzi, M.A., Piacente, S., d'Aquino, L. and Montoro, P., 2025. *Glucosinolate variation among organs and growth stages in Eruca sativa*

cultivated in a closed system. Abstract presented at: Il Contributo dei Giovani Chimici in Campania, 3–4 July 2025, SCI Campania, Department of Chemistry and Biology, University of Salerno.

- Monzillo, F., **Della Mura, B.**, Crescenzi, M.A., Piacente, S., d’Aquino, L. and Montoro, P., 2025. *Glucosinolate variation among organs and growth stages in Eruca sativa cultivated in a closed system*. Poster presented at: 12th MS J-Day, 22–23 May 2025, Pisa.
- Monzillo, F., **Della Mura, B.**, Crescenzi, M.A., Piacente, S., d’Aquino, L. and Montoro, P., 2025. *Rocket (Eruca sativa) microgreens versus plants in full vegetative phase cultivated in a newly developed closed system: Metabolomics by UHPLC-Q-Exactive-MS/MS analysis*. Poster presented at: 29° Corso di Spettrometria di Massa, 10–14 March 2025, Certosa di Pontignano, Siena.
- Ambrico, A., Magarelli, R.A., Trupo, M., Larocca, V., Martino, M., Palazzo, S. and **Della Mura, B.**, 2024. *Dried cell-free supernatant of Bacillus subtilis strain ET-1 against Penicillium digitatum on clementine fruits*. Abstract presented at: XLII Meeting “Microbe and Microbiome management for a better planet”, 18–20 September 2024, Bari.
- **Della Mura, B.**, Ambrico, A., Trupo, M., Magarelli, R.A., Palazzo, S. and d’Aquino, L., 2024. *Evaluation of the phytostimulant activity of microbial biomass containing Bacillus subtilis*. Poster presented at: Agritech: Coltivare innovazione per un futuro sostenibile, 6 September 2024, Milan.
- Trupo, M., Magarelli, R.A., Martino, M., Larocca, V., **Della Mura, B.** and Ambrico, A., 2023. *Utilization of suitable microorganisms for production of substances with antimicrobial effects from agro-industrial waste*. Poster presented at: Agritech: Le sfide dell’economia circolare in ambito agroalimentare, September 2023, Milan.

Annex B

Data and observations on the biostimulant activity of microbial biomass

The following are the phenotypic observations, biometric measurements and Chlorophyll Content Index obtained from *in vivo* tests evaluating the biostimulant effect of microbial biomass containing *B. subtilis* ET-1.

Pilot trial on Basilico

Phenotypic observations and data obtained from the pilot test evaluating the biostimulant activity of microbial biomass containing *B. subtilis* ET-1 on Basil variety 'Genovese' are reported below.

In particular, the theses considered are:

- B: plants treated with microbial biomass.
- C (negative control): plants treated with spring water.
- S (positive control): plants treated with ammonium sulphate.

Phenotypic observations

The plants grew healthily and vigorously throughout the trial.

Fourteen days after transplanting, the basil roots became visible through the transparency of the cylinders (Figure B1).



Figure B1. Details of basil roots 14 days after transplanting.

Thirty-one days after transplantation, the beginnings of flower buds appeared (Figure B2).



Figure B2. Detail of the floral axis primordium of basil 31 days after transplanting.

Forty-three days after transplantation, elongation of the flower stalks was observed in plants in these B1, B2, C2, and S1 (Figure B3).



Figure B3. Details of the elongation of basil flower stems 43 days after transplanting.

Forty-five days after transplanting, the overall condition of the plants was good.

The plants treated with microbial biomass appeared taller and more luxuriant than those treated with water and ammonium sulphate (Figure B4).



Figure B4. General condition of basil plants 45 days after transplanting.

Biometric measurements

The data obtained 45 days after transplanting, relating to the number of stems, height and number of nodes per plants, are shown below (Table B1):

Table B1. Data regarding the number of stems, height and number of nodes of basil plants treated with microbial biomass (B), untreated (C) and treated with ammonium sulphate (S).			
Treatment	Number of stems	Height (cm)	Number of nodes
B1	4	24,0	7
B2	4	34,5	8
C1	4	19,5	6
C2	4	19,0	6

S1	4	24,5	6
S2	4	16,5	7

The fresh weights of leaves, flower stalks and stems of each thesis obtained 57 days after transplanting are shown below (Table B2):

Table B2. Fresh weights of flowers, leaves and stems of basil plants treated with microbial biomass (B), untreated (C) and treated with ammonium sulphate (S).			
Treatment	Fresh weight (g)		
	Leaves	Flowers	Stems
B1	57,17	3,01	12,25
B2	75,79	5,98	19,61
C1	57,37	0,62	12,32
C2	65,87	1,89	14,93
S1	84,75	5,82	24,40
S2	68,68	0,78	14,32

The dry weights of leaves, flower stalks and stems of each thesis obtained 71 days after transplanting are shown below (Table B3):

Table B3. Dry weights of flowers, leaves and stems of basil plants treated with microbial biomass (B), untreated (C) and treated with ammonium sulphate (S).			
Treatment	Dry weight (g)		
	Leaves	Flowers	Stems
B1	4,38	0,34	1,25
B2	6,46	0,73	2,58
C1	4,50	0,06	1,19
C2	4,83	0,36	1,57
S1	7,38	0,82	2,87
S2	5,46	0,06	1,45

Chlorophyll Content Index

The chlorophyll content indices obtained 45 days after transplanting are shown below (Table B4):

Table B4. Chlorophyll content index recorded for the middle and apical leaves of basil plants treated with microbial biomass (B), untreated (C) and treated with ammonium sulphate (S).

Treatment	Chlorophyll Content Index (C.C.I.)			
	Apical leaves		Median leaves	
	F1	F2	F3	F4
B1	70,3	46,1	29,5	31,2
B2	36,9	41,1	35,6	37,6
C1	40,4	39,7	40,3	32,1
C2	42,3	45,5	44,4	30,2
S1	48,6	45,6	34,5	35,6
S2	45,2	85,3	41,6	41,3

Summary evaluation of results

During and at the end of the trial, the following assessments were made:

- In the experimental setup, all plants grew well, showing phenotypic development consistent with expectations.
- The overall plant health was good, and the microbial biomass treatments did not cause stress to the plants.
- From a phenotypic point of view, plants treated with microbial biomass performed better in terms of height, number of nodes and floral axis elongation rate than plants treated with water and ammonium sulphate.
- The C.C.I. of plants treated with biomass is higher than that of plants treated with spring water, but lower than that of plants treated with ammonium sulphate.
- Plants treated with microbial biomass have a higher fresh weight than plants treated with spring water, and the fresh weight of the flower stalks is higher than that of plants treated with ammonium sulphate.
- The dry weight of plants treated with microbial biomass is higher than that of plants treated with spring water, and the dry weight of flower stalks is higher than that of plants treated with ammonium sulphate.

In general, plants treated with microbial biomass showed better results than plants treated with spring water, as well as comparable and sometimes better results than plants treated with ammonium sulphate.

Not only did the microbial biomass not cause stress, but it also had a positive effect on the vigour of the treated plants.

Pilot trial on potato plants

Phenotypic observations and data obtained from the pilot test evaluating the biostimulant activity of microbial biomass containing *B. subtilis* ET-1 on the Potato variety ‘Ricciona di Napoli’ are reported below.

Phenotypic observations

The plants grew healthily and vigorously throughout the trial.

The plants quickly overcame the transplant shock.

Eight days after transplanting, the potato roots began to show through the transparency of the cylinders.

Ten days after transplanting, sprouting began (Figure B5).



Figure B5. Details of potato roots and shoots 8 and 10 days after transplanting, respectively.

Flowering began 36 days after transplantation (Figure B6).



Figure B6. Detail of potato flower buds 36 days after transplanting.

Forty-three days after transplanting, anthesis occurred on the plants in theses B1, C1 and S1 (Figure B7).



Figure B7. Details of potato anthesis 43 days after transplanting.

A couple of days after anthesis, the flowers began to fall.

Fifty days after transplanting, the aerial part appeared greatly elongated and the root system highly developed.

At harvest time, only thesis C1 produced a single tuber, while the other theses did not make any tubers.

Biometric measurements

The tuber produced by the C1 thesis plant is well-formed and measures approximately 6 cm in length and approximately 6.5 cm in width at its widest points (Figure B8).

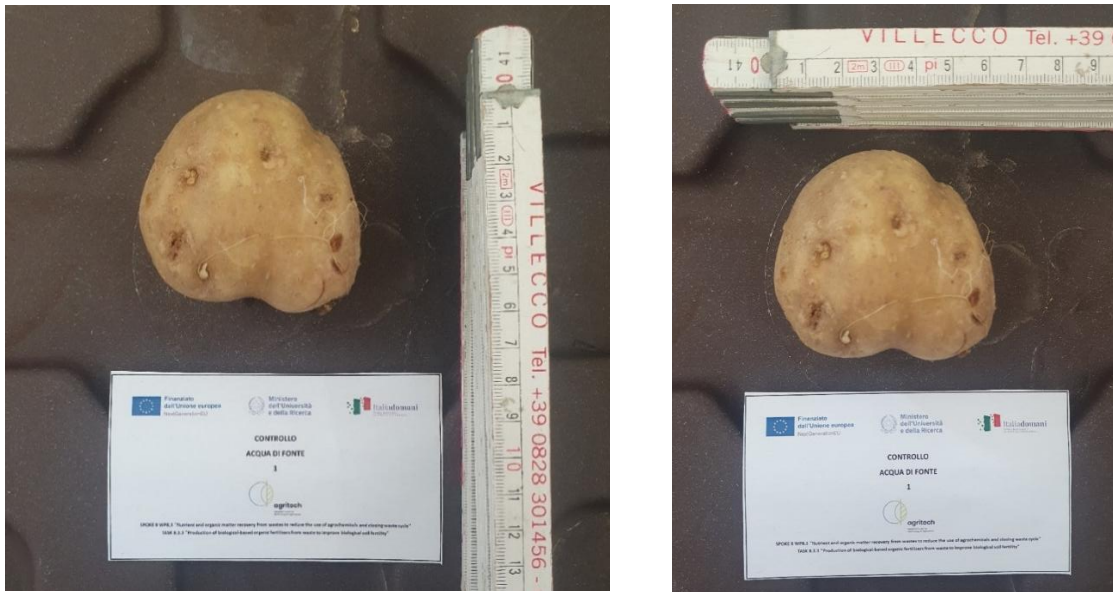


Figure B8. Details of the tuber of thesis C1 50 days after transplanting.

The tuber weighs 117.82 g.

Summary evaluation of results

During and at the end of the trial, the following was assessed:

- In the experimental setup, all plants showed phenotypic development characterised by excessive elongation of the aerial part.
- Theses B1, C1 and S1, in which anthesis occurred, showed flower drop.
- The general phytosanitary status was good and the treatments with microbial biomass did not cause stress to the plants.
- In terms of yield, only plot C1 produced a single tuber.

All plants grew, showing phenotypic development inconsistent with expectations, probably due to the growing conditions of the trial.

Further tests may be useful to investigate the results obtained in greater depth.

Biostimulation test on basil

Phenotypic observations and data obtained from the pilot test evaluating the biostimulant activity of microbial biomass containing *B. subtilis* ET-1 on Basil variety ‘Fenix’ are reported below.

In particular, the theses considered are:

- B: plants treated with microbial biomass.
- C (negative control): plants treated with spring water.
- S (positive control): plants treated with ammonium sulphate.

Biometric measurements

The data obtained 51 days after transplanting, relating to the number of stems, height and number of nodes per plant, are shown below (Table B5):

Table B5. Data regarding the number of stems, height and number of nodes of basil plants treated with microbial biomass (B), untreated (C) and treated with ammonium sulphate (S).			
Treatment	Number of stems	Height(cm)	Number of nodes
B1	3	32,7	12
B2	3	44,3	12
B3	3	39,6	12
B4	3	41,2	12
C1	3	46,0	12
C2	3	37,4	13
C3	3	40,5	13
C4	3	40,5	13
S1	3	31,5	11
S2	3	47,0	12
S3	3	35,7	12
S4	2	31,0	11

The fresh weights of leaves, flower stalks and stems of each thesis obtained 51 days after transplanting are shown below (Table B6):

Table B6. Fresh weights of leaves, flowers and stems of basil plants treated with microbial biomass (B), untreated (C) and treated with ammonium sulphate (S).	
Treatment	Fresh weight (g)

	Leaves	Flowers	Stems
B1	38,27	0,04	10,76
B2	50,09	1,98	18,01
B3	53,01	0,13	15,79
B4	53,69	0,95	18,24
C1	46,90	0,57	13,74
C2	42,93	0,14	11,68
C3	39,75	0,67	16,30
C4	41,40	0,12	11,43
S1	43,89	-	11,83
S2	49,98	1,07	17,68
S3	31,36	-	7,60
S4	40,16	0,00	9,65

The dry weights of leaves, flower stalks and stems of each thesis obtained 57 days after transplanting are shown below (Table B7):

Treatment	Dry weight (g)		
	Leaves	Flowers	Stems
B1	3,33	0,00	1,28
B2	5,42	0,34	3,47
B3	5,25	0,03	2,69
B4	6,26	0,18	4,42
C1	4,70	0,11	2,03
C2	3,88	0,00	1,53
C3	4,35	0,11	2,93
C4	3,86	0,02	1,32
S1	4,49	-	1,55
S2	5,50	0,21	4,27
S3	2,58	-	0,83

S4	3,30	0,00	1,10
----	------	------	------

Chlorophyll Content Index

The chlorophyll content indices obtained 41 days after transplanting are shown below (Table B8):

Table B8. Chlorophyll content index recorded for the middle and apical leaves of basil plants treated with microbial biomass (B), untreated (C) and treated with ammonium sulphate (S).				
Treatment	Chlorophyll Content Index (C.C.I.)			
	Apical leaves		Median leaves	
	F1	F2	F3	F4
B1	32,5	43,4	29,8	71,6
B2	37,3	36,7	39,7	33,2
B3	46,3	39,3	31,5	36,1
B4	45,5	44,0	40,4	37,2
C1	43,2	32,8	58,7	52,3
C2	42,1	38,2	37,3	40,3
C3	48,2	39,3	40,8	36,4
C4	38,8	41,2	40,9	43,2
S1	35,5	41,2	32,8	38,6
S2	45,2	42,1	37,9	37,8
S3	32,2	30,5	48,2	48,8
S4	35,8	37,0	36,1	38,2

Testing chitosan coating on basil

The following data refer to the germination percentage and phenotypic observations obtained from the coating test of “classic Italian” basil seeds with chitosan.

The theses considered are:

- ST: seeds treated with chitosan.
- SNT: seeds not treated with chitosan.

Germination percentage

The germination percentages calculated at different times after sowing (days) in Petri dishes and in pots are shown below (Table B9 and Table B10):

Table B9. Germination percentage recorded for chitosan-coated (ST) and uncoated (SNT) basil seeds after 4, 5, 6, 7 days from sowing.				
Thesis	Percentage of germination in Petri dishes (%)			
	+ 04	+ 05	+ 06	+ 07
ST	22,22	25,00	25,00	33,33
SNT	66,66	66,66	72,22	75,00

Table B10. Germination percentage recorded for chitosan-coated (ST) and uncoated (SNT) basil seeds after 7, 9 and 16 days from sowing.			
Thesis	Percentage of germination in pots (%)		
	+ 07	+ 09	+ 16
ST	2,77	11,11	8,33
SNT	2,77	2,77	2,77

Phenotypic observations

Seeds arranged in Petri dishes

Two days after sowing, rootlets began to emerge in both Petri dish tests, with a greater number of seeds affected in the “untreated” test.

This trend remained unchanged even three and four days after sowing. In particular, 4 days after sowing, 24 out of 36 untreated seeds began to sprout rootlets, and some even started to elongate.

Four days after sowing, 8 out of 36 treated seeds sprouted rootlets, 5 of which began to elongate (Figure B9).

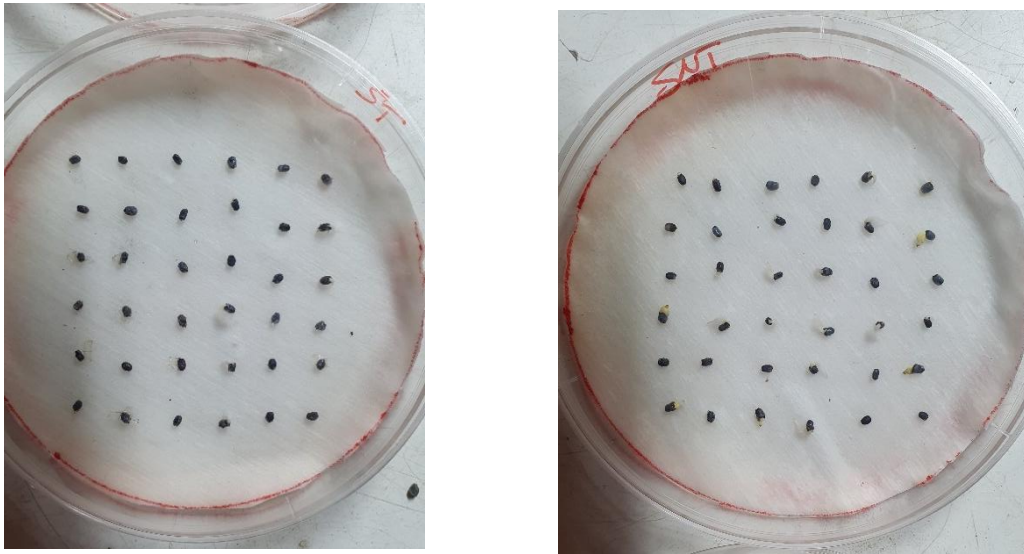


Figure B9. Comparison between treated basil seeds (left) and untreated seeds (right) four days after sowing in Petri dishes.

In general, four days after sowing, untreated seeds showed greater germinability and faster germination than treated seeds.

Six days after sowing in Petri dishes, untreated seeds showed more advanced rootlet development than treated seeds, as can be seen in the following photos (Figure B10):

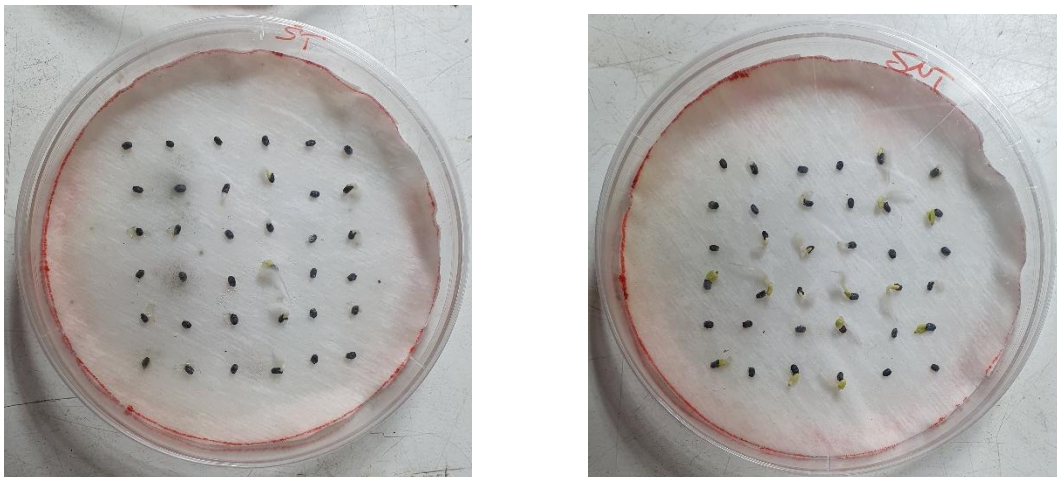


Figure B10. Comparison between treated (left) and untreated (right) basil seeds 6 days after sowing in Petri dishes.

In addition, the cotyledons became visible, especially in the “untreated seeds” thesis.

Mould also formed in the Petri dish of the “treated” seeds.

Eight days after sowing, the untreated seeds showed longer and more branched rootlets, as well as more developed cotyledons than the treated seeds, as can be seen in the following photos (Figure B11):

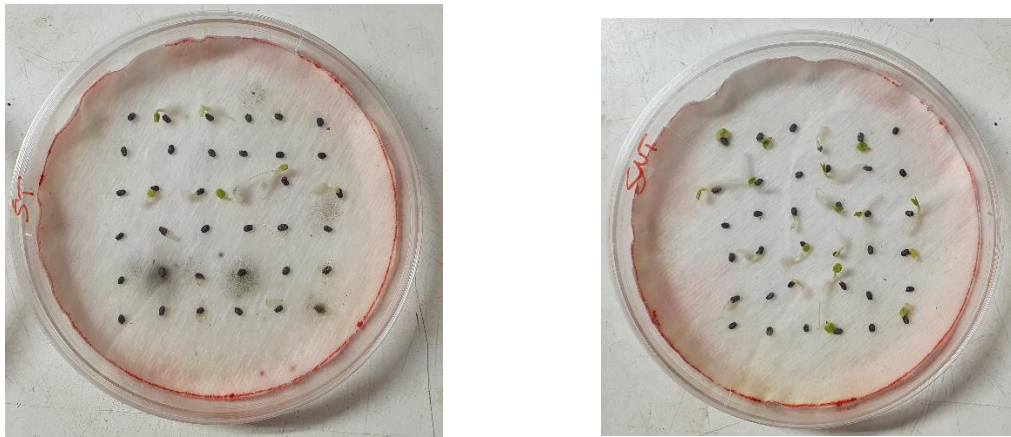


Figure B11. Comparison between treated (left) and untreated (right) basil seeds 8 days after sowing in Petri dishes.

Eight days after sowing, three treated seeds have moulded.

This marked the end of the germination test in Petri dishes.

Seeds arranged in pots

Seven days after sowing, germination began for both treated and untreated seeds.

Specifically, there was one sprout in “pot 1” of treated seeds and one sprout in “pot 3” of untreated seeds (Figure B12).

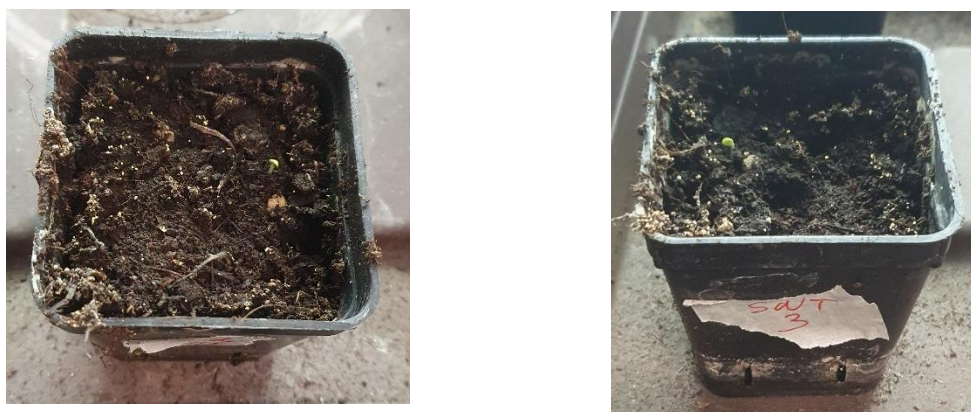


Figure B12. Germination rate of treated (left) and untreated (right) basil seeds 7 days after sowing.

Nine days after sowing, the number of sprouts increased from 1 to 4 for the “treated seeds” hypothesis. These sprouts were distributed individually in pots 1, 3, 4 and 5 (Figure B13).



Figure B13. Germination of treated (left) and untreated (right) basil seeds 9 days after sowing.

The number of shoots in the ‘untreated’ group remained at 1.

Sixteen days after sowing, the number of shoots in the ‘treated’ group decreased from 4 to 3, while the number of shoots in the ‘untreated’ group remained unchanged.

Given the stability of germination, the test was terminated 16 days after sowing.

Summary evaluation of results

During and at the end of the germination tests, the following was assessed:

- Germination began simultaneously for both theses, both in Petri dishes and in pots. In particular, for both treatments, the rootlets became visible 2 days after sowing, while the cotyledons became visible 7 days after sowing.
- The treated seeds placed in the dish had a lower germination rate and slower development than the untreated seeds placed in the dish.
- Unlike the untreated seeds placed in Petri dishes to germinate, some of the seeds in the “treated” experiment became mouldy.
- The treated seeds placed in pots filled with soil showed a higher germination rate than their untreated counterparts.

In conclusion, the behaviour of the treated seeds placed in Petri dishes was different from that of the treated seeds placed in pots.

The chitosan used to coat the basil seeds not only did not inhibit seed germination when grown in soil, but may have had a stimulating effect.

However, the moulding of some seeds treated in the dish could be indicative of possible problems in storage and cultivation in particularly humid environments.

Testing of microbial biomass coating on basil

The following are the germination percentage, biometric measurements and chlorophyll content index obtained from the test carried out on Prospera F1 basil seeds coated with microbial biomass.

The theses considered are:

- B: seeds coated with microbial biomass in an aqueous pectin solution.
- C: seeds coated with pectin.
- N: uncoated seeds.

Germination percentage

The germination percentages calculated 13 and 19 days after sowing are shown below (Table B11 and Table B12):

Table B11. Germination percentage and number of basil seeds coated with microbial biomass and pectin (B), coated with pectin (C) and uncoated (N) germinated.		
Treatment	+ 13 days after sowing	
	No. of germinated seeds out of total	Germination percentage (%)
B1	6/20	30
B2	4/20	20
B3	6/20	30
B4	7/20	35
C1	13/20	65
C2	12/20	60
C3	14/20	70
C4	14/20	70
N1	14/20	70
N2	17/20	85
N3	16/20	80
N4	17/20	85

Table B12. Germination percentage and number of basil seeds coated with microbial biomass and pectin (B), coated with pectin (C) and uncoated (N) germinated.		
Treatment	+ 19 days after sowing	
	No. of germinated seeds out of total	Germination percentage (%)
B1	6/20	30
B2	7/20	35
B3	6/20	30
B4	7/20	35
C1	16/20	80
C2	13/20	65
C3	17/20	85
C4	18/20	90
N1	14/20	70
N2	18/20	90

N3	18/20	90
N4	17/20	85

Biometric measurements

The data obtained 60 days after sowing, relating to the number of stems, height and number of nodes per plant, are shown below (Table B13):

Treatment	Number of stems	Height (cm)	Number of nodes
B1	4	39,5	5
B2	4	41,5	5
B3	4	38,0	5
B4	4	42,5	5
C1	4	40,5	5
C2	4	38,0	5
C3	4	41,5	5
C4	4	42,5	5
N1	4	37,3	5
N2	4	41,2	5
N3	4	41,3	5
N4	4	38,2	5

The fresh weights of leaves, flower stalks and stems of each thesis obtained 60 days after sowing are shown below (Table B14):

Treatment	Fresh weight (g)		
	Leaves	Flowers	Stems
B1	28,86	0,23	15,22
B2	25,86	0,21	13,97
B3	25,39	0,20	13,64
B4	29,16	0,25	16,91

C1	29,83	0,27	16,50
C2	28,48	0,28	15,38
C3	24,30	0,22	15,83
C4	27,33	0,15	17,06
N1	30,57	0,15	17,13
N2	24,41	0,29	15,00
N3	24,85	0,28	15,16
N4	28,51	0,28	16,15

The dry weights of leaves, flower stalks and stems of each thesis obtained 95 days after sowing are shown below (Table B15):

Table B15. Dry weight of leaves, flowers and stems of basil plants treated with microbial biomass (B), pectin (C) and untreated (N).			
Treatment	Dry weight (g)		
	Leaves	Flowers	Stems
B1	2,38	0,04	1,29
B2	2,25	0,03	1,24
B3	2,24	0,02	1,23
B4	2,73	0,07	1,58
C1	2,51	0,00	1,35
C2	2,48	0,02	1,31
C3	2,56	0,06	1,74
C4	2,47	0,00	1,57
N1	2,65	0,00	1,39
N2	2,11	0,05	1,38
N3	2,17	0,04	1,45
N4	2,38	0,04	1,33

Chlorophyll Content Index

The chlorophyll content indices obtained 60 days after sowing are shown below (Table B16):

Table B16. Chlorophyll content indices recorded for the middle and apical leaves of basil plants treated with microbial biomass (B), pectin (C) and untreated (N).	
--	--

Treatment	Chlorophyll Content Indices (C.C.I.)			
	Apical leaves		Median leaves	
	F1	F2	F3	F4
B1	33,4	33,3	63,5	33,5
B2	37,7	32,2	31,5	34,3
B3	31,7	32,1	65,6	30,6
B4	35,7	32,1	31,6	33,7
C1	36,0	36,1	29,7	33,2
C2	31,7	26,8	61,1	35,2
C3	32,1	39,7	63,5	29,2
C4	28,2	30,9	29,9	26,8
N1	36,1	34,2	29,9	28,6
N2	34,9	34,1	47,9	27,9
N3	44,0	36,0	27,4	33,3
N4	34,6	31,6	65,2	29,3

Annex C

Data on the assessment of *P. granadensis* CT364's ability to colonise plant tissues

Below are the results related to the biometric data and Fv/Fm values obtained during the evaluation test of the plant growth-promoting bacterium *P. granadensis* CT364's ability to colonise the root and aerial tissues of Micro-Tom tomato. Also reported are the sterilisation procedures carried out on Cochise wheat seeds and their outcomes.

Tomato Micro-Tom tissues colonisation

To assess the ability of *P. granadensis* CT364 to colonise plant tissues and improve the fitness of host plants, two hypotheses were considered.

- Treatment with *P. granadensis* CT364 (PG).
- Treatment with magnesium sulfate (MS).

Biometric measurements

The data obtained 52 days after transplanting, relating to the height per plant, are shown below (Table C1):

Plant	Plant height (cm)
PG1A*	66,7
PG1B	55,5
PG1C	62,2
PG1D	57,4
PG2A	73,5
PG2B*	44,4
PG2C	50,4
PG2D	76
PG3A	74,5

PG3B	59,2
PG3C	58
PG3D*	70,3
MS1A	72
MS1B	65,8
MS1C	65,1
MS1D*	69,8
MS2A	71,2
MS2B	76
MS2C*	61,4
MS2D	83
MS3A*	47,5
MS3B	73,2
MS3C	66,8
MS3D	45,8

The fresh weights of leaves, flowers and stems of each plant obtained 52 days after transplanting are shown below (Table C2):

Table C2 relating to the fresh weights recorded for plants treated with <i>P. grandensis</i> CT364 (PG) and control (MS), concerning leaves, stems and flowers			
Plant	Fresh weight (g)		
	Leaves	Flowers	Stems
PG1B	16,86	0,67	19,08
PG1C	19,37	0,45	12,85
PG1D	28,22	0,028	10,76
PG2A	23,17	1,45	15,71
PG2C	17,6	0,17	7,87
PG2D	16,37	0,36	14,39
PG3A	18,18	1,25	18,02
PG3B	17,51	0,21	7,98

PG3C	19,87	0,14	8,35
MS1A	23,65	0,47	15,08
MS1B	23,54	0,48	12,76
MS1C	21,63	0,27	12,47
MS2A	16,86	0,58	15,06
MS2B	16,36	0,1	14,09
MS2D	15,86	1,16	15,49
MS3B	19,46	0,21	11,19
MS3C	14,6	0,19	10,09
MS3D	18,03	0,08	10,13

The dry weights of leaves, flower stalks and stems of each thesis obtained 59 days after sowing are shown below (Table C3):

Table C3 relating to the dry weights recorded for plants treated with <i>P. grandensis</i> CT364 (PG) and control (MS), concerning leaves, stems and flowers.			
Plant	Dry weight (g)		
	Leaves	Flowers	Stems
PG1B	3,49	0,17	3,3
PG1C	3,84	0,12	2,24
PG1D	4,07	0,02	1,63
PG2A	4,27	0,26	3,03
PG2C	3	0,01	1,14
PG2D	3,19	0,09	2,5
PG3A	3,14	0,25	3,23
PG3B	2,88	0,07	1,26
PG3C	3,47	0,07	1,51
MS1A	3,95	0,17	2,69
MS1B	4,35	0,12	2,25
MS1C	4,09	0,06	2,27

MS2A	3,4	0,18	2,51
MS2B	2,82	0,06	2,21
MS2D	2,99	0,26	2,69
MS3B	2,74	0,05	1,43
MS3C	2,32	0,03	1,43
MS3D	3,17	0,05	1,55

Measurement of Chlorophyll fluorescence

The data obtained 28 days after the transplant and related to Fm (maximum fluorescence), Fv (variable fluorescence) and Fv/Fm values are reported below (Table C4):

Table C4 shows the Fm (maximum fluorescence), Fv (variable fluorescence), and Fv/Fm values recorded for plants treated with <i>P. granadensis</i> CT364 (PG) and control (MS).			
Plant	Fm	Fv	Fv/Fm
PG1A	10863,83	8431,97	0,78
PG1A	11593,05	8826,80	0,76
PG1A	10893,81	8254,87	0,76
PG2B	12771,47	9658,62	0,76
PG2B	11874,80	8896,80	0,75
PG2B	11116,17	8288,14	0,75
PG3D	14213,71	11087,73	0,78
PG3D	12303,14	9615,24	0,78
PG3D	10710,94	8296,46	0,77
MS1D	11779,88	8577,68	0,73
MS1D	12486,66	9127,89	0,73
MS1D	10550,92	7588,36	0,72
MS2C	11253,01	8511,52	0,76
MS2C	10518,96	8023,15	0,76
MS2C	11045,70	8332,31	0,75
MS3A	12792,04	9793,59	0,77
MS3A	11068,21	8531,42	0,77
MS3A	12126,59	9576,21	0,79